The Role of Na^+/H^+ Exchanger Isoform 5 (NHE5) in Glioma

by

Hung-Yi Fan

B.Sc., The University of British Columbia, 2011

A THESIS SUBMITTED IN PARTIAL FULFILLMENT OF

THE REQUIREMENTS FOR THE DEGREE OF

MASTER OF SCIENCE

in

The Faculty of Graduate and Postdoctoral Studies

(Biochemistry and Molecular Biology)

THE UNIVERSITY OF BRITISH COLUMBIA

(Vancouver)

November, 2015

Abstract

Up-regulation of the receptor tyrosine kinases (RTKs) signalling cascades constitutes the basis of tumorigenesis. Signal termination that normally occurs through receptor degradation is disrupted in various cancers. Therefore, persistent receptor-mediated signal occurs through increased recycling and elevated surface expression of these receptors. Previous discoveries of endosomal pH modulators that promote tumour progression suggest the potential roles of acidic endosomal pH in receptor turnover from the endosomes and oncogenic signalling. In this thesis study, I showed that neuron-enriched Na^+/H^+ exchanger NHE5 plays an important role in trafficking of c-Met RTK in C6 glioma cells. NHE5 is predominantly expressed in recycling endosomes of C6 cells. By fluorescence ratiometric analysis, I showed that NHE5 depletion with short-hairpin RNA significantly increases pH of Tfn positive recycling endosomes, implicating a prominent role of NHE5 in endosomal acidification. By cell surface biotinylation, I found that cell surface abundance of hepatocyte growth factor (HGF) receptor c-Met is significantly reduced in NHE5-deficient cells. Further analysis revealed that recycling circuitry is impaired and degradation of c-Met is enhanced by a previously uncharacterized, non-proteasomal degradation when NHE5 is depleted. Consequently, reduced expression of c-Met by NHE5 knockdown (KD) causes severe migratory defect and loss of cell polarity. Stable expression of shRNA-resistant human NHE5 into NHE5 KD cells acidifies endosomal pH, increases surface c-Met abundance, restores Rac1 activity, and enhances cell migration. In summary, this thesis study highlights critical role of endosomes pH in regulating receptor-mediated signalling through vesicular trafficking, and a potential role of NHE5 in promoting sustained signalling essential for the tumorigenicity of glioma.

Preface

The work presented in this thesis has been a collaborative effort between myself, my supervisor, Dr. Masayuki Numata, and members of Numata lab. The experiments presented in this thesis were designed through collaborative effort between myself and my supervisor, Dr. Numata. Preparation of materials used in the experiments for this thesis was a collaborative effort of members of Numata lab. Some of the constructs used in this study, such as cDNA for hNHE5 and Rab11, were cloned by Dr. Numata. Subcloning of plasmids used in this study was designed by Dr. Numata and the works were carried out by myself with the help of volunteer students, Andy Chen, Winston Huang, Stephanie Cheung and Yue Wu. Most of the experiments presented in this thesis were performed by myself, with the exception of figure 4.7A, which was done by Dr. Yuka Numata (Numata lab). Preparation of astrocyte lysates for figure 3.1A was done by Dr. Caroline Perronnet (Moukhles lab). Preparation of data figures were done by myself with assistance from Dr. Yuka Numata. I received training and technical support from many colleagues, in particular from my supervisor Dr. Numata, and Dr. Yuka Numata.

A combined version of chapter 3 and 4 has been prepared as a manuscript for publication. I prepared the first draft of the manuscript, which was revised by my supervisor Dr. Numata, and Dr. Yuka Numata.

Fan, S. H., Numata, Y. Numata, M. Endosomal Na^+/H^+ exchanger NHE5 influences MET recycling and cell migration. Submitted

The research presented in this thesis was approved by the UBC Bio-Safety Committee (Certificate LB-2013-125257).

Table of contents

List of tables

List of figures

List of abbreviations

ADHD - Attention deficit hyperactivity disorder
AE - Anion (Cl^-/$HCO3^-$) exchanger
AQP – Aquaporin
Arf - ADP-ribosylation factor
Baf - Bafilomycin A1
BDNF - Brain-derived neurotrophic factor
BSA - Bovine serum albumin
β - Buffering capacity
β2AR - β-2 adrenergic receptor
CFTR - Cystic fibrosis transmembrane conductance regulator
CHO - Chinese hamster ovary
CIE - Clathrin-independent endocytosis
CK2 - Casein kinase 2
ClC - Chloride channel
CLIC - Chloride intracellular channel
CLIC/GEEC - Clathrin-independent carriers/GPI-enriched early endosomal compartment
CME - Clathrin-mediated endocytosis
c-Met - Hepatocyte growth factor receptor
    HGF - Hepatocyte growth factor
ECL - Enhanced chemiluminescence
ECM - Extracellular matrix
EDTA - Ethylenediaminetetraacetic acid
EE - Early endosome
    EEA1 - Early endosome antigen 1
EGFR - Epidermal growth factor receptor
    EGF - Epidermal growth factor
    TGFα - Transforming Growth Factor α
EIPA - 5-(*N*-ethyl-*N*-isopropyl) amiloride
FBS - Foetal bovine serum
GBM - Glioblastoma multiforme
GGA3 - Golgi-localized γ-ear-containing ARF-binding protein 3
GLAST - Glutamate/Aspartate transporter
GLUT - Glucose transporter
GST - Glutathione S-transferase

IPTG - Isopropyl β-D-1-thiogalactopyranoside
KD - Knockdown
KO – Knockout
LE - Late endosome
LDLR - Low-density lipoprotein receptor
LRIG1 - Leucine rich repeats and immunoglobin-like domains protein 1
NBC - Sodium/Bicarbonate co-transporter
NDCBE - Sodium-driven chloride/bicarbonate exchanger
NGF - Nerve growth factor
NHE - Sodium/Proton exchangers
    pNHE - Plasmalemmal NHE
    CNO-NHE – Cation non-specific organeller membrane type NHE
    NHERF – NHE regulatory factor
    rNHE5 – Rat NHE5
NKA - Sodium/Potassium ATPase
NMDA - N-methyl-D-aspartate
PAGE - Polyacrylamide gel electrophoresis
Pak1 - p21 protein-activated kinase 1
    PBD - p21 binding domain
PBS - Phosphate-buffered saline
PC12 - Pheochromocytoma-12
PI - Protease inhibitor
PIP - Phosphatidylinositol phosphate
PKA - Protein kinase A
PKC - Protein kinase C
PM - Plasma membrane
PQ – Primaquine
RACK1 - Receptor for activated c-kinase 1
RAVE - Regulator of H^+-ATPase of the vacuolar and endosomal membranes
RE - Recycling endosome
RIPA - Radioimmunoprecipitation assay buffer
RTK - Receptor tyrosine kinase
SCAMP - Secretory carrier membrane protein
SDS - Sodium dodecyl sulfate
SGLT - Sodium-glucose linked transporter
Tfn - Transferrin

TfR - Transferrin receptor
TGN - Trans-Golgi network
USP8 - Ubiquitin specific protease 8
V-ATPase - Vacuolar type H^+-ATP hydrolases

Acknowledgments

I would like to express my gratitude to my supervisor, Dr. Masayuki Numata, for giving me this opportunity to work on this project with complete freedom, training me with laboratory techniques required, and providing guidance throughout the hardships. Without his mentorship and encouragement, I would not have been able to complete this work. I would also like to thank my committee members, Dr. I. Robert Nabi and Dr. Elizabeth Conibear for their constructive feedback and guidance throughout this thesis study. Much of the experiments that I have done were inspired through discussion with the committee members. I would like to thank the members of Numata lab, past and present, for their helps with my projects and lab chores, but most importantly, for their companionship. I would especially like to thank Dr. Yuka Numata, for having a lot of patience training and helping me with many of the experiments, as well as providing constructive feedbacks to make my work more presentable.

Many thanks to members of Nabi lab, Cullis lab, Roberge lab and Moukhles lab, especially Ray Feng, Dr. Jay Shankar, Aruna Balgi, Sam Chen, Dr. Paulo Lin, and Dr. Caroline Perronnet, for training me how to use the equipments and generously shared reagents and protocols for my experiments.

I would also like to thank my family for their continuous support and encouragement to work hard, and for tolerating my (occasional) bad temper when things failed…

For funding, I would like to acknowledge the Natural Science and Engineering Research Council of Canada, which provided the financial support for this project.

1. Introduction

1.1 Cellular pH and homeostasis

Many cellular processes are modulated by pH. Small variations in intracellular or extracellular pH can change the protonation states of proteins, which affect the structure and functions of the proteins, have profound effects on cellular processes such as signal activation, cell motility, membrane dynamics, and protein turnover. Generation of proton gradients (or proton motive force) stores considerable amount of cellular energy that drives various processes. Because of this, cellular pH is tightly regulated to ensure proper cellular functions. Cellular pH homeostasis is safe-guarded by multiple mechanisms to prevent fluctuations of pH away from the physiological range that can potentially damage the cells. First, cellular pH is protected by the high pH buffering capacity (β), which consists of $\beta_{intrinsic}$ provided by intracellular weak bases and acids, including phosphates and amino acids, and $\beta_{bicarbonate}$ (Casey, Grinstein et al. 2010). $\beta_{bicarbonate}$ stems from the ability of the cell to convert CO_2 to bicarbonate acid (catalyzed by carbonic anhydrase), which is readily dissociated into H^+ and HCO_3^-. When coupled with ion transporters, the bicarbonate makes a strong buffering system that holds the cytosolic pH at a slightly acidic range. Secondly, ion gradients and membrane potential (net negative in cytosol) also prevent continuous influx or efflux of proton as it requires tremendous energy to overcome the gradient and electrostatic barrier (Casey, Grinstein et al. 2010). Lastly, many pH-regulating transporters are allosterically regulated by pH and the movement of protons through transporters alleviates cellular stress. For instance, an acid extruder Na^+/H^+ exchanger NHE1 is activated by cytosolic acidification and inhibited by cytosolic alkalinization (Wakabayashi, Hisamitsu et al. 2003; Lacroix, Poet et

al. 2004; Hisamitsu, Yamada et al. 2007; Casey, Grinstein et al. 2010; Brisson, Driffort et al. 2013). The negative feedback regulation of transporters allows for fine-tuning of pH within physiological range for cellular functions.

1.2 Regulators of cellular pH

Specific intracellular distributions and regulated activities of different transporters allow the organelles to be maintained at distinct pH. These include proteins that directly transport proton or others that indirectly influence proton flux by generating ion/counter-ion gradients and membrane potentials. In the following sections, some of the major transporters involved in cellular pH regulation will be discussed.

1.2.1 Vacuolar type H^+-ATP hydrolases (V-ATPases)

V-ATPases pump proton against its gradient using ATP as an energy source. V-ATPases consist of two complexes: a V_0 membrane complex that translocates protons and a V_1 peripheral complex that hydrolyzes ATP to provide energy required for V_0 (Forgac 2007). On the plasma membrane (PM), V-ATPases play an important role in maintenance of extracellular acidity as in the case for osteoclast (Qin, Cheng et al. 2012), gastric, and renal epithelial cells (Brown, Paunescu et al. 2009; Shin, Munson et al. 2009). V-ATPases are primary active transporters that acidify the organellar pH as inhibition of V-ATPase activity by macrolide antibiotics (*i.e.* Bafilomycin A1) markedly alkalinizes intracellular compartments (Johnson, Dunn et al. 1993; Presley, Mayor et al. 1997; Forgac 2007). Since organelles have varying pH, it is likely that activities of V-ATPases are differentially regulated. This could be affected by variation in distribution of V-ATPases or isoforms specificity in different organelles (Casey, Grinstein et al. 2010).

Uncoupling of proton pump and ATP expenditure through disassembly of the V_0 and V_1 complexes had been proposed as one way to modulate rate of proton transport. The RAVE (regulator of H^+-ATPase of the vacuolar and endosomal membranes) complex had been suggested to stabilize the V_0 and V_1 complexes and thus plays an important role in modulating V-ATPases activity (Smardon, Diab et al. 2014). Translocations of protons generate membrane potential across the membrane (net positive inside lumen), thereby preventing further influx of proton. This limitation can be alleviated by coupling the influx of protons into organellar lumen with the efflux of cations (*i.e.* Na^+), or by counter-ion conductance through parallel influx of anions (*i.e.* Cl^-). Thus non-proton transporting ion transporters also participate in regulating organellar pH. The established membrane potential presents an energy barrier that limits the movement of proton and effectively maintains organellar pH homeostasis (Casey, Grinstein et al. 2010).

1.2.2 Anion transporters

As described in the previous section, extracellular or luminal acidification by V-ATPases requires concomitant influx of counter-ions to achieve electroneutral transport. The members of the chloride channel family (ClC) , the Cl^-/HCO_3^- exchanger family (AE), and the Cystic fibrosis transmembrane conductance regulator (CFTR) are known transporters that mediate primarily chloride transport, but also HCO_3^- to a lesser extent (Casey, Grinstein et al. 2010; Scott and Gruenberg 2011). Of note, ClCs also mediate proton transport through exchange of two Cl^-, but whether or not they directly participate in endosomal acidification is still under debate (Mohammad-Panah, Harrison et al. 2003; Hara-Chikuma, Yang et al. 2005; Wellhauser, D'Antonio et al. 2010; Scott and Gruenberg 2011). The precise role of these chloride channels in intracellular pH

regulation thus depends largely on the established ion gradient of the compartments.

1.2.3 Bicarbonate transporters

As a major buffer for cellular pH, transport of bicarbonate across the membrane has significant influences on pH homeostasis. Bicarbonate transporters are generally coupled with Na^+ or Cl^-. Depending on the ion specificity, bicarbonate transporters can be base-extruders or acid extruders. Members of the Na^+/HCO_3^- co-transporter (NBC) family mediate parallel HCO_3^- and Na^+ transport into the cytoplasm. Of note, some isoforms of the NBC catalyze electroneutral transport of HCO_3^- and Na^+ in 1:1 stoichiometry, while others are electrogenic that transport 1 Na^+ for two or three HCO_3^-. Whereas the transporter activities of electroneutral isoforms are solely driven by the Na^+ gradient and mediate unidirectional transport (*i.e.* alkalinizes cytosol), the direction of the transport by the electrogenic isoforms is controlled by both Na^+ gradient and membrane potential (net negative in cytosol). Thus, if the electrical component outweighs the concentration gradient, the transporters would instead mediate efflux of Na^+ and HCO_3^- and acidify the cytosol (Gross, Hawkins et al. 2001; Cordat and Casey 2009; Casey, Grinstein et al. 2010).

Bicarbonate can also be transported along with Cl^- as in AE and Na^+-driven chloride/bicarbonate exchanger (NDCBE). In the case of AE, the export of HCO_3^- is driven by an influx of Cl^- toward lower concentration gradient ($[Cl^-]_{ext} > [Cl^-]_{cyt}$) and therefore acidifies the cytosol. In contrast, NDCBE transports HCO_3^- and Cl^- in the opposite direction at the expense of Na^+ gradient, thus increasing the cytosolic pH (Casey, Grinstein et al. 2010; Honasoge and Sontheimer 2013). Altogether, these transporters keep the ion gradient and membrane potential at the physiological range.

1.2.4 Na^+/H^+ exchangers

Na^+/H^+ exchangers (NHE) are evolutionary conserved secondary active transporters that utilize electrochemical gradient of monovalent cations to transport protons. The substrates of NHE are typically Na^+ and H^+ (Orlowski and Grinstein 2007; Donowitz, Ming Tse et al. 2013). Eleven mammalian isoforms have been identified, of which NHE1-NHE9 were shown to exhibit ion transporter activity. They commonly have an N-terminal transmembrane domain containing 11 or 12-alph-helical segments, which is involved in electroneutral proton/cation transport and an isoform-specific cytosolic C-terminal domain that regulates individual transporter activity. Mammalian NHEs can be sub-divided into two groups. The plasmalemmal NHEs (pNHEs, NHE1-5) exert Na^+/H^+ exchange across the PM when expressed in NHE-deficient cells, although some isoforms such as NHE5 and NHE3 shuttle between intracellular compartments and the PM. Besides NHE1, which is found in almost all tissue, other isoforms of pNHEs are tissue-specific (Donowitz, Ming Tse et al. 2013; Fuster and Alexander 2014). The organellar NHEs (NHE6-9) are found in intracellular compartments of most cells and typically do not show Na^+/H^+ exchange activity across the PM upon expression in NHE-deficient cells. NHE6-NHE9 possess unique monovalent cation transporter activity with a higher affinity to K^+ than Na^+, which is the likely reason for the incapability of these transporters to "complement" pNHE activity on the PM (Nakamura, Tanaka et al. 2005; Kondapalli, Hack et al. 2013; Ouyang, Lizarraga et al. 2013). Thus, depending on the intracellular localization of the transporter and the substrate used, the role of *c*ation *n*on-specific *o*rganelle-membrane type NHEs (CNO-NHEs) in pH regulation may vary. It had been suggested that CNO-NHEs function primarily as “proton-leak” pathways and play critical roles in fine-tuning organellar pH. In the following sections, nine isoforms of

mammalian NHEs are briefly introduced.

Plasmalemmal NHEs

NHE1

NHE1 is the most extensively studied isoform of the NHE family. In human, it is encoded by SLC9A1 gene and consists of 815 amino acids with an apparent molecular weight of ~91 kDa. It is ubiquitously expressed and resides primarily in the PM. NHE1 facilitates transport of H^+ out of the cytosol and plays a housekeeping role in relieving cells from acidic stress. NHE1 is also a major contributor of Na^+ influx into the cells and modulates cell volume through intake of salt and water by coupling with Cl^-/HCO_3^- exchanger, AE2, and the water channel aquaporin, AQP1 (Stock and Schwab 2006; Casey, Grinstein et al. 2010; Donowitz, Ming Tse et al. 2013; Fuster and Alexander 2014). In addition, it had been suggested that the local pH shift mediated by NHE1 is critical in modulating the dynamics of actin filaments and focal adhesion complexes, and the activities of enzymes that degrade extracellular matrix (ECM) (Bourguignon, Singleton et al. 2004; Stock and Schwab 2006; Magalhaes, Larson et al. 2011; Choi, Webb et al. 2013). NHE1 may also function as a membrane scaffold for the assembly of signalling complex that promotes cell proliferation, migration, invasion, and suppresses apoptosis (Denker, Huang et al. 2000; Baumgartner, Patel et al. 2004; Cardone, Casavola et al. 2005; Stock and Schwab 2006)**.** The implication that NHE1 plays a role in cancer arose from an early study that reported a positive correlation between tumour frequency with expression level of NHE1 (Lagarde, Franchi et al. 1988). Despite the extensive research of NHE1 in promoting cell motility, there is no clinical evidence supporting NHE1-based inhibitors as effective anti-metastatic therapeutics (Donowitz, Ming Tse et al. 2013;

Fuster and Alexander 2014). One possible explanation is that other NHEs or transporters may play a compensatory role when NHE1 function is disrupted, as several plasmalemmal NHEs share similar distribution and functional redundancy (Donowitz, Ming Tse et al. 2013).

NHE2

Human NHE2 is encoded by SLC9A2 gene and consists of 812 amino acids with calculated molecular weight of ~91 kDa (Malakooti, Dahdal et al. 1999). It is highly expressed in kidney, intestinal and gastric epithelium (Praetorius, Andreasen et al. 2000; Dixit, Xu et al. 2004). It is localized to the apical surface of renal and intestinal epithelial cells (Bailey, Giebisch et al. 2004; Dixit, Xu et al. 2004; Guan, Dong et al. 2006), with the exception of basolateral expression in inner medullary collecting duct (Sun, Liu et al. 1998) and gastric parietal cell (Schultheis, Clarke et al. 1998). NHE2 plays an important role in Na^+/HCO_3^- absorption in kidney (Bailey, Giebisch et al. 2004; Dixit, Xu et al. 2004) and contributes to the intracellular pH regulation of duodenum epithelium (Praetorius, Andreasen et al. 2000). In the distal tubule, increased flow of bicarbonate into the lumen is countered by secretion of H^+ into the extracellular space by apical NHE2, NHE3, and V-ATPases, as well as absorption of HCO_3^- to the interstitial place, resulting in increased Na^+ and HCO_3^- reabsorption (Bailey, Giebisch et al. 2004). In addition, NHE2 is highly expressed in the crypt of intestinal epithelial lining (Chu, Chu et al. 2002). Loss of NHE2 in mice reduces transport of Na^+ and HCO_3^- into the intestinal cells (Bailey, Giebisch et al. 2004; Guan, Dong et al. 2006), but exhibits no major pathological consequences likely due to compensatory effects from other transporters, such as NHE3 (Bachmann, Riederer et al. 2004). In the gastric epithelium, loss of NHE2 is associated with reduced

viability of parietal cells, leading reduced gastric secretion and increased pH (Schultheis, Clarke et al. 1998).

NHE3

Human NHE3 is encoded by SLC9C3 gene and consists of 834 amino acids with calculated molecular weight of 93 kDa (Brant, Yun et al. 1995). It is most abundantly expressed in the gastrointestinal system and kidney, and to a lesser extent in heart, and lungs (Fuster and Alexander 2014). Basolateral and apical subcellular localization of NHE3 in different tissues and species had been reported (Biemesderfer, Rutherford et al. 1997; Bazzini, Botta et al. 2001; Sabolic, Herak-Kramberger et al. 2002; Hayashi, Szaszi et al. 2004). The role of NHE3 in guts and kidney had been studied extensively. In intestinal epithelium, the activity of NHE3 is suggested to be inhibited by Ca^{2+} and cAMP (Yun, Oh et al. 1997; Weinman, Steplock et al. 2000; Cinar, Chen et al. 2007). This is likely to occur by retrieval of NHE3 from the PM through PKA-mediated phosphorylation of NHE3 and the disassembly of the c-terminal PDZ domain of NHE3 from NHE regulatory factor (NHERF) 2 and Ezrin (Weinman, Steplock et al. 2000; Cha and Donowitz 2008; Lin, Murtazina et al. 2011). The binding of clathrin complex adaptor protein synaptotagmin 1 to NHE3 is required for endocytosis of NHE3 (Musch, Arvans et al. 2009). Conversely, PM targeting and activity of NHE3 is coupled to uptake of D-glucose mediated by SGLT1 (Sodium-Glucose linked transporter-1) and concomitant activation of PI3K, Akt, and NHERF2 at the apical surface of intestinal epithelial (Lin, Murtazina et al. 2011). In kidney, NHE3 is expressed in proximal tubules, where it is involved in reabsorption of Na^+, HCO_3^-, and water (Fuster and Alexander 2014). Knockout of NHE3 in mice impairs renal and intestinal absorption of electrolyte, leading

to mild acidosis (Schultheis, Clarke et al. 1998).

NHE4

Human NHE4 consists of 798 amino acids and has a calculated molecular weight of 90 kDa. It is highly expressed in stomach but also found in macula densa cells, ascending limb of loop of Henle, proximal and distal tubules in kidney, hippocampus, zymogen granule of pancreas, acinar and duct cells of salivary glands. In polarized epithelial cells, NHE4 is mostly localized with NHE1 at the basolateral surface (Pizzonia, Biemesderfer et al. 1998; Donowitz, Ming Tse et al. 2013). In stomach, NHE4 is expressed in parietal cells, where it couples with other transporters such as AE2 and NKA to mediate uptake of electrolyte and maintains cell volume (Gawenis, Greeb et al. 2005). NHE4-null mice develop hypochlorhydria similar to NHE2-null mice (Bailey, Giebisch et al. 2004; Gawenis, Greeb et al. 2005). Loss of NHE4 is associated with impaired secretory membrane development, reduced viability of parietal cells, defective gastric secretion, and reduction in cell volume of parietal cell, similar to that of AE2 knockout (KO) (Gawenis, Greeb et al. 2005). It is therefore presumed that NHE4 (and its coupled basolateral transporters) functions primarily in establishing the intracellular electrolyte gradient required to drive constant gastric secretion at the apical surface. In kidney, NHE4 mediates transport of NH_4^+ / Na^+ exit out of ascending loop of Henle into medullary interstitium where gradients are established for ammonia excretion in distal tubule. This is supported by the finding that loss of NHE4 in mice reduces accumulation of ammonia in inner medulla and failure to increase urinary ammonia and acid excretion following acid challenge (Gawenis, Greeb et al. 2005).

NHE5

Human NHE5 consists of 896 amino acids and has an apparent molecular weight of ~99 kDa. Its mRNA is predominantly expressed in the nervous system, but expression in testes, spleen and skeletal muscles had also been found (Attaphitaya, Park et al. 1999; Fuster and Alexander 2014). Within the human brain, NHE5 mRNA is most abundantly expressed in the hippocampus, the hypothalamus, and the thalamus, whereas limited expression was observed in the glia-enriched corpus callosum, leading to the dogma that NHE5 is "neuron-specific" (Baird, Orlowski et al. 1999). Very little was known about the protein expression levels of NHE5 until our laboratory developed anti-NHE5 antibodies that specifically recognize rat NHE5 (Diering, Mills et al. 2011; Diering, Numata et al. 2013). NHE5 is most closely related to NHE3, sharing about 50% of primary sequence identity and similar intracellular localization. In comparison, NHE5 shares about 40% primary sequence identity with NHE1 (Brett, Donowitz et al. 2005). NHE5 resides predominantly in the recycling endosomes and is occasionally targeted to the PM (Donowitz, Ming Tse et al. 2013). Vesicular trafficking and activity of NHE5 at the PM is regulated by interaction with various proteins through the C-terminal cytosolic tail. For example, internalization of NHE5 requires association with β-arrestin and c-terminal phosphorylation by Casein Kinase 2, CK2, (Lukashova, Szabo et al. 2011). The secretory carrier membrane protein, SCAMP2, small GTPases, Arf6, and Rab11 modulate PM targeting of NHE5 and its activity on the plasma membrane (Diering, Church et al. 2009). In addition, PI-3K and the actin cytoskeleton appear to play a regulatory role in distribution of NHE5 between endosomes and the PM (Szaszi, Paulsen et al. 2002), whereas PKA, PKC (Attaphitaya, Nehrke et al. 2001), and the Receptor for Activated C-Kinase 1, RACK1 (Onishi, Lin et al. 2007), regulate the PM activity of NHE5.

More recently, NHE5 had been reported to play an inhibitory role on NMDA receptor through acute recruitment to the synaptic cleft, where it mediates local acidification to terminate NMDA activity and thus limits growth of dendritic spines (Diering, Mills et al. 2011). Moreover, NHE5 acidifies recycling endosomes of neuroendocrine pheochromocytoma (PC12), positively regulates cell-surface targeting and signalling of NGF receptor tyrosine kinase, TrkA, and promotes neurite extensions (Diering, Numata et al. 2013). Thus, NHE5 appears to play a critical role during neurogenesis. These studies implicate that NHE5 is of paramount importance in shaping neuroplasticity and is essential for neural functions.

Cation non-specific Organellar NHEs (CNO-NHEs)

NHE6

Human NHE6 is encoded by SLC9A6 gene. It is ubiquitously expressed with higher expression observed in brain (Brett et al. 2005) and osteoblasts (Fuster and Alexander, 2014). NHE6 is localized to the recycling endosomes in most cells, although PM distributions have also been reported in certain types of cells including osteoblasts (Liu, Schlesinger et al. 2011) and inner ear cells (Hill, Brett et al. 2006). Unlike plasmalemmal NHEs, the CNO-NHEs preferentially catalyze K^+/H^+ exchange over Na^+/H^+ exchange (Fuster and Alexander 2014). Due to the higher $[K^+]$ in the cytsol than that in organellar lumens, CNO-NHEs are thought to be endosomal alkalinizers. In support of this, knockdown of NHE6 in HEPG2 and HeLa cells resulted in acidification of endosomal compartments and disrupted polarized protein distribution to apical and basolateral membranes, thereby affecting polarity establishment and inhibiting clathrin-dependent endocytosis (Ohgaki, Matsushita et al. 2010; Xinhan, Matsushita et al. 2011). The

significance of NHE6 in neural functions had been reported in previous studies (Stromme, Dobrenis et al. 2011; Ouyang, Lizarraga et al. 2013). In mice, loss of NHE6 is associated with late endosomal and lysosomal accumulation of GM2 ganglioside and unesterified cholesterol in neurons of specific brain region, accompanying with motor coordination defect (Stromme, Dobrenis et al. 2011). Neurons without NHE6 or expressing NHE6 E255Q, a transporter-inactive mutant, exhibit impaired BDNF/TrkB signalling due to over-acidification of early endosome and these result in impaired endosomal signalling, reduced neuron branching, and immature development of neurocirucuit . Mutations in SLC9A6 gene had been correlated to neurological diseases in human, including X-linked Angelman-like syndrome, corticobasal degeneration associated with tau deposition, and severe mental disability (Christianson, Stevenson et al. 1999; Gilfillan, Selmer et al. 2008; Garbern, Neumann et al. 2010; Takahashi, Hosoki et al. 2011; Fuster and Alexander 2014)

NHE7

Human SLC9A7 encodes for NHE7, which is consist of 725 amino acids and has a calculated molecular weight of 80 kDa. It is predominantly localized to the *trans*-Golgi network (TGN) but is also present in endosomes and the PM (Numata and Orlowski 2001). The terminal region is responsible for translocation of NHE7 to the TGN, as well as binding with multiple partners, including SCAMPs, caveolins, CD44, and GLUT1 (Lin, Williams et al. 2005; Lin, Williams et al. 2007; Kagami, Chen et al. 2008). However, the role of these interactions in transporter activity and function are only partially understood. Overexpression of NHE7 in MDA-231 had been shown to promote breast cancer cell invasion, cell-cell adhesion, anchorage-independent growth, and implicate a potential

role of organellar pH in cancer biology (Onishi, Lin et al. 2012). The pathophysiological significance of elevated expression of NHE7 in carcinogenesis and progression of malignant tumours requires further studies.

NHE9

Human SLC9A9 gene encodes NHE9, which is consist of 645 amino acids and has a calculated molecular weight of 72 kDa. In most cells, NHE9 is localized to late and recycling endosomes (Nakamura, Tanaka et al. 2005; Kondapalli, Hack et al. 2013; Fuster and Alexander 2014). In vestibular hair bundles, NHE9 is present on the plasma membrane, functions in K^+/H^+ exchange by utilizing high [K^+] of endolymph, and removes excess cytosolic proton generated by Ca^{2+}-ATPase (Hill, Brett et al. 2006). As a common feature of the CNO-NHEs, NHE9 interacts with RACK1 through its c-terminus and this regulates PM targeting of the transporter (Ohgaki, Matsushita et al. 2010). Loss of NHE9 function had been associated with neurological disorders such as autism, attention deficit hyperactivity disorder (ADHD), and mental retardation (de Silva, Elliott et al. 2003; Morrow, Yoo et al. 2008; Markunas, Quinn et al. 2010; Schwede, Garbett et al. 2014). In astrocytes, over-expression of NHE9 contributes to alkalinization of the endosomal compartment, increased uptake of transferrin and glutamate, and stabilized surface expression of transferrin receptor and glutamate transporter GLAST. Conversely, autism-associated NHE9 mutations (L236S, S438P, V176I) showed loss of transporter activity, reduced surface expression of synaptic protein Glut1 and glutamate clearance (Kondapalli, Hack et al. 2013; Kondapalli, Prasad et al. 2014), suggesting a potential role of NHE9 in modulating synaptic activity.

NHE8

NHE8 is distinct from other NHEs in that it shares only about 25% primary sequence identity and has a much shorter C-terminal tail with no sequence homology to other isoforms (Brett, Donowitz et al. 2005; Donowitz, Ming Tse et al. 2013). It is highly expressed in kidney, liver, skeletal, muscle, and testis (Donowitz, Ming Tse et al. 2013; Fuster and Alexander 2014). In Chinese hamster ovary (CHO) or HeLa cells, NHE8 was predominantly found in the *mid*- and *trans*-Golgi, but some expression in endosomes was also observed (Nakamura, Tanaka et al. 2005). Depletion of NHE8 in HeLa cells disrupted protein sorting within multivesicular bodies (MVBs) and enhanced EGFR (Epidermal growth factor receptor) degradation. Interestingly, NHE8 knockdown did not affect pH of MVBs, implicating an alternative role of NHE8 besides transporter activity in modulating endosome morphology and vesicular trafficking (Lawrence, Bright et al. 2010). In rat kidney epithelium, NHE8 is expressed on the plasma membrane (Zhang, Bobulescu et al. 2007). In kidney and intestine, NHE8 is found in intracellular compartment and at the apical plasma membrane of proximal tubules and intestinal brush border epitheliums (Donowitz, Ming Tse et al. 2013). As such, it is possible that the intracellular localization and functions of NHE8 is affected by cell-type and/or context-dependent factors. While NHE3 is expressed and functional in adult renal proximal tubule, NHE8 is a dominant NHE in newborns and later translocates to intracellular compartments (Goyal, Mentone et al. 2005; Becker, Zhang et al. 2007; Xu, Chen et al. 2008; Donowitz, Ming Tse et al. 2013). This switch from NHE8 to NHE3 activity during post natal renal development appears to be regulated by glucocorticoid or thyroid hormones level (Gattineni, Sas et al. 2008; Xu, Zhang et al. 2010; Baum, Twombley et al. 2012), but the relevance of the isoforms switch is current not known.

However, it had been shown that NHE8 plays a compensatory role in proximal tubule acidification when NHE3 is knocked out (Joseph, Gattineni et al. 2013), suggesting the functional redundancy between these two isoforms provides a protective mechanism in renal functions.

1.3 Endocytic trafficking of membrane receptors

The complexity of endocytic circuitry provides spatial and temporal regulations required for basic cellular processes. Entry of cargoes into cells occurs via two major routes: clathrin-mediated endocytosis (CME), and clathrin-independent endocytosis (CIE) includes caveolar-, ARF6-, and CLIC/GEEC-dependent pathways (Mayor and Pagano 2007; Huotari and Helenius 2011). These two modes of endocytosis occur in different membrane domains, thus allow for spatially regulated internalization of specific cargoes. For instance, Major histocompatibility complexes I and II (MHCI,II), ion and nutrient transporters (Glucose transporter I, L-type amino acid transporter 1, potassium channel Kir3.4), adhesion molecules (E-cadherin, ICAMI, CD44, Integrin β1), and a subset of signalling receptors (β2-adrenergic receptors, M3-muscarinic receptors, metabotropic glutamate receptor 7) are some of the identified cargoes of CIE (Maldonado-Baez et al. 2013). Low-density lipoprotein receptor (LDLR), Transferrin receptor (TfR), and many receptor tyrosine kinases (RTKs) are endocytosed through CME (Goh and Sorkin 2013; Maldonado-Baez, Williamson et al. 2013). However, some RTKs such as EGFR and c-Met (Hepatocyte growth factor receptor) internalize through both pathways (Sigismund, Argenzio et al. 2008; Maldonado-Baez, Williamson et al. 2013).

The internalized vesicles first arrive at early endosomes (EEs), where cargoes are

either passively sorted by geometry of the endomembrane or through recognition of specific targeting signals by adaptor proteins/protein complexes (Maxfield and McGraw 2004). EEs are generally found in the cell periphery and are associated with markers including Rab5, Rab4, and early endosome antigen-1 (EEA1). The turnover rates of cargoes of EEs are about 5-10 min (Maxfield and McGraw 2004; Huotari and Helenius 2011). During this time, the cargoes could be directly recycled to the PM through Rab4-dependent fast recycling pathway, or sorted to recycling endosomes for slower recycling, or retained in EEs for degradation (Scita and Di Fiore 2010). Rab5 remains on the EEs for the entire time and is required for the maturation of EEs to late endosomes (LEs) (Huotari and Helenius 2011). Active Rab5, along with VPS34-p150, a class III PI3K, produces phosphatidylinositol 3-phosphate (PI(3)P) (Zerial and McBride 2001). The clustering of active Rab5 and PI(3)P then recruits EEA1, which functions in endosomes docking and fusion (Simonsen, Lippe et al. 1998; Christoforidis, McBride et al. 1999; Zerial and McBride 2001). The EEs and LEs also communicate with the TGN through bi-directional pathways. The anterograde trafficking supplies the endosomes with enzymes required for protein degradation whereas the retrograde transport provides a return route for membrane proteins from endosomes back to TGN (Huotari and Helenius 2011).

Sorting of cargoes in endosomes occurs in part through geometry of the endosomes. Bulks of membrane proteins are preferentially sequestered to tubular recycling compartments whereas soluble proteins that contain lysosomal targeting motif are retained in the EEs and eventually delivered to LEs (Maxfield and McGraw 2004). However, with the discovery of sorting signals on several receptors and accessory proteins that affects the transport of these receptors, it is now accepted that recycling of

some receptors are regulated by additional factors (Gage, Kim et al. 2001; Dai, Li et al. 2004; Parachoniak, Luo et al. 2011; Hsu, Bai et al. 2012). For instance, the recycling of β2 adrenergic receptor (β2AR) requires SNX27, an adaptor protein that binds to β2AR and recruits it to retromers (Temkin, Lauffer et al. 2011). It was initially thought that recycling of β2AR involves retrograde transport from endosomes to the TGN and subsequently to the PM through the secretory pathway. However, a later study showed that β2AR is directly targeted to the PM from sorting endosomes, suggesting a direct role of retromers in recycling (Puthenveedu, Lauffer et al. 2010; Huotari and Helenius 2011). For c-Met, recycling takes place in the small GTPase Arf6-positive-endosomes, and requires recruitment of an Arf6 effector GGA3 (Golgi-localized γ-ear-containing ARF-binding protein 3) and its adaptor protein, Crk (Parachoniak, Luo et al. 2011). In other cases, sorting and recycling cargoes involves post-translational modification. As is the case with most RTKs, receptor activation and phosphorylation promote ubiquitination, which target the receptors to late endosomes for degradation (Levkowitz, Waterman et al. 1999; Yokouchi, Kondo et al. 1999; Abella, Peschard et al. 2005; Lemmon and Schlessinger 2010). Absence of the ubiquitin tag by disrupting the recruitment of Cbl, an E3 ubiquitin ligase, to the activated receptors has been shown to promote recycling of EGFR (Pennock and Wang 2008).

Emerging studies on altered RTKs trafficking in promoting receptor turnover and sustained signalling suggest a potential role in tumorigenesis (Abella, Peschard et al. 2005; Mak, Peschard et al. 2007; Sigismund, Argenzio et al. 2008; Joffre, Barrow et al. 2011). Endosomal pH regulators such as V-ATPases, CLICs (Chloride Intracellular Channels), and organelle-membrane-bound NHEs, have been suggested to modulate

trafficking of signalling receptors and promote cell motility, proliferation, persistent signalling, and tumour formation (Dozynkiewicz, Jamieson et al. 2012; Wiedmann, von Schwarzenberg et al. 2012; Poea-Guyon, Ammar et al. 2013; Kondapalli, Llongueras et al. 2015), implicating the pathological significance of endosomal pH homeostasis in cancer biology. In this thesis study, I have shown that NHE5 protein, previously known as the "neuronal" NHE is abundantly expressed in rat glioma C6 cells and human glioma U87 cells, but not in normal rat astrocytes, and have investigated the roles of NHE5 in C6 glioma cells. Unexpectedly robust expression of NHE5 in C6 glioma cells raises the question as to whether this neuron-specific transporter plays a role in signalling in non-neuronal cells and possibly in tumorigenesis. I first showed that NHE5 is localized to recycling endosomes in C6 cells and is functional in these compartments (See chapter 3). This led me to the next chapter, where I examined the role of NHE5 in vesicular trafficking, signalling, and cell motility. The finding of this thesis study has provided one of the first molecular mechanisms for endosomal pH regulation in glioma cells, which modulates cargo-specific targeting of RTK.

2. Materials and methods

2.1 Cell culture and transfection

C6 rat glioma cells were a generous gift from Dr. Sin, Wun Chey (LSI, UBC). Cells were cultured in DMEM containing 10% foetal bovine serum (FBS). Stable knockdown clones were generated by transfecting the cell with corresponding shRNA plasmid and maintaining them in DMEM + 10% FBS supplemented with either G418 or hygromycin. The target sequences for NHE5 are A) GTTTGCTCTTGGTGAAACAGATGTTA, B) ATAGTGGTGGCCACAAAGTAGTCCT, and C) TTTGTGGTAATCACTCCTCTTCACC (Diering, Mills et al. 2011; Diering, Numata et al. 2013). C6 cells were transfected with BioRad GenePulser Xcell electroporation system (BioRad, Hercules, CA, USA). Cells were resuspended in ice-cold 1M HEPES Buffer, mixed with plasmid DNA, subjected to electric shock (250V, 200μF), and immediately placed into pre-warmed culture media.

2.2 Antibodies, reagents, and DNA construct

Rabbit anti-rat NHE5 (rNHE5) antibody was generated in our laboratory and tested previously (Diering, Mills et al. 2011; Diering, Numata et al. 2013). Anti-phospho-Erk1/2 (pT185/pY187, #44-680G), transferrin receptor (clone H68.4, #13-6800), Alexa-Fluo conjugated phalloidin (#A-22287 and #A-12379), Alexa-Fluor conjugated goat anti-mouse (#A-21235 and #A-11004) and anti-rabbit (#A-11079 and #A-21210) secondary antibodies were obtained from Invitrogen (Carlsbad, CA, USA). Anti-EEA1 (clone 14/EEA1, #610456), Rab11 (clone 47/Rab11, #610656), GM130 (clone 35/GM130, #610822), and RACK1 (clone20/RACK1, #610177) antibodies were obtained from BD Bioscience (Mississauga, ON, Canada). Anti-Rac1 (clone 23A8, #05-389)

antibody was purchased from Millipore (Billerica, MA, USA). Mouse monoclonal anti-Cdc42 (clone B-8, #sc-8401), rabbit polyclonal anti-c-Met (SP260, #sc-162), Rac1 (C-14, #sc217), and EGFR (1005, #sc-03) antibodies were obtained from Santa Cruz Biotechnology (Dallas, TX, USA). Anti-HA (clone 16B12) antibody was obtained from Covance (Princeton, NJ, USA). Anti-Na^+/K^+ ATPase (clone α5) and β-tubulin (clone E7) antibodies were obtained from Developmental Study Hybridoma Bank (Iowa city, IA, USA). Rabbit polyclonal anti-SCAMP1 (#PA1-739) was obtained from Thermo Fisher Scientific (Waltham, MA, USA). Rabbit polyclonal Anti-phospho-Akt (pT308, #9275), Akt (#9272), Erk1/2 (#9102), and mouse monoclonal anti-c-Met (clone 25H2, #3127) antibodies were obtained from Cell Signaling Technology (Danvers, MA, USA). Hoechst 33342 was obtained from Sigma Aldrich (St.Louis, MO, USA). DRAQ5^{TM} (#62251, Thermo Fischer Scientific) was a generous gift from Dr. P.R Cullis (UBC, Canada).

Bafilomycin A1 (#B-1080) was purchased from LC Laboratories (Woburn, MA, USA). Hepatocyte Growth Factor (HGF, #CYT-090) and Epidermal Growth Factor (EGF, #CYT-217) were obtained from ProSpec-Tany TechnoGene Ltd (Rehovot, Israel). Nigericin (#BML-CA421) was obtained from Enzo Life Sciences, Inc (Farmingdale, NY, USA). Alexa-568- (#T-23365) and FITC-conjugated Tfn (#T-2871) were purchased from Invitrogen. Isopropyl β-D-1-thiogalactopyranoside (IPTG, #I5502), Primaquine bisphosphate (#160393), MG-132 (#C2211), and sodium orthovanadate (#S6508) were obtained from Sigma Aldrich. NSC-23766 was a generous gift from Dr. I.R. Nabi, (UBC, Canada). SNARF-1 (Seminaphtharhodafluor) pH sensor was a generous gift from Dr. J. Church (UBC, Canada)

Human NHE5 36HA, NHE5- and NHE1-specific shRNA constructs were previously described (Diering, Mills et al. 2011; Diering, Numata et al. 2013). YFP-Rac1 pEYFP-C1

(#11391) and GST-Pak1 PBD pGEX2TK (#12217) were purchased from Addgene (Cambridge, MA, USA).

Table 2.2A - Dilutions of antibodies and fluorescence probes used for immunoblotting and immunofluorescence.

Primary Antibodies	Immunoblotting	Immunofluorescence
Akt	5,000X	-
pAkt	10,000X	-
Cdc42	250X	200X
EEA1	-	200X
EGFR	1,000X	-
Erk1/2	2,000X	-
pErk1/2	10,000X	-
GM130	-	200X
HA	5,000X	500X
c-Met (mouse/rabbit)	1,000X/1,000X	200X/100X
rNHE5	1,000X	50X
NKA	100X	-
Rab11	-	200X
RACK1	2,500X	500X
Rac1 (mouse/rabbit)	10,000X/1,000X	100X/100X
SCAMP1	30,000X	-
TfR	10,000X	1,000X
β-tubulin	1,000X	200X

Secondary Antibodies	Immunoblotting	Immunofluorescence
Goat-anti-Mouse Alexa Fluor 647/568	-	500X
Goat-anti Mouse HRP	20,000X	-
Goat-anti Rabbit Alexa Fluor 568/488	-	500X
Goat-anti Rabbit HRP	20,000X	-

Fluorescent Probes	Immunofluorescence
DRAQ5™	1,000X
Hoechst	500 ng/mL
Phalloidin Alexa Fluor 647/488	100X

Unless otherwise noted, the values represent folds of dilution from laboratory or manufacturers' stocks.

Table 2.2B Concentration of stimulants and inhibitors used for assays.

Compounds	**Final Concentrations Used**
Bafilomycin A1	50 nM
EGF	50 nM
HGF	50 nM
IPTG	1 mM
MG-132	20 μM
Nigericin	10 μM
NSC-23766	100 μM
Primaquine bisphosphate	100 μM
SNARF-1	10 μM
Sodium Orthovanadate	2 mM
Tfn-AlexaFluor 568	25 μg/mL
Tfn-FITC	30 μg/mL

2.3 Immunofluorescence

Cells were grown on the slides overnight and fixed with 3% PFA for 10 min at room temperature (RT) followed by permeabilization with 0.1% Triton X-100 in PBS for 10 min. To visualize endogenous NHE5, cells were fixed and permeabilized in cold 1:1 methanol/acetone at -20ºC for 10 min. The cells were then blocked with 1% BSA-PBS solution, probed with primary antibodies diluted with 0.1% BSA-PBS at 4°C overnight, and incubated with Alexa Fluor conjugated secondary antibodies in 0.1% BSA-PBS at RT for 45 min. After extensive wash, cover slips were mounted in ProLong Gold Antifade Reagent (Invitrogen). For fixed samples, images were collected with Leica TCS-SP8 laser scanning confocal microscope (63x/NA1.40 oil objective, Diode/Argon/HeNe lasers, and SP detector, Wetzlar, Germany).

2.4 Immunoblotting

Cells were lysed on ice in 1% NP-40 in PBS or Radioimmunoprecipitation Assay (RIPA) buffer (50 mM Tris-HCl [pH 7.2], 150 mM NaCl, 0.1% SDS, 0.5% sodium deoxycholate, 1% NP-40) with protease inhibitor (PI) cocktail (Roche Diagnostic Corporation, Indianapolis, IN, USA). Cell debris was cleared by centrifugation at 16,000 x g at 4°C for 15 min and protein concentration was determined by Bradford assay (BioRad). Proteins were separated by SDS-PAGE and electrotransferred onto PVDF membranes. The membrane was blocked with 5% non-fat milk in PBS-Tw (0.075% Tween-20) at RT for 1 h, incubated overnight with primary antibody at 4ºC, followed by brief washes with PBS-Tw, then, incubated with HRP-conjugated secondary antibody (Jackson ImmunoResearch Laboratories, Inc. West Grove, PA, USA) at RT for 40 min, washed again with PBS-Tw, and detected by enhanced chemiluminescence (ECL) using

Luminata Forte Western HRP substrate (Millipore). Quantifications of the blots were done by densitometry analysis using Image J software (NIH, Bethesda, MD, USA).

2.5 Endosomal pH measurement

Endosomal pH measurements were done as previously described (Diering, Numata et al. 2013). Cells were grown on 8-well chamber glass slides (Lab-Tek™ II, Thermo Fischer Scientific) overnight and serum starved for 2 h prior to the experiment. Serum-starved cells were incubated with 30 µg/mL of Tfn-fluorescein and 25 µg/mL of Tfn-Alexa 568 at 37ºC for 30 min, follow by 15 min chase in the absence of Tfn. For the V-ATPases inhibition experiments, 200 nM Bafilomycin A1 was added during the Tfn labelling step and maintained throughout the experiments. Perinuclear fluorescences were captured under live cell conditions using a spinning-disk confocal microscopy (Carl Zeiss Axiovert 200M, Jena, Germany) using 100x/NA1.45 oil objective with appropriate filters. Fluorescein and Alexa-568 were excited by a 488-nm or a 546-nm laser, respectively. The background reading obtained from imaging cell-free area was subtracted from the readings of both fluorophores. Since fluorescein is pH-sensitive (pKa~6.4) (Diehl and Markuszewski 1989; Klonis and Sawyer 1996) and Alexa568 is pH-insensitive, endosomal pH can be quantified by ratiometric analysis of the two fluorophores. The obtained fluorescein/Alexa-568 ratios were converted to pH using a calibration curve. To generate the calibration curve, Tfn-loaded cells were incubated in buffered high-K^+ solution containing nigericin (140 mM KCl, 10 mM glucose, 1 mM $MgCl_2$, 2 mM $CaCl_2$, 20 mM HEPES [pH7.0]/PIPES [pH6.5]/MES [pH6.0, 5.5], 10 µM Nigericin) to clamp intracellular pH (Presley, Mayor et al. 1997; Brett, Tukaye et al. 2005). The fluorescence ratios at corresponding pH were plotted.

2.6 Cytosolic pH measurement

$3x10^4$ cells were grown overnight in 8 well chamber slide. Cells were cultured in HEPES-based culture media (20 mM HEPES bicarbonate-free DMEM + 10% FBS) at 37ºC, 0.03% CO_2. Bicarbonate was eliminated from the culture medium to minimize the potential perturbation of cytosolic pH by the bicarbonate transporters, NBC and NDCBE. Cells were then incubated with 10 μM SNARF-1 for 30 min at 37ºC. SNARF-1 is a single excitation, dual emission pH-sensitive biosensor that allows quantification of cellular pH through ratiometric analysis (Sheldon, Cheng et al. 2004). Following cellular uptake of SNARF1, the cells were washed twice with pre-warmed HEPES-based culture media and imaged with scanning confocal microscopy (Olympus FV1000 laser scanning microscope, Tokyo, Japan). The filter and capture settings were modified from previously described protocol (Sheldon, Cheng et al. 2004). The biosensor was excited by 488 nm laser and the fluorescence emission was split by two dichoric mirrors which reflected emission below 640 nm to the first detector and emission between 640 nm to 650 nm to the second detector. The detectors were set to capture emission from 550 nm to 600 nm (Hv: 700, Gain: 1X, Offset: 9%) and at 647 nm (Hv: 650, Gain1X, Offset: 9%), corresponding to two peaks of fluorescence emission of the biosensor, respectively. The fluorescent ratios of the two emission peaks were converted to pH with a calibration curve. To generate the calibration curve, cells loaded with SNARF1 dye were clamped between pH 6 to 8 using high K^+/Nigericin technique described above (See section 2.5). The fluorescence ratio at corresponding pH were recorded and plotted.

2.7 HGF-induced Akt/Erk activation assay

Cells were grown at 37ºC and serum starved overnight prior to HGF stimulation.

Cells were incubated with 50 ng/mL of HGF in pre-warmed serum-free DMEM (Cai, Rook et al. 2000) for 0, 2, 5, 15, 30, 60, or 120 min in the CO_2 incubator at 37ºC. Cells were then quickly washed with ice-cold PBS, lysed in 1%NP40-TBS containing 2 mM sodium orthovanadate and PI, and quantified cell lysates were analyzed by Immunoblotting. Activated Akt and Erk were probed with phosphor-Akt(pT308) or phospho-Erk1/2(pT185/pY187) antibody. The densitometric analysis was performed using ImageJ. Relative Erk and Akt activities were obtained as ratios of phosphorylated (active) and respective total proteins that were normalized to peak intensity of control at 15 min.

2.8 Surface labeling assay

Semi-confluent cells were rinsed twice with ice-cold PBS-CM (1 mM $MgCl_2$, 0.1 mM $CaCl_2$) and incubated with 0.5 mg/mL of membrane impermeable amino-reactive biotinylation reagent (EZ-Link™ Sulfo-NHS-SS-Biotin, #21331, Thermo Fischer Scientific), in PBS-CM at 4ºC for 45 min. Unreacted biotinylation reagent was then quenched with 20 mM glycine in PBS-CM for 10 min at 4˚C. Cells were washed with ice-cold PBS three times, and lysed in RIPA buffer with PI. Fifty µg of protein were incubated with NeutrAvidin conjugated agarose beads (Thermo Fischer Scientific) at 4˚C overnight, washed with ice-cold RIPA, buffer and eluted with SDS sample buffer (112 mM Tris [pH 6.8], 4.5% (w/v) SDS, 0.23% (w/v) Bromophenol Blue, 23% glycerol, 0.1 M DTT) at 65°C for 30 min. Eluted protein and 4 µg of input were analyzed by immunoblotting. For c-Met or EGFR, surface abundance was calculated by taking the ratio of the surface receptor signal and surface NKA signal. Relative surface abundance was obtained by normalizing to the value of control.

2.9 Internalization and recycling assays

Internalization and Recycling assays were done as previously described with some modifications (Le, Yap et al. 1999). Surface proteins were labeled with biotin as described in section 2.8. Cells were then incubated with pre-warmed culture media for 0 or 30 (Intern. 30) min at 37ºC, followed by 15 min of incubation with the cleavage buffer twice (50 mM glutathione, 90 mM NaCl, 1 mM $MgCl_2$, 0.1 mM $CaCl_2$, 0.2% BSA, pH 8.6) at 4ºC, washed with PBS, and lysed in RIPA buffer with PI. No cleavage controls (SL.0 and SL.30) were included for to account for the loss of biotinylated proteins due to intrinsic degradation during the 30 min incubation. Quantified cell lysates were incubated with NeutrAvidin beads overnight, washed, and eluted with SDS sample buffer. Eluted proteins were analyzed by Immunoblotting using anti-c-Met or anti-NHE1 antibody. For c-Met experiment, Five times more proteins were used for NHE5 knockdown (KD, 200 µg) to normalize the surface abundance of the receptor to control (40 µg). The blots were quantified by densitometry. Relative internalization of c-Met was calculated by normalizing the ratio of total internalized population and the total surface c-Met (SL.0) to the level of control. The total internalized population includes the internal pool (Intern.30) and the degraded pool (SL.0 – SL.30). The formula for quantification is as followed: [Intern.30 + (SL.0-SL.30)] / SL.0

For recycling assay, biotin-internalized cells were further incubated in culture media for 15 min at 37˚C. The cells were subjected to two additional rounds of cleavage to remove biotin that recycled back to plasma membrane (Recycle), followed by washes and lysis. A non-cleaved sample (Degrad.) was included to determine intracellular degradation of c-Met after receptor internalization. For primaquine experiment, cells were treated with 100 µM of primaquine for 4 h prior biotin labeling and maintained in the

culturing media for the duration of the experiment. Protein concentrations were quantified by Bradford assay. 150 µg of proteins from control or 750 µg of NHE5 KD were incubated overnight with NeutrAvidin beads. The eluted proteins were then analyzed by Immunoblotting and probed for c-Met, Integrin β1, and TfR. The blots were quantified by densitometric analysis. Recycling of receptor was represented by the ratio of Recycled population (Degrad. – Recycle) and the internalized pool (Intern.). Relative recycling was obtained by normalizing to the value of control.

2.10 HGF-dependent c-Met degradation assay

$5x10^5$ cells were grown in 60 mm plates and serum starved for 16 h. Cells were then treated with 50 ng/mL for 0, 30, 60, and 120 min prior to lysis. To examine the effects of specific degradation pathway, cells were treated with 20 µg/mL MG-132 or 200 nM of Bafilomycin A1 for 3 h prior to as well as during the incubation period with HGF. Cells were then lysed on ice in RIPA buffer with PI. Equal amount of proteins were analyzed by Immunoblotting and the blot were simultaneously probed for c-Met and NHE1. Degradation of c-Met was quantified by densitometric analysis. For each sample, expression of c-Met relative to that of NHE1 was normalized to the unstimulated sample.

2.11 Rho GTPases assay

Pak-PBD (p21-binding domain of p21 activated protein kinase 1) immobilized agarose beads were prepared as previously described (Mezzacappa, Komiya et al. 2012). BL-21 cells were transformed with PBD-GST plasmids and the culture was incubated in 2YT media with ampicillin (16 g/L Tryptone, 10 g/L Yeast Extract, 5 g/L NaCl, 100 µg/mL ampicillin, pH 7.0) at 30°C until OD600 reached 1.0. Expression of PBD-GST

was then induced with 1 mM IPTG for 3 h at 30°C. Cells were then spun-down, resuspended in PBS, and lysed by sonication. Supernatants were collected and proteins were separated by 10% SDS-PAGE. PBD-GST yield was quantified by Coomassie staining with BSA standard. Two µg of PBD-GST per sample were incubated with glutathione agarose beads (GE healthcare, Little Chalfont, UK) for 45 min at 4°C. The beads were then washed and resuspended in Rac1 lysis buffer (50 mM Tris, pH 7.5, 200 mM NaCl, 2% NP-40, 10% glycerol, 10 mM $MgCl_2$, PI). C6 cells were grown to about 60% confluency and lysed on ice with Rac1 lysis buffer. Protein concentrations were quantified by Bradford assay. Twenty-five µg (Rac1) or 100 µg (Cdc42) of proteins were incubated with PBD-GST beads at 4ºC for 1 h. Beads were then washed and eluted with SDS sample buffer. Rac1 or Cdc42 bound to the beads were analyzed by immunoblotting using anti-Rac1 or Cdc42 antibody. The blots were quantified by densitometric analysis. Activities of GTPases were obtained as ratios of pulldown (activated) and total proteins, relative to the value of control.

To inhibit Rac-1 activity, cells were treated with 100 µM of NSC-23766 (Santa Cruz Biotechnology) for 24 h prior to lysis. For HGF-induced Rac-1 activity assay, cells were serum starved overnight, followed by addition of 50 ng/mL HGF for 5 min before lysis. Lysates were then subjected to PBD pulldown as described above.

2.12 Membrane fractionation

Cells were collected and resuspended in sucrose buffer (250 mM sucrose, 1 mM EDTA, 10 mM Tris, pH 7.4, PI). Cell membrane was sheared by passing the cell suspension through a 26.5 Gauge needle 20 times at 4ºC. Cell debris was cleared by centrifugation at 800 x g for 15 min at 4ºC twice, followed by ultracentrifuge at 98,000 x g

for 30 min at 4ºC (Beckman TLS55 rotor, Brea, CA, USA). The supernatant was collected as the cytosolic fraction. The pellet was gently washed with ice cold PBS once and resuspended in RIPA buffer. Insoluble pellet debris was cleared by centrifugation at 16,000 x g for 15 min and the supernatant was collected as membrane fraction. Proteins in each fraction were quantified by Bradford and analyzed by Immunoblotting with Rac1, SCAMP1 (Membrane control), or RACK1 (Cytosol control) antibodies.

2.13 3D Migration assay

Cells were seeded into the Transwell™ permeable support insert (Corning Inc., Corning, NY, U.S.A) at $4x10^4$ cells/ 200 μL per insert and incubated inside the 24-well plate containing 300 μL of DMEM with 20% FBS per well for 6 h at 37°C, 5% CO_2. Cells were then fixed with 3% PFA for 15 min. Cells that remained on the upper side of membrane were scraped off with a cotton swab. The inserts were incubated with 0.1% crystal violet for 20 min to stain the migrated cells. The inserts were then rinsed with water and air dried. Images were taken using inverted light microscope using 40x objective (Nikon Eclipse TS100, Tokyo, Japan). Five randomly selected image of each cell line were scored. Five to eight experiments per cell line were conducted.

2.14 Wound healing assay

Wound healing assay was done with Incucyte ZOOM™ automated imaging system (Essen BioScience, Ann Arbor, MI, USA). 30,000 cells were seeded to a 96-well plate and incubated at 37°C, 5% CO_2 overnight. The wells were gently washed and wounds were generated using 96-well Woundmaker™ tool (#4493, Essen Bioscience). The plate was then incubated at 37ºC inside Incucyte, where images were taken every 30 min for

16 h. Relative wound closure was calculated with preset algorithm in manufacturer's software, as a function of cell density and open wound area.

For c-Met and Rac1 localization assay, cells were grown overnight on glass cover slips in a 35 mm culture dish into a monolayer. Pipette tip was used to generate multiple equal-sized wounds across the coverslips. The well was then gently washed with PBS to remove detached cells and incubated for 9 h at 37°C. Cells were fixed and label with corresponding antibodies as described in Immunofluorescence section and confocal images were taken. Membrane translocation was determined by fluorescent signals of the proteins on the plasma membrane that is discontinuous with the cytosolic fluorescence. Percentage of cell expressing positive Rac1 or c-Met translocation at the leading edge was quantified.

2.15 Polarity assay

Cells were grown overnight into a monolayer on glass cover slips. Equal-width wounds were generated with a pipette tip and the cover slips were gently washed with PBS to remove detached cells. Cells were then incubated at 37°C for 6 h, fixed, and probed with anti-mouse GM130, DRAQ5 fluorescent nucleus dye, and phalloidin-Alexa488 and images were taken with confocal microscope. Polarity establishment was presented by an arbitrary unit, Polarity Index, defined by the percentage of cells exhibiting correct orientation at the leading edge. Orientations of the cells were determined by placing a 120°plane on the cell with its tip at the center of nucleus and the longest axis parallel to the wound. Correct orientation is scored if Golgi resides within the plane.

2.16 Statistical analysis

To determine statistical significance, Student's paired or unpaired *t*-tests were performed using Microsoft Excel software (Microsoft Corporation, Remund, WA, USA). *p*-values are indicated as follows: *$p<0.05$, **$p<0.01$, ***$p<0.001$, n.s=not significant.

3. NHE5 is a potent recycling endosomal acidifier in C6 glioma.

Introduction

NHE5 had been long recognized as the brain-specific NHE due to the abundant mRNA expression in neurons (Attaphitaya, Park et al. 1999; Baird, Orlowski et al. 1999; Diering, Mills et al. 2011). However, little was known about expression of NHE5 in non-neuronal cell types. In this chapter, I examine the expression and function of NHE5 in C6 glioma cells. Given that NHE5 had been implicated in regulating receptor signalling, cell adhesion, and migration (Onishi, Lin et al. 2007; Diering, Numata et al. 2013; Jinadasa, Szabo et al. 2014), elevated NHE5 expression levels may have pathological consequences in cancer biology. Here, I present my results on characterization of NHE5 in C6 cells and show that NHE5 is predominantly localized to and acidifies recycling endosomes.

3.1 NHE5 is up-regulated in C6 glioma cells and resides predominantly in recycling endosomes

Preliminary experiments done by others in our laboratory suggested that the C6 glioma cell line expresses appreciable amount of NHE5. Interestingly, Dr. Nicole Basler had noted in her thesis that mRNA expression levels of NHE5 were higher in samples obtained from grade IV glioblastoma multiforme (GBM) patients and from patients with shorter than mean survival time (Basler, 2013. "*Studies on the expression and function of pH - regulatory transporters in Glioblastoma multiforme (German to English."* (Doctoral dissertation http://d-nb.info/1046071394/34), raising an interesting possibility that NHE5 could contribute to the malignancy of glioma.

Using polyclonal antibodies generated against a polypeptide EEPTQEPGPLGEPP

corresponding to first extracellular loop of rat NHE5, I detected a single band at 95 kDa corresponding to NHE5 in C6 glioma with immunoblotting (Fig. 3.1A). To examine the relative expression level of NHE5 in C6 cells, I compared the abundance of NHE5 between hippocampal astrocytes obtained from postnatal day 1 Sprague Dawley rat (Noel, Tham et al. 2009), C6 glioma, and neuroendocrine pheochromocytoma (PC12) by immunoblotting. Using β-tubulin as a loading control, I showed that NHE5 is more abundantly expressed in C6 cells compared to astrocytes, but NHE5 expression in C6 cells was lower than in PC12 cells. In contrast, expression of housekeeping plasma membrane NHE, NHE1, was similar between the tested cells (Fig. 3.1A).

To identify the intracellular localization of NHE5, I performed immunofluorescence analysis using antibodies against NHE5 and endosomal markers including early endosome antigen-1 (EEA1), transferrin receptor (TfR) and Rab11. NHE5 partially co-localized with TfR and Rab11 at the perinuclear region (Fig. 3.1B-C). No overlapping signal was observed with EEA1 in the cell periphery (Fig. 3.1D). This is consistent with our previous finding in PC12 and exogenous expression of NHE5 in NHE-deficient CHO cells, in which NHE5 co-localized with Rab11 and TfR but not with an early endosomal marker Rab5 (Diering, Numata et al. 2013). In addition, exogenous NHE5 is transiently targeted to the PM in CHO cells and primary neurons (Onishi, Lin et al. 2007; Diering, Church et al. 2009; Jinadasa, Szabo et al. 2014). To test if endogenous NHE5 is also targeted to the PM, I performed cell-surface biotinylation that labelled proteins present on the PM but not cytosolic proteins or membrane proteins on the intracellular membrane. I was unable to detect NHE5 in the surface fraction whereas robust surface expression of NHE1 was detectable (Fig. 3.1E).

(Fig 3.1)

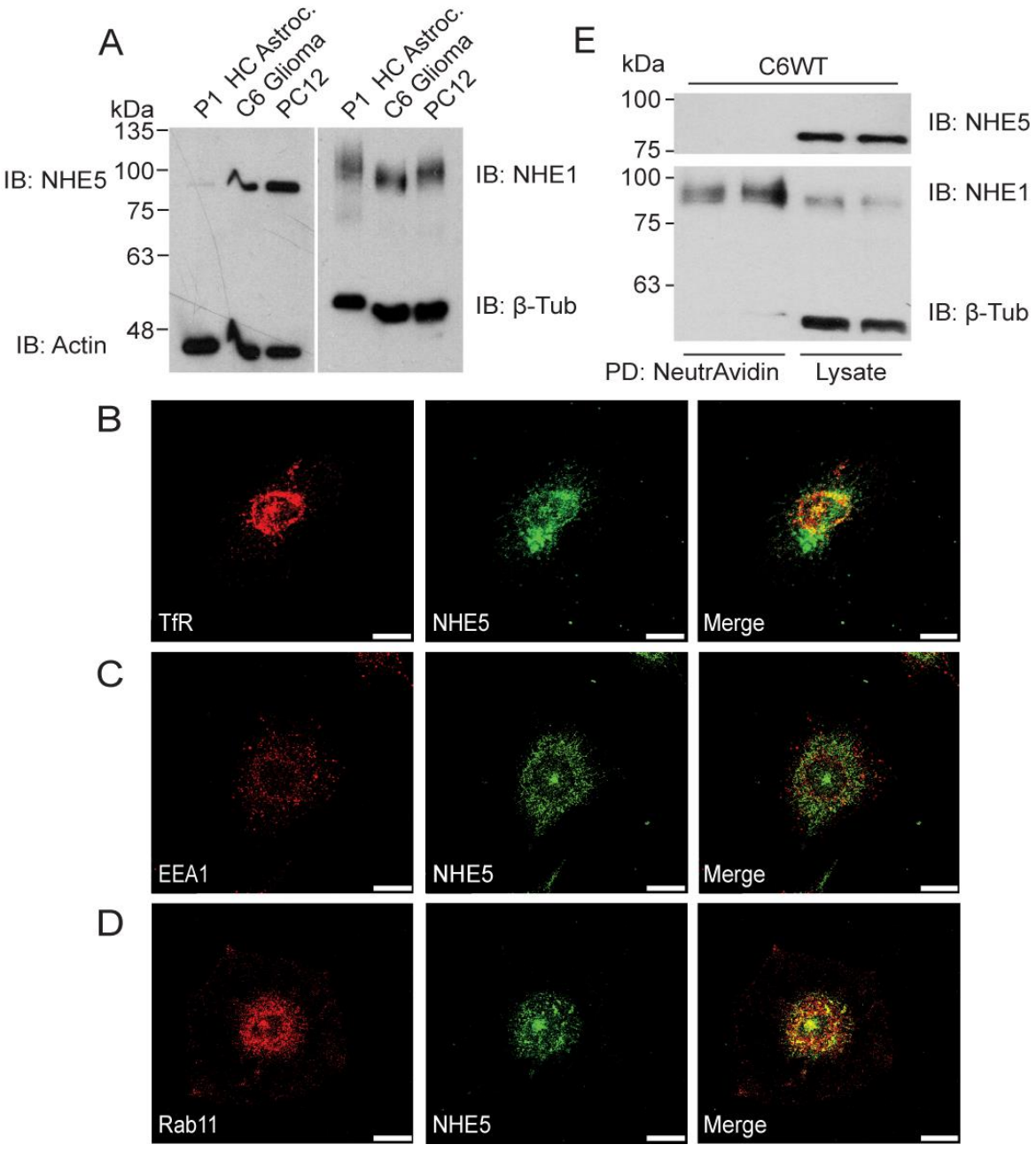
A
P1
HC Astroc.
C6 Glioma
PC12
kDa
135
100
75
63
48
IB: NHE5
IB: Actin
IB: NHE1
IB: β-Tub
E
kDa
C6WT
100
75
IB: NHE5
IB: NHE1
IB: β-Tub
PD: NeutrAvidin
Lysate
B
TfR
NHE5
Merge
C
EEA1
NHE5
Merge
D
Rab11
NHE5
Merge

(Cont.) Figure 3.1 - NHE5 is highly expressed in C6 glioma and resides predominantly in recycling endosomes.

(A) Expression of NHE5 in rat astrocyte, C6 rat glioma, and rat pheochromocytoma (PC12) were analyzed by Immunoblotting. Two µg of total protein from post natal day 1 rat hippocampal astrocytes (P1 HC Astroc.), C6, and PC12 cells were subjected to immunoblotting. Anti-NHE5, NHE1, actin, and β-tubulin antibodies were used to detect corresponding proteins. Higher expression of NHE5 was observed in glioma compared to non-malignant astrocytes. (B-D) Intracellular localization of NHE5 in C6 cells was analyzed by immunofluorescence microscopy. C6 cells were double stained for Transferrin Receptor (TfR, Red, A), Early Endosome Antigen-1 (EEA1, Red, B), or Rab11 (Red, C), and NHE5 (Green). Bars = 20 µm. NHE5 localizes with recycling endosomal markers, TfR and Rab11, but not with an early endosomes marker EEA1. (D) Surface and total NHE5, NHE1, and β-tubulin were analyzed by surface biotinylation and immunoblotting. Semi-confluent cells were incubated with membrane impermeable biotinylation reagent to label surface proteins and lysed. Proteins were affinity purified with NeutrAvidin beads and surface expression of NHE5, NHE1 and β-tubulin was detected by Immunoblotting using corresponding antibodies. Two µg of total proteins were loaded as input. NHE5 was not observable in the biotin-purified fraction, indicating that it is not present on the PM.

3.2 Generating knockdown and rescue stable clones with rat NHE5 and NHE1 specific shRNA and human NHE5 36HA plasmids

To investigate the function of NHE5 in C6 glioma, I transfected C6 cells with three independent NHE5 specific short hairpin RNA plasmids to reduce NHE5 expression. C6 cells were also transfected with an NHE1-specific shRNA plasmid or an empty vector. Transfected cells were selected by an appropriate marker for four to eight weeks to establish stable cell lines. Monoclonal stable clones were isolated once the colonies became visible. The degree of protein knockdown (KD) in each isolated clone was analyzed by immunoblotting. Three NHE5 KD clones and one NHE1 KD clones were isolated, with approximately 50% of NHE5 or 20% of NHE1 expression remaining, respectively. NHE5 rescue stable clone was generated by stably expressing rat NHE5 (rNHE5) shRNA-resistant human NHE5 (hNHE5) 36HA into one of the stable NHE5 KD cells (Fig. 3.2).

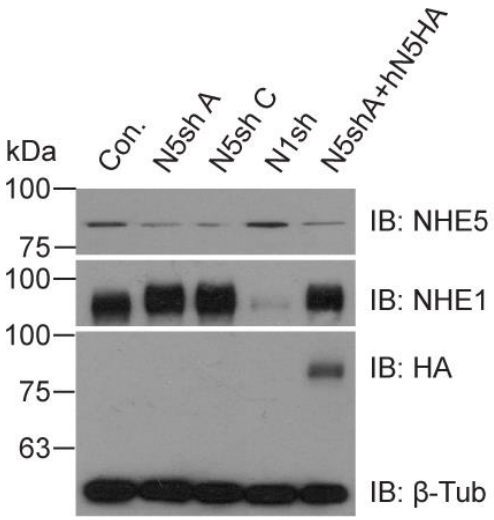

Figure 3.2 - Generating knockdown and rescue stable clones with rNHE5 and rNHE1 specific shRNA and hNHE5 36HA plasmids.

Expression of NHE5 in control, two independent stable clones expressing different rat NHE5-specific shRNA (N5sh) plasmids, NHE1shRNA (N1sh) expressing clone, and NHE5shRNA stable clone expressing human NHE5HA (hN5HA) were determined by immunoblotting using anti-rat NHE5 or NHE1 antibody to detect endogenous proteins, or anti-HA antibody to detect exogenous hNHE5 expression. β-tubulin was probed as a loading control.

3.3 NHE5 acidifies recycling endosomes

Next, I examined the function of NHE5 in recycling endosomes. Since the concentration of Na^+ in endosomes (~120 mM) is higher than that of the cytosol (~10mM) (Sage, Rink et al. 1991; Scott and Gruenberg 2011), I hypothesized that NHE5 functions as an endosomal acidifier that pumps Na^+ into the cytosol in exchange for H^+ into endosomes. To test this, I measured the endosomal pH of control and stable clones by fluorescence ratiometric analysis as previously described (Diering, Numata et al. 2013). Control and NHE5 KD cells were incubated with Tfn conjugated with fluorescent dyes (see below) and subjected to a chase incubation for an extended period of time to label the recycling endosomes (Fig. 3.3A). Confocal imaging of the pH-sensitive, Tfn-Fluorescein (green), and pH-insensitive (red), Tfn-568, revealed that NHE5 KD cells typically exhibit much higher green fluorescence within the recycling compartments as compared to controls, NHE1 KD, or hNHE5-complemented NHE5 KD cells (Fig. 3.3B-C). Since the fluorescence intensity of fluorescein positively correlates with pH, this indicated that the recycling compartments of NHE5 KD cells were more alkaline. I employed the high K^+/Nigericin technique (Presley, Mayor et al. 1997; Brett, Tukaye et al. 2005) to generate a calibration curve (Fig. 3.3D), which was used to convert fluorescence ratios to pH. The recycling endosomal pH of control and NHE1 KD cells were between 5.9 to 6.0 whereas the endosomes in NHE5 KD cells were significantly more alkaline (~pH 6.3). Expression of hNHE5 in NHE5 KD cells restored the recycling endosomal pH to ~5.9, suggesting that NHE5 is a recycling endosomal acidifier in C6 cells. Inhibition of V-ATPases by Bafilomycin A1 alkalinizes endosomal pH in both control (pH~6.2) and NHE5 KD (pH~6.4) cells, suggesting that V-ATPases contribute to acidification of recycling endosomes.

(Fig.3.3)

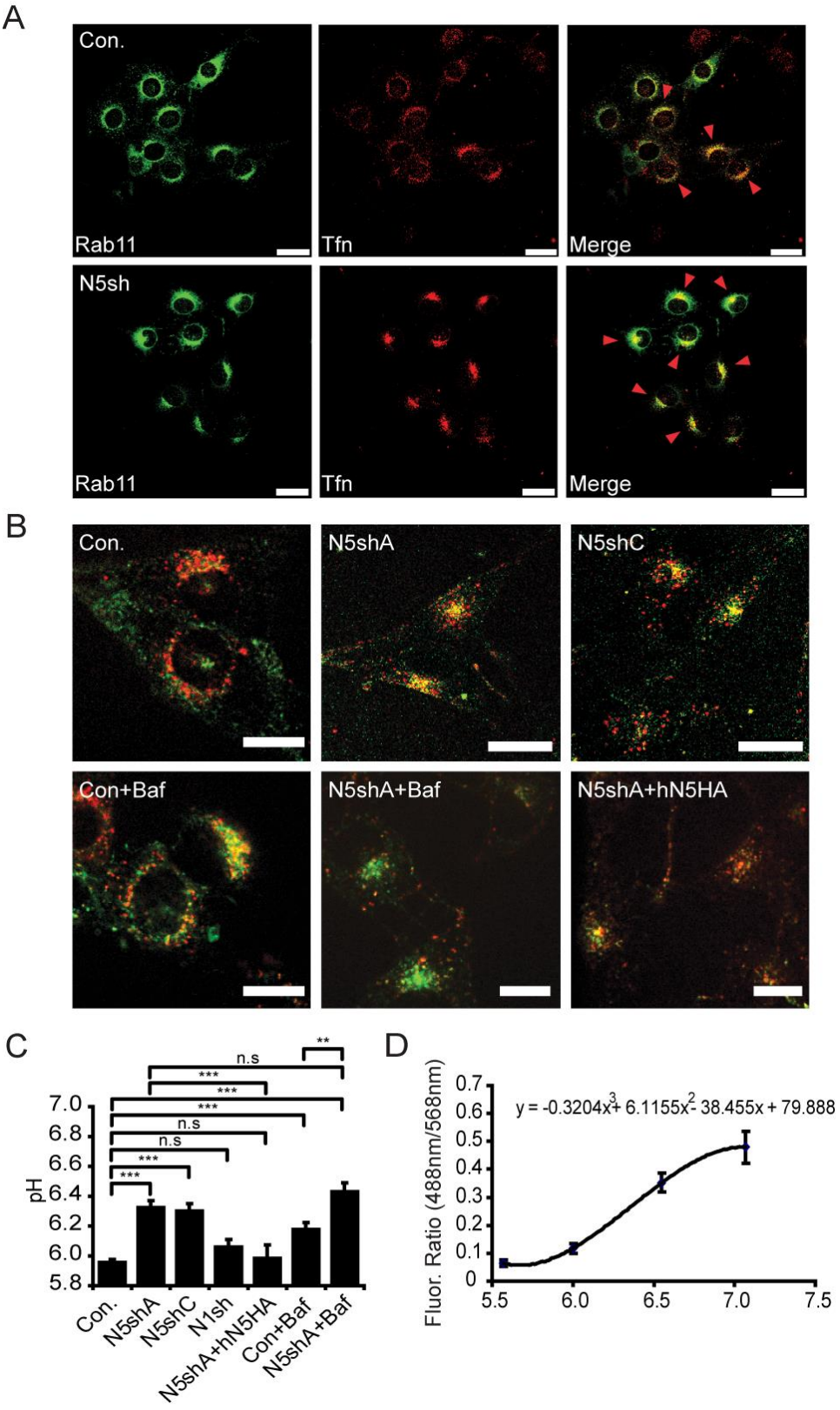
A
Con.
Rab11
Tfn
Merge
N5sh
Rab11
Tfn
Merge
B
Con.
N5shA
N5shC
Con+Baf
N5shA+Baf
N5shA+hN5HA
C
pH
7.0
6.8
6.6
6.4
6.2
6.0
5.8
n.s
**
***
***
***
n.s
n.s
***
***
Con.
N5shA
N5shC
N1sh
N5shA+hN5HA
Con+Baf
N5shA+Baf
D
Fluor. Ratio (488nm/568nm)
y = -0.3204x3 + 6.1155x2 - 38.455x + 79.888
0.7
0.6
0.5
0.4
0.3
0.2
0.1
0
5.5
6.0
6.5
7.0
7.5

(Cont.) Figure 3.3 - NHE5 acidifies recycling endosomes.
(A) Transferrin (Tfn) uptake assay. Overnight serum-starved GFP-Rab11 transfected cells were incubated with Alexa Fluor 568 conjugated Tfn (Tfn-568) at 37°C for 30 min and fixed. Representative confocal images of control and N5sh cells fluorescently labelled for Rab11 (Green) with Tfn (Red) are shown. Red arrow heads point to the endosomal compartments where Rab11 and Tfn colocalize. Bars = 25 µm. **(B)** Endosomal pH measurement of control cells, two stable N5sh clones, stable N1sh clone, stable hN5HA complemented N5sh clone and Bafilomycin A1 (Baf) treated control and N5sh cells. Cells were preloaded with Tfn-Fluorescein and Tfn-568 under conditions described above. For Baf experiments, 200 nM Baf was added during the Tfn labelling step and maintained through out the experiments. Endosomal pHs were extrapolated with a standard curve of Fluorescence ratio by pH (*p<0.05, ***p<0.001, n.s.= not significant, n=5, Student's unpaired t-test). **(C)** Representative confocal images of live cells labelled with Tfn dyes are shown. Bars = 10 µm. (**D**) Standard curve of Fluorescence Ratio by pH. Tfn-dye loaded cells were incubated in high K^+/nigericin solution buffered at pH 5.6, 6.0, 6.55, or 7.07.

3.4 NHE1, but not NHE5, regulates cytosolic pH

Since NHE1 is the predominant NHE on the PM of C6 glioma cells (Fig. 3.1E), I tested whether knockdown of NHE1 affects the cytosolic pH. Using the single excitation, dual-emission pH sensitive dye, SNARF1, cytosolic pH of C6 cells under bicarbonate-free conditions was examined by fluorescence ratiometric analysis. The fluorescence intensities at 650-nm and 580-nm, corresponding to the two pH-sensitive emission peaks of SNARF-1, were background adjusted and presented as ratios. To convert the ratio into pH, a calibration curve was generated by clamping the SNARF-loaded cells at specific pH using high K^+/nigericin technique (Fig 3.4A-B). The steady state cytosolic pH of control and NHE5 KD cells was around 7.45, whereas the intracellular pH of NHE1 KD cells was more acidic (pH~7.35, Fig. 3.4C-D). Furthermore, NHE1 is sensitive (K_i = 1-1.6 μM) to 5-(*N*-ethyl-*N*-isopropyl) amiloride (EIPA) while NHE5 is more resistant (K_i = 21 μM) (Masereel, Pochet et al. 2003). Thus, the treatment of cells with EIPA at 10 μM inhibits NHE1 (Masereel, Pochet et al. 2003), but not NHE5. Indeed, EIPA treatment reduced cytosolic pH of control cells to ~7.3 (Fig. 3.4C-D). This confirmed that NHE1 is an acid extruder on PM that maintains the steady state cytosolic pH at a slightly alkaline range, while NHE5 does not play a prominent role in cytosolic pH regulation in C6 cells.

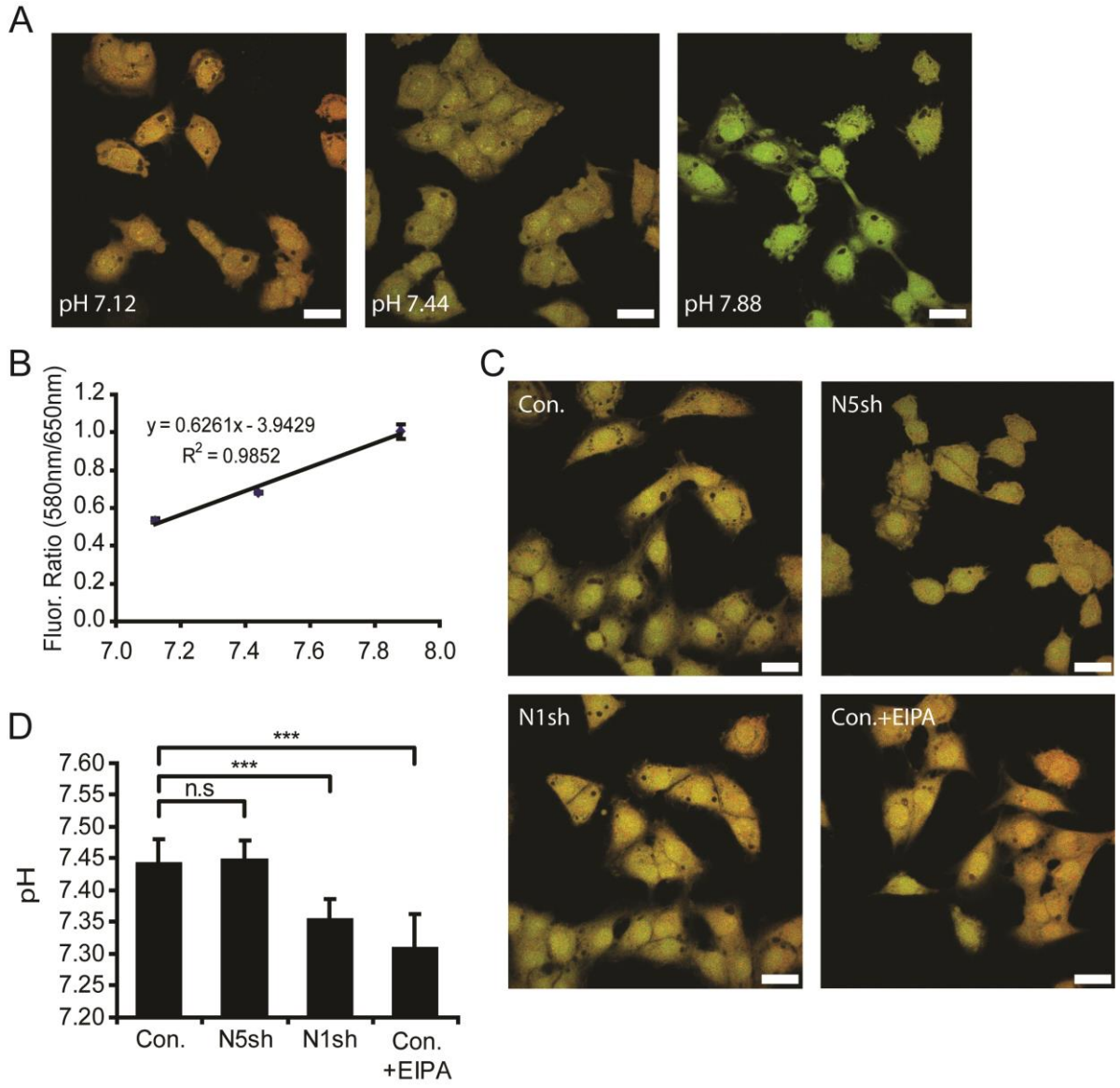

Figure 3.4 - NHE1, but not NHE5, regulates steady state cytosolic pH.
Cells were incubated with 10 μM SNARF for 30 min at 37°C under bicarbonate-free conditions, and then imaged by confocal microscopy (See section 2.6). For 5-(N-Ethyl-N-isopropyl) Amiloride (EIPA) experiments, cells were pre-treated with 10 μM EIPA for 2 h prior to imaging. Cells were clamped at pH 7.12, 7.44, and 7.88 (A), using nigericin/High K^+ technique, to generate a calibration curve (B). (C) Representative confocal images of SNARF-loaded control, N5sh, N1sh, and EIPA-treated control cells are shown. Bars = 25 μm. (D) Steady state cytosolic pH (± SD) of C6 and EIPA-treated cells. Both NHE1 KD and EIPA treated cells exhibit more acidic cytosolic pH, where as NHE5 KD cells were unaffected, implicating that NHE1 is the predominant isoform on the PM (***p<0.001, n.s.= not significant, n=5, Student's paired t-test).

4. Role of NHE5 in RTK targeting and signalling in C6 glioma

Introduction

In a simplistic view, the endocytic circuit consists of 3 components: the endocytosis path, the degradation path, and the recycling path. The endocytic circuit provides cells with the ability to modulate turnover, activity, and distribution of membrane proteins on the PM, which is important for many basic cellular processes. Maintaining endosomal pH homeostasis is crucial to ensure proper function of these compartments. For instance, mildly acidic pH (5.8-6.0) in the early endosome is required for the dissociation of ligands from their receptors and affects the sorting of the cargoes to different compartment thereafter. Increasing acidity from late endosomes to lysosomes is required for activation of lysosomal enzymes and provides optimal environment for protein degradation (Huotari and Helenius 2011). In the classical model, endosomes are responsible for the transport of membrane proteins for degradation or to the PM for further use. However, emerging evidence has challenged this classical view by showing that many important cellular events take place inside endosomes (Sorkin and Von Zastrow 2002; Gould and Lippincott-Schwartz 2009; Scita and Di Fiore 2010). Furthermore, endosomal pH regulators have become increasingly recognized as a modulator of trafficking and endosomal signalling (Dozynkiewicz, Jamieson et al. 2012; Wiedmann, von Schwarzenberg et al. 2012; Diering, Numata et al. 2013; Kondapalli, Hack et al. 2013; Kondapalli, Llongueras et al. 2015). In the previous chapter, I investigated the cellular distribution and transporter activity of NHE5 in rat glioma C6 cells, concluding that NHE5 is a potent endosomal acidifier. Here, I look into the effect of endosomal pH disruption by NHE5 KD on RTK trafficking, signalling, and cell migration.

4.1 Effects of NHE5 knockdown on PI3K-Akt signalling and Ras-Raf-Mek-Erk (MAPK) pathways

In chapter 3, I have shown that depletion of NHE5 alkalinizes recycling endosomes (Fig. 3.2). In contrast, NHE1 plays a limited role in recycling endosomes and is therefore a suitable control to distinguish cellular processes modulated by endosomal pH homeostasis. In light of a series of studies conducted by a former lab member, Dr. Graham Diering, who showed that NHE5 acidifies recycling endosomal pH in PC12 cells and modulates trafficking and signalling of TrkA (Diering, Numata et al. 2013), I decided to test whether RTKs in C6 cells are affected by NHE5. Given the potential role of EGF and HGF in proliferation and motility of glioma (Hu, Shi et al. 2009; Kondapalli, Llongueras et al. 2015), I tested the role of NHE5 in EGFR and HGFR(c-Met) signalling. Binding of growth factors to RTKs activates signalling pathways through a series of steps involving receptor dimerization, autophosphorylation, and recruitment of downstream adaptor/signalling proteins to the phosphorylated docking sites (Lemmon and Schlessinger 2010). Activation of c-Met by HGF increases PI3K and MEK activities, as noted by the increase in T308 and T185/Y187 phosphorylation of Akt and Erk, respectively (Fig 4.1 A-B,D). In control cells, the signals peaked at 15 min and gradually decreased overtime. In contrast, knocking down NHE5 reduced the peak activation of both Erk and Akt (Fig 4.1 D-E), suggesting that NHE5 modulates the c-Met signalling axis.

(Fig. 4.1)

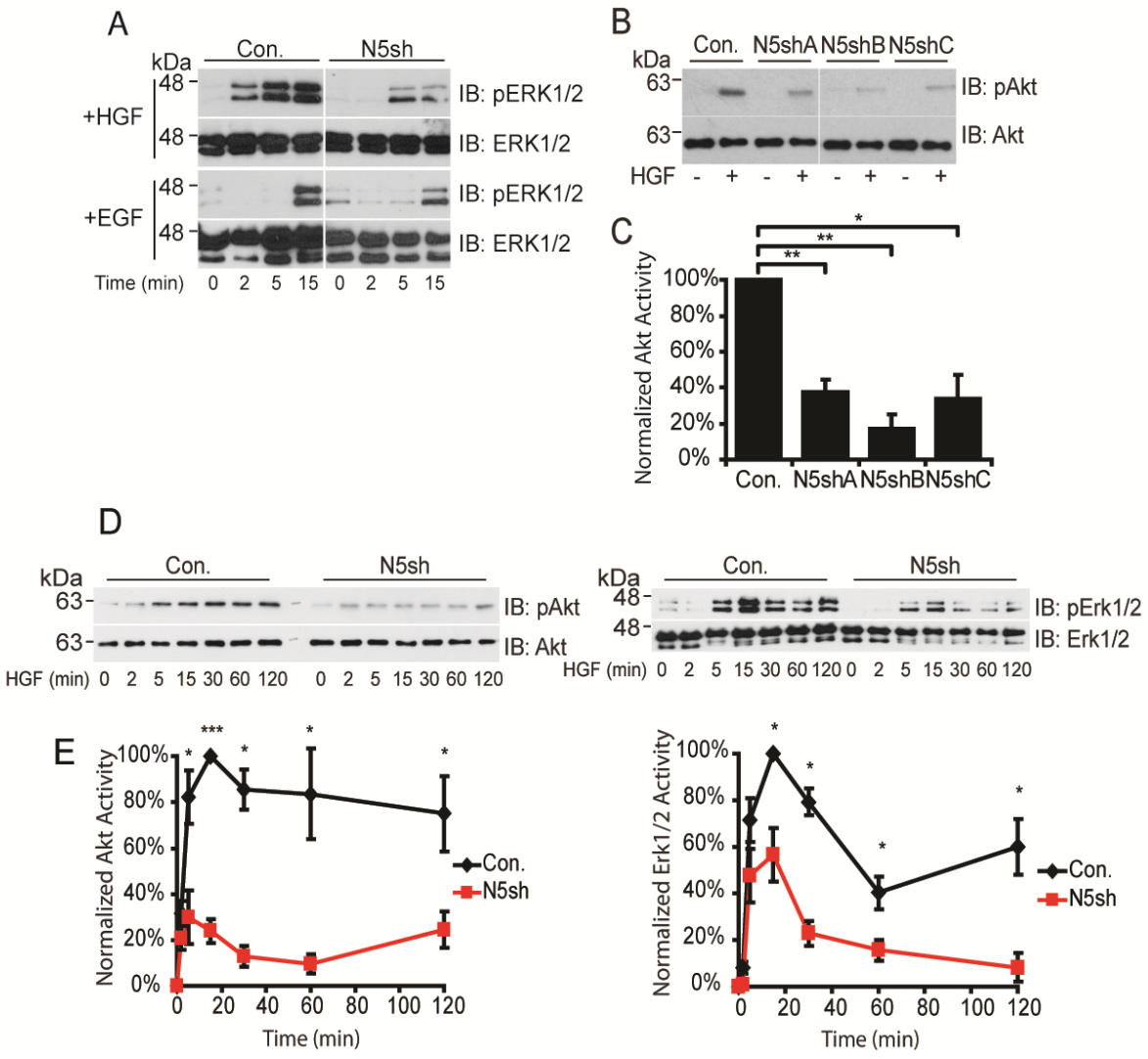
A
kDa
Con.
N5sh
+HGF
+EGF
48
IB: pERK1/2
IB: ERK1/2
Time (min) 0 2 5 15 0 2 5 15
B
Con. N5shA N5shB N5shC
63
IB: pAkt
IB: Akt
HGF - + - + - + - +
C
Normalized Akt Activity
100%
80%
60%
40%
20%
0%
Con. N5shA N5shB N5shC
D
HGF (min) 0 2 5 15 30 60 120 0 2 5 15 30 60 120
IB: pErk1/2
IB: Erk1/2
E
Normalized Akt Activity
Normalized Erk1/2 Activity
Time (min)
Con.
N5sh

(Cont.) Figure 4.1 - Effects of NHE5 knockdown on PI3K-Akt signalling and Ras-Raf-Mek-Erk (MAPK) pathways.

(A) Overnight serum-starved control and N5sh cells were treated with 50 ng/mL EGF or 50 ng/mL HGF for indicated times. Cells were then lysed in 1%NP40 supplemented with 2 mM sodium orthovanadate and protease inhibitor (PI) cocktail. Erk activation (phosphorylation) was determined by immunoblotting using phosphor-Erk1/2 antibody. (B) Serum-starved control and three independent N5sh stable clones were treated with 50 ng/mL HGF for 5 min. Akt phosphorylation was determined by immunoblotting using phospho-Akt antibody. (C) Akt phosphorylation was calculated by densitometric analysis of phosphorylated Akt and total Akt. The values were normalized to controls. The data represent mean activity ± SEM of Akt (*p<0.05, **p<0.01, n=3, Student's paired t-test). (D) Overnight serum-starved control and N5sh cells were incubated with 50 ng/mL HGF for the indicated time. Akt and Erk activation were assessed by immunoblotting as described above. (E) Activation of Akt and Erk were calculated by densitometric analysis of phosphorylated proteins and corresponding total proteins. The values were normalized to the peak values of control (at 15 min) and plotted against time. The data represent mean activity ± SEM of Akt or Erk over time (*p<0.05, ***p<0.001, n=4, Student's paired t-test).

4.2 NHE5 regulates surface expression of c-Met and EGFR

Impaired c-Met activation affecting both PI3K and MAPK as a result of NHE5 deficiency could be the result of altered vesicular trafficking of c-Met. Previous studies have reported the significance of endosomal pH in trafficking of receptors, including Integrin, EGFR, TrkA, and TfR (Presley, Mayor et al. 1997; Dozynkiewicz, Jamieson et al. 2012; Wiedmann, von Schwarzenberg et al. 2012; Diering, Numata et al. 2013). As a proton transporter that resides primarily in recycling endosomes, it is possible that NHE5 plays an important role in modulating recycling of RTKs. To test this hypothesis, I first investigated the surface expression of c-Met and EGFR in C6 cells, which reflects the steady state turnover of the receptors on the plasma membrane. Cell-surface biotinylation experiment showed that NHE5 KD cells have significantly lower c-Met (20% of control) and EGFR (30% of control) on the PM compared to that of control and NHE1KD cells. Interestingly, no difference in surface abundance of Na^+/K^+ ATPase (NKA), a PM resident protein, was observed between NHE5 KD and control cells (Fig. 4.2A-D), implicating that NHE5 may modulate cargo-specific transport. In addition, polarized targeting of c-Met to leading edge during direct migration was also drastically impaired in NHE5 KD cells. Whereas 64% of control and 50% of NHE1 KD were positive for c-Met staining at the leading edge, less than 30% of NHE5 KD cells or Bafilomycin A1 treated cells displayed leading edge translocation of c-Met (Fig. 4.2E-F). Collectively, these results suggest that acidic endosomal pH modulates membrane abundance of c-Met.

(Fig. 4.2)

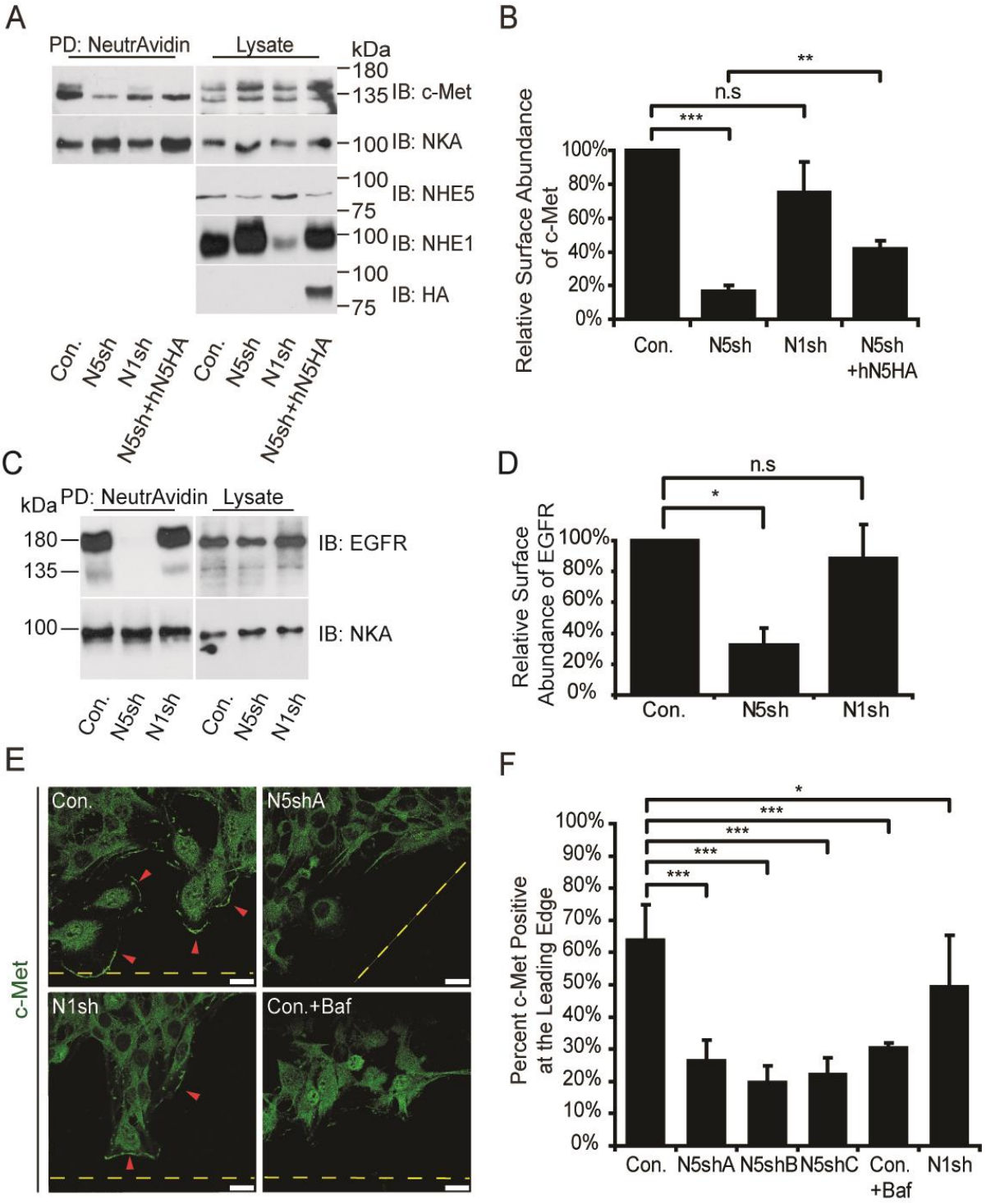
A
PD: NeutrAvidin
Lysate
kDa
180
135
IB: c-Met
100
IB: NKA
100
IB: NHE5
75
100
IB: NHE1
100
75
IB: HA
Con.
N5sh
N1sh
N5sh+hN5HA
Con.
N5sh
N1sh
N5sh+hN5HA
B
Relative Surface Abundance of c-Met
100%
80%
60%
40%
20%
0%
**
n.s
***
Con.
N5sh
N1sh
N5sh +hN5HA
C
kDa
PD: NeutrAvidin
Lysate
180
135
IB: EGFR
100
IB: NKA
Con.
N5sh
N1sh
Con.
N5sh
N1sh
D
Relative Surface Abundance of EGFR
100%
80%
60%
40%
20%
0%
n.s
*
Con.
N5sh
N1sh
E
c-Met
Con.
N5shA
N1sh
Con.+Baf
F
Percent c-Met Positive at the Leading Edge
100%
90%
80%
70%
60%
50%
40%
30%
20%
10%
0%
*
***
***
***
***
Con.
N5shA
N5shB
N5shC
Con. +Baf
N1sh

(Cont.) Figure 4.2 - NHE5 regulates surface expression of c-Met and EGFR.
(A and C) Surface expression of c-Met and EGFR in control, N5sh, N1sh, and hNHE5 complemented N5sh (c-Met only) cells was examined with cell-surface biotinylation experiment. Cells were incubated with biotinylation reagent, quenched with glycine, and lysed. Biotin-labelled proteins were affinity purified with NeutrAvidin beads. Surface expression of c-Met, EGFR, and Na^+/K^+ ATPase (NKA) was detected by immunoblotting. **(B and D)** Surface expression of RTKs was normalized to surface NKA. Data represent mean relative surface expression ± SEM. (**p*<0.05, ***p*<0.01, ****p*<0.001, n=3-5, Student's paired *t*-test). Knockdown of NHE5 reduces surface abundance of c-Met and EGFR. (**E**) Polarized targeting of c-Met was examined by immunofluorescence of migrating N5sh, N1sh, and control cells as described in section 2.14. Where indicated, control cells were incubated with 50 ng/mL of Bafilomycin A1 for 11 h total. Representative high magnification confocal images of control, N5shA, N1sh and Bafilomycin A1-treated control cells are shown. Yellow dotted lines indicate the direction of open wound. Red arrow heads point to the leading edge displaying positive membrane c-Met fluorescence that is discontinuous with the intracellular fluorescence. Bars = 10 µm. (**F**) The data represent means of percentages of cells positive for c-Met (± SD) from three experiments. At least 100 cells of each cell line were scored in each experiment. (**p*<0.05, ****p*<0.001, n=3, Student's paired *t*-test).

4.3 NHE5 regulates recycling of c-Met RTK back to the PM but not internalization

Reduced cell-surface expression of c-Met reflects perturbations in the turnover of the receptor, which could be affected by collective changes in endocytosis, recycling, and/or degradation. To distinguish the role of NHE5 in these processes, I set up cell-surface biotinylation and internalization experiments (see sections 2.8 and 2.9). Using these approaches, I found that the internalization of c-Met between control and NHE5 KD were not significantly different (Fig. 4.3A-B). Next, I tested whether NHE5 increases recycling of c-Met back to the plasma membrane. Significantly higher biotin-c-Met signal after post-incubation cleavage was observed in NHE5 KD cells, suggesting that recycling of c-Met is significantly impaired (39% of control) when NHE5 is depleted. In contrast, recycling of TfR and Integrin β1 were independent of NHE5 (Fig 4.3C-D, F-G). To further examine the pH-dependence in vesicular trafficking, I treated the cell with primaquine, a lysosomotropic amine that interferes with recycling of most of the recycling membrane receptors including transferrin receptors (Hiebsch, Raub et al. 1991; van Weert, Geuze et al. 2000), and tested whether PM targeting of receptors was impaired. First, I showed that primaquine does not interfere with endocytosis of Tfn, as Tfn-dyes still internalized into intracellular puncta in primaquine-treated cells in agreement with previous studies. These compartments were significantly more alkaline and prolonged exposure to the drug causes swelling of intracellular vesicles (Fig. 4.3E). Under this condition, recycling of both c-Met and TfR was significantly reduced to approximately 10% and 47% of non-treated control cells, respectively (Fig. 4.3D-E). Altogether, these results implicate prominent roles of endosomal pH homeostasis in vesicular trafficking and highlight NHE5 as a critical pH regulator that modulates the movement of specific cargoes/compartments.

(Fig. 4.3)

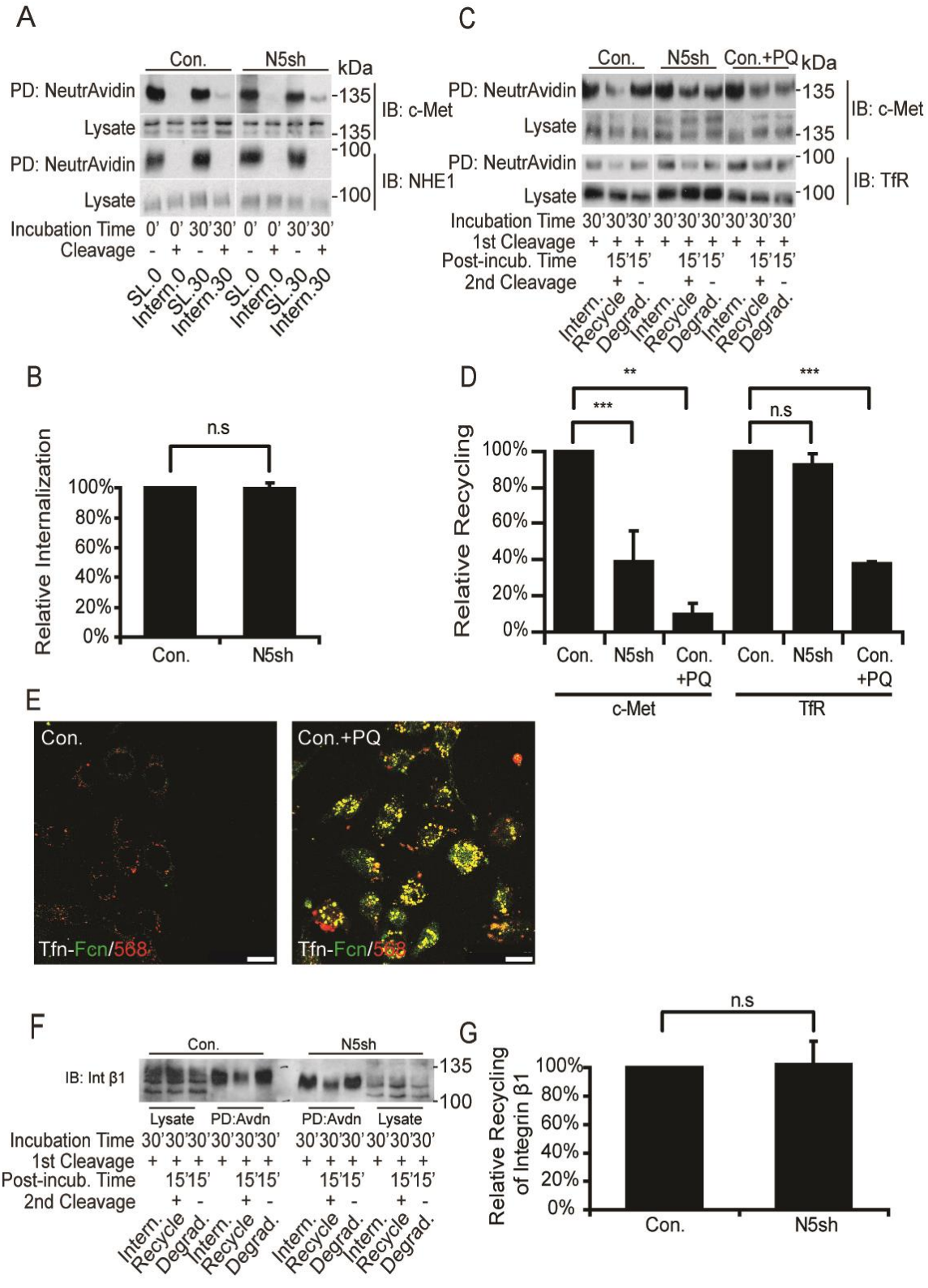
A
Con.
N5sh
kDa
PD: NeutrAvidin
Lysate
IB: c-Met
IB: NHE1
-135
-100
Incubation Time 0' 0' 30'30' 0' 0' 30'30'
Cleavage - + - + - + - +
SL.0
Intern.0
SL.30
Intern.30
C
Con.+PQ
IB: TfR
Incubation Time 30'30'30' 30'30'30' 30'30'30'
1st Cleavage + + + + + + + + +
Post-incub. Time 15'15' 15'15' 15'15'
2nd Cleavage + - + - + -
Intern.
Recycle
Degrad.
B
n.s
Relative Internalization
100%
80%
60%
40%
20%
0%
Con.
N5sh
D
**
***
n.s
Relative Recycling
Con.
N5sh
Con. +PQ
c-Met
TfR
E
Con.
Con.+PQ
Tfn-Fcn/568
F
IB: Int β1
Lysate
PD:Avdn
Incubation Time 30'30'30'30'30'30' 30'30'30'30'30'30'
1st Cleavage + + + + + + + + + + + +
Post-incub. Time 15'15' 15'15' 15'15' 15'15'
2nd Cleavage + - + - + - + -
G
Relative Recycling of Integrin β1

(Cont.) Figure 4.3 - NHE5 regulates recycling of c-Met RTK back to PM but not internalization.

(A) Internalization of c-Met in control and N5sh cells was examined (section 2.9). Semi-confluent cells were labelled with biotinylating reagent, incubated at 37°C with culture media for 0 or 30 min, and then treated with glutathione to remove biotin from un-internalized receptors (Intern.0 and Intern.30). Non-cleaved samples were included to represent total surface labelled protein at indicated time point (SL.0 and SL.30). Biotinylated proteins were affinity purified with NeutrAvidin beads and eluted proteins were analyzed by Immunoblotting with anti-c-Met or NHE1 antibody. For the c-Met experiment, five times more protein from N5sh than control cells was used for Neutravidin pulldown in order to normalize the surface abundance of c-Met between the N5sh and control cells. Four µg of total protein was loaded as input. **(B)** Internalization of c-Met was quantified by densitometry. Relative internalization of c-Met (± SD) is presented as control-normalized internal c-Met relative to total surface c-Met (n.s.= not significant, n=5, Student's paired *t*-test). **(C)** Recycling of c-Met and TfR to PM in control, N5sh, and primaquine (PQ) treated control cells were examined (section 2.9). Surface membrane proteins were labelled and internalized as described in Fig. 4.3A. Cells were then subjected to an additional 15 min of incubation in culture media at 37°C, additional round of glutathione cleavage to remove biotin from recycled receptors. Affinity purified biotinylated proteins were subjected to immunoblotting with anti-c-Met or TfR antibody. Five times more protein from N5sh than control cells was used for pulldown in order to normalize the difference in internalized c-Met. Equal amount of total protein from each cell line was used for the TfR analysis. To block recycling of membrane proteins, cells were treated with 100 µM of primaquine for 4 h prior to biotin labelling and throughout the incubation in culture media. Four µg of total proteins was loaded as input. **(D)** Relative recycling of c-Met and TfR were quantified by densitometry. Recycling of receptors (± SD) is presented as the control-normalized recycled population relative to the internalized pool. (***p*<0.01, ****p*<0.001, n.s=not significant, n=3-5, Student's paired *t*-test). **(E)** Representative confocal images of control and primaquine-treated Tfn-Fluorescein(Fcn)/568 loaded cells are shown. Bars = 20 µm. The increased green fluorescence in the primaquine-treated cells indicates alkalinized endosomal compartments. **(F and G)** Recycling of Integrin β1 in control and N5sh cells was tested and quantified as described above.

4.4 HGF-induced c-Met degradation is enhanced in NHE5-depleted cells

Internalization and subsequent degradation of receptors following HGF-mediated activation is the primary pathway for attenuation of c-Met signalling (Hammond, Urbe et al. 2001; Abella, Peschard et al. 2005; Lefebvre, Ancot et al. 2012). Oncogenic mutations in c-Met have been shown to facilitate escape from degradation and enhanced recycling of the receptor to the PM (Joffre, Barrow et al. 2011). Since NHE5 KD attenuated recycling of c-Met, I next asked if the internalized receptor was degraded. Indeed, loss of the receptor was observed over time after HGF stimulation (Fig. 4.4A). Interestingly, the degree of degradation was significantly higher in NHE5 KD cells. Whereas about 50% of c-Met was still detectable in control, only approximately 10% was observed in NHE5 KD cells after 60 min of HGF treatment. To determine the pathway for ligand-mediated degradation of c-Met, Bafilomycin A1 or MG-132 was used to inhibit lysosomal or proteasomal degradation, respectively. Incubating the cells in MG-132 along with HGF prevented degradation of c-Met, as 90% of c-Met in control and 50% of c-Met in NHE5 KD cells were detectable after 60 min of HGF treatment. In contrast, blocking lysosomal acidification had no apparent inhibitory effect on c-Met degradation (Fig. 4.4B-C). Altogether, these results suggest that NHE5-depletion facilitates receptor down-regulation and that proteasomal degradation plays a more prominent role in HGF-induced degradation of c-Met in C6 cells.

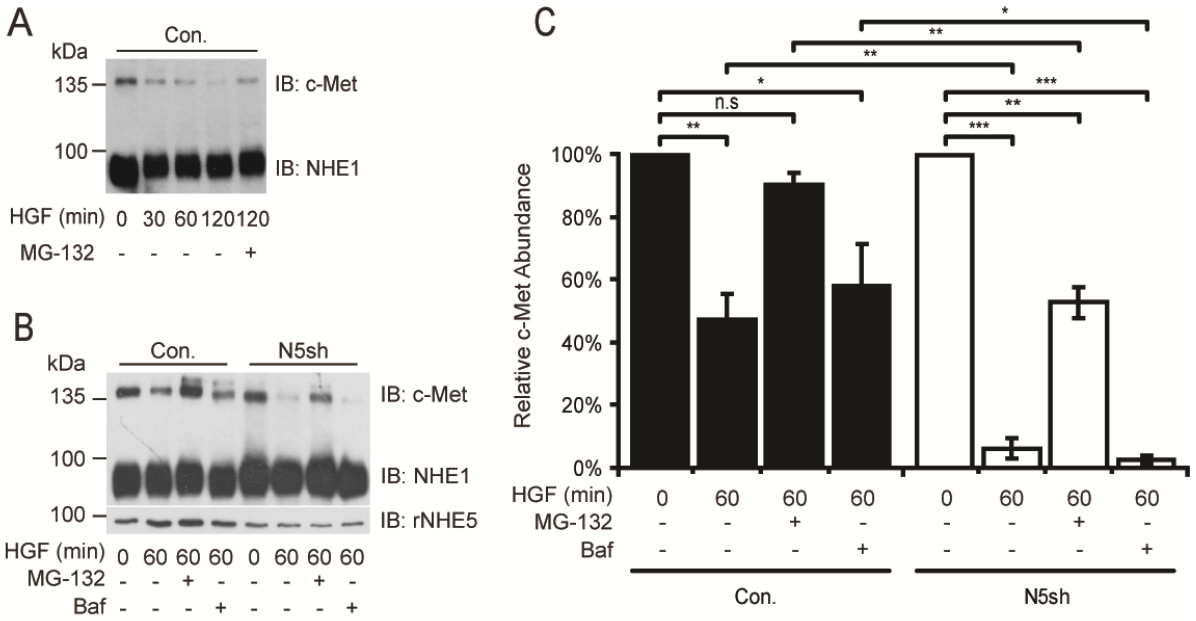

Figure 4.4 - HGF-induced c-Met degradation is enhanced in NHE5-depleted cells. (A) HGF-dependent c-Met degradation in control and N5sh cells was examined by immunoblotting. Overnight-starved control cells were stimulated with 50 ng/mL of HGF in culture media for indicated time and lysed. To inhibit proteasomal degradation, cells were incubated with 20 µM of MG-132 for 4 h. Four µg of total protein was loaded for immunoblotting analysis using anti-c-Met and NHE1 antibodies. (B) HGF-dependent degradation of c-Met for control or N5sh cells at 60 min with degradation inhibitors was examined. Cells were treated with MG-132 or Bafilomycin A1(Baf) for 4 h to inhibit proteasomal or lysosomal degradation, respectively. Three µg of total protein was loaded for immunoblotting and probed with anti-c-Met and NHE1 antibodies. (C) Quantification of c-Met degradation was analyzed by densitometry and expressed as HGF-minus-normalized mean (± SEM) c-Met/NHE1 expression (*p<0.05, **p<0.01, ***p<0.0001, n.s= not significant, n=3, Student's paired t-test).

4.5 NHE5 modulates membrane recruitment and activities of Rho family GTPases, Rac1 and Cdc42

The Rho family GTPases, Rac1 and Cdc42, are downstream signalling molecules of HGF/c-Met (Lemmon and Schlessinger 2010; Gherardi, Birchmeier et al. 2012) and are best known for their roles in modulating cytoskeletal remodelling, cell motility and polarity establishment (Nobes and Hall 1995; Etienne-Manneville 2004). Aberrant activities of Rho family GTPases have been associated with cancer metastasis (Sahai and Marshall 2002; Fortin Ensign, Mathews et al. 2013). The pathological significance of HGF-induced Rac-1 activities in promoting tumour invasion is especially well-recognized (Palamidessi, Frittoli et al. 2008; Hu, Shi et al. 2009; Joffre, Barrow et al. 2011; Menard, Parker et al. 2014). Upon activation, Rho family GTPases are recruited to the PM along with the corresponding Guanine Exchange Factor (GEF), where formation of protein complex with membrane receptors and other adaptor proteins induces local remodeling of the actin cytoskeleton and drives membrane protrusion (Symons 2011). To examine whether membrane targeting of Rho family GTPases is affected by NHE5 knockdown, I performed membrane fractionation experiment (section 2.12) to study membrane association of the Rho family GTPases. Interestingly, more Rac1 was associated with the membrane in control and NHE1 KD than NHE5 KD cells (Fig. 4.5A-B). Next, I looked into the leading edge targeting of Rac1 by immunofluorescence. Similarly, significantly less NHE5 KD cells (<30%) showed positive Rac1 leading edge staining than control (66%) or NHE1 KD cells (57%) (Fig. 4.5C-E). Altogether, these results suggest that NHE5 influences recruitment of Rho family GTPases to the plasma membrane.

Since activation of c-Met and PI3K is attenuated in NHE5 KD cells, activities of downstream targets, Rac1 and Cdc42, could also be affected. Activities of Rac1 and

Cdc42 were determined by affinity purification using Pak-PBD-GST (GST-tagged p21 binding domain of p21 activated kinase 1), which binds to GTP bound Rac1 and Cdc42. The specificity of Rac1 pulldown was tested by treating the cells with Rac GEF inhibitor, NSC23766, which drastically reduced activation of Rac1 (Fig. 4.5E). Next, I showed that activity of Rac1 in control cells is increased after HGF treatment, confirming that Rac1 is indeed downstream of c-Met signalling (Fig. 4.5F). Interestingly, NHE5 KD cells exhibit impaired HGF-mediated activation of Rac1 and significantly reduced steady state activities of Rac1 (~25% of control) and Cdc42 (~42% of control) when compared to the control cells and NHE1 KD cells. When HA-tagged human NHE5 that has unmatched sequence against the shRNA was re-expressed to the NHE KD cells, the reduced Rac1 activity was restored whereas re-expression of an ion-binding deficient mutant did not complement the phenotype (Fig. 4.5G-J).

(Fig. 4.5)

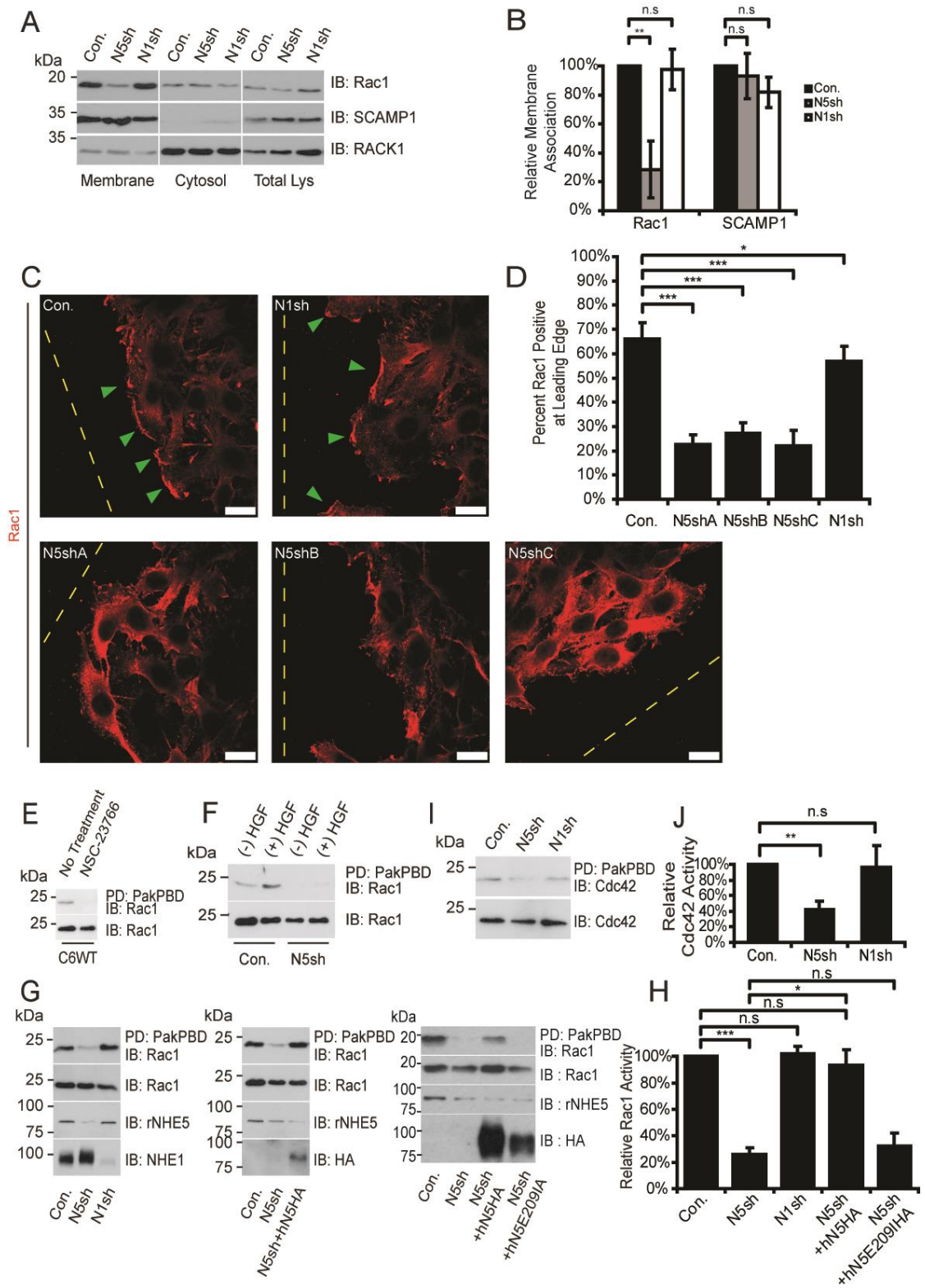
A
kDa
Con.
N5sh
N1sh
IB: Rac1
IB: SCAMP1
IB: RACK1
Membrane
Cytosol
Total Lys
B
Relative Membrane Association
Con.
N5sh
N1sh
Rac1
SCAMP1
C
Con.
N1sh
N5shA
N5shB
N5shC
Rac1
D
Percent Rac1 Positive at Leading Edge
Con.
N5shA
N5shB
N5shC
N1sh
E
No Treatment
NSC-23766
PD: PakPBD
IB: Rac1
C6WT
F
(-) HGF
(+) HGF
Con.
N5sh
I
IB: Cdc42
J
Relative Cdc42 Activity
G
IB: rNHE5
IB: NHE1
IB: HA
N5sh+hN5HA
H
Relative Rac1 Activity
+hN5HA
+hN5E209IA

(Cont.) Figure 4.5 - NHE5 modulates membrane recruitment and activities of Rho family GTPases, Rac1 and Cdc42.

(A) Sub-confluent cells were lysed by physical membrane disruption using 26-gauge syringe. Membrane and cytosol fractions (section 2.12) were analyzed by immunoblotting with anti-Rac1, SCAMP1, or RACK1 antibody. SCAMP1 and RACK1 were used as membrane and cytosol controls, respectively. **(B)** Relative membrane association (± SD) of Rac1 and SCAMP1 was quantified by densitometric analysis (***p*<0.01, n.s= not significant, n=3, Student's paired *t*-test). **(C)** Polarized targeting of Rac1 in control and three independent N5sh clones was examined. Migrating cells were fixed and labelled for Rac1. Cells that displayed Rac1 staining on the leading edge that is discontinuous with cytosolic fluorescence were scored as positive. Representative confocal images from one of the three experiments are shown. The green arrowheads point to positive Rac1 localization at the leading edge. Yellow dotted lines indicate direction of open wound. Bars = 75 μm. **(D)** Mean percentages of cells (± SD) at the leading edge that had positive Rac1 staining are shown (****p*<0.001, n=3, Student's paired *t*-test). **(E-F,G,I)** Rac1 and Cdc42 activities in control, N5sh, N1sh, N5sh+hN5HA, and N5sh+hN5 E209I HA cells were examined by Rho GTPases assay. Sub-confluently grown cells were lysed and equal amounts of protein was incubated with PBD-conjugated beads at 4°C to pulldown Rac1- and Cdc42-GTP. Eluted samples were analyzed by Immunoblotting and probed with anti-Rac1 or Cdc42 antibody. Two μg of protein was loaded as input. For Rac1 inhibitor experiment, cells were pre-treated with 100 μM of NSC-23766 for 24 h prior to PBD pulldown. For HGF stimulation experiment, cells were serum-starved overnight and incubated with 50 ng/mL of HGF for 5 min prior to lysis and PBD pulldown. **(H and J)** Relative GTPase activities (± SEM) were represented by the densitometric ratio of the pulled-down (active form) and total protein, normalized to the level of control (**p*<0.05, ***p*<0.01, ****p*<0.001, n=3, Student's paired *t*-test).

4.6 Cytoskeletal dynamics, cell motility and polarity establishment are impaired in NHE5 KD cells

Activation of Rho GTPases through HGF/c-Met signalling mobilizes cytoskeleton reorganization on the plasma membrane (Bosse, Ehinger et al. 2007; Joffre, Barrow et al. 2011; Menard, Parker et al. 2014). Here, the change in actin dynamics was assessed by the appearance of increased actin staining and mesh-like or spicule structures (here on after termed membrane ruffles), at the cell periphery. To induce membrane ruffles, serum starved cells were incubated with HGF for 30 min, followed by fluorescence staining using Alexa Fluor 647-Phalloidin. In untreated cells, approximately 20% of all cells were observed with membrane ruffles. However, after HGF-stimulation, between 70 to 80% of control, NHE1 KD cells, or hNHE5 complemented NHE5 KD cells were positive for membrane ruffles, whereas only 36% of NHE5 KD cells were observed with membrane ruffles (Fig. 4.6A-B). Similarly, membrane ruffle formation in migrating NHE5 KD cells was reduced compared to control cells (Fig. 4.6C).

Having shown that actin remodelling is impaired in NHE5 KD cells, I next asked whether cell migration is affected by NHE5-depletion. In wound healing assays, scratches were introduced to confluent monolayer of cells to produce wounds of equal size, followed by incubation of 16 h to monitor the rate of wound closure. NHE1 was reported to be an important regulator of cell migration in melanoma cells (Stock and Schwab 2006) and depletion of NHE1 significantly reduced cell motility (~35% wound closure) compare to control (~60%). Interestingly, NHE5 KD cells exhibit more drastically impaired cell migration (~28%) than control. The migration defect in NHE5 KD cells was partially rescued by hNHE5 complementation or over-expression of Rac1 (Fig. 4.6D-E). To test if luminal pH modulates cell migration, Bafilomycin A1 was used as an alternative

approach to disrupt endosomal pH homeostasis. As shown in Fig. 4.6F, Bafilomycin A1 impairs cell migration in a dose-dependent manner, suggesting that cell migration is modulated by endosomal pH. Since knocking down NHE5 hampers PI3K and MAPK signalling and both pathways promote cell proliferation (Seger and Krebs 1995; Vivanco and Sawyers 2002), potential complication due to differential cell growth must be taken into consideration when extended period of incubation (as in wound healing assay) is required. To minimize the effect of proliferation, cell migration was also tested by transwell assays. Significantly less NHE5-deficient (33% of control) cells migrated through the membrane as compared to control cells. It is of note that the effect of NHE5-knockdown is much more significant than that of NHE1-knockdown (79%), and hNHE5-complemented NHE5 KD cells (52%) (Fig. 4.7A-B). These results suggest that NHE5 directly modulates cell migration independent of its effect on cell proliferation and growth.

Cdc42-Par3/6-aPKC complex plays a pivotal role in establishing epithelial cell polarity and activation of Cdc42 is essential for the assembly of this complex (Joberty, Petersen et al. 2000; Lin, Edwards et al. 2000; Etienne-Manneville 2004). Since Cdc42 activity appears to be modulated by NHE5, it follows that polarity establishment could be impaired in NHE5 KD cells. To test this hypothesis, I compared polarity establishing capability between migrating control and NHE5 KD cells. During cell migration, cells establish polarity. Cell polarity is assessed by the relative position of microtubule organizing center (MTOC), which typically resides close to Golgi stacks, to the position of nucleus and the migrating edge ((Bornens 2008), Fig. 4.7C). Here, I determined polarity of migrating cells by immunolabeling the Golgi apparatus and examined its relative position (in relation to the nucleus) in directly migrating cells. Approximately 50% of

control cells showed correct Golgi orientation, while only 32% of NHE5 KD cells were positive for polarity. A moderate but significant rescue was observed by stable expression of hNHE5 in NHE5 KD cells, as noted by 42% of correct Golgi orientation (Fig. 4.7D-E). In agreement to the migration and polarity data, I also observed a drastic effect of NHE5 depletion in impairing integrin-dependent cell adhesion than NHE1 KD or scramble shRNA control cells (Fig. 4.8), which further implicates the potential involvement of NHE5 in early stage of cell adhesion and spreading.

(Fig. 4.6)

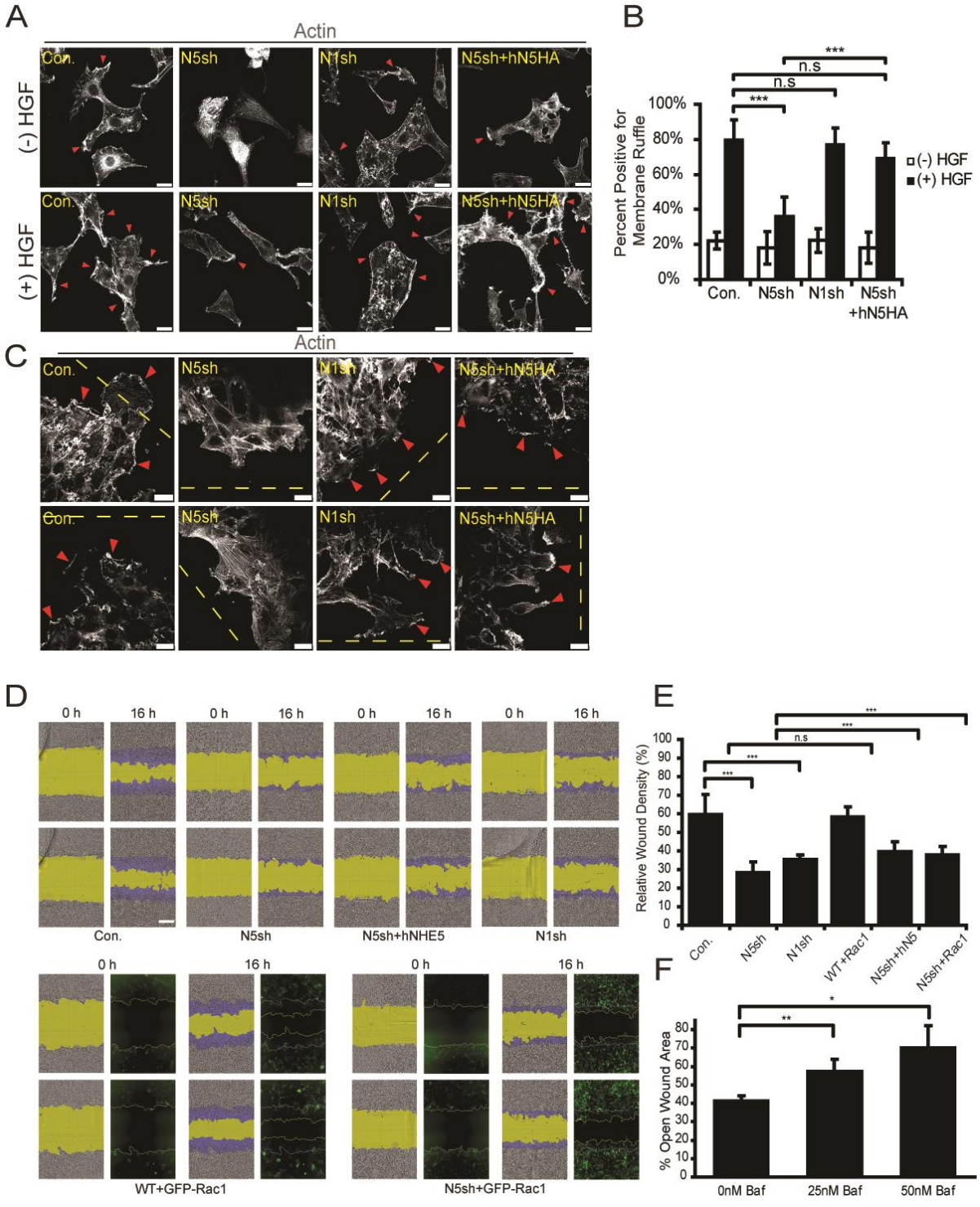
A
Actin
Con.
N5sh
N1sh
N5sh+hN5HA
(-) HGF
(+) HGF
B
Percent Positive for Membrane Ruffle
100%
80%
60%
40%
20%
0%
***
n.s
n.s
***
(-) HGF
(+) HGF
Con.
N5sh
N1sh
N5sh +hN5HA
C
Actin
Con.
N5sh
N1sh
N5sh+hN5HA
D
0 h
16 h
Con.
N5sh
N5sh+hNHE5
N1sh
WT+GFP-Rac1
N5sh+GFP-Rac1
E
Relative Wound Density (%)
Con.
N5sh
N1sh
WT+Rac1
N5sh+hN5
N5sh+Rac1
F
% Open Wound Area
0nM Baf
25nM Baf
50nM Baf

(Cont.) Figure 4.6 - Cytoskeletal dynamics and directed cell migration are impaired in NHE5 KD cells.

(A) HGF-induced change in peripheral actin morphology was examined by fluorescent phalloidin staining. Overnight serum-starved control, N5sh, N1sh, and N5sh+hN5HA cells were kept serum-starved or incubated with 50 ng/mL HGF for 60 min. Cells were then fixed and stained with fluorescent phalloidin to visualize actin structure. Representative images from one of the three sets of experiment are shown. Red arrow heads point to the positive membrane ruffling observed as increased phalloidin staining associated with wave-like protrusions or tiny spicules. Bars = 20 μm. **(B)** Cells were categorized by their patterns of membrane ruffles. Mean percentages of cells positive for membrane ruffling (± SD) are shown (***p<0.001, n=3, Student's paired t-test). **(C)** Directed migration was setup as described in section 2.14. Cells were fixed and stained with fluorescent phalloidin. Yellow dotted lines indicate direction of open wound. Red arrow heads point to membrane ruffle structures. Bars = 25 μm. **(D)** Directed migration of control, N5sh, N5sh+hN5HA, N1sh, and GFP-Rac1 expressing control or N5sh cells were analyzed by wound healing assay using IncuCyte Zoom™ live cell imaging system. Cells were grown into monolayer in 96 wells plate. Cells were scratched with a 96-pin WoundMaker™ tool and incubated at 37°C for 16 h. A program was set up to capture a set of phase-contrast image (and green fluorescence image where applicable) every hour. Relative Wound Density (a function of cell density and open wound area) was analyzed using the manufacturer's preset algorithm. Representative images from one of the three experiments are shown. Yellow shaded area represent open wound. Blue shade is the area migrated. Bar = 300 μm. **(E)** Averages (± SD) of relative wound density after 16 h of incubation are shown (***p<0.001, n=3, Student's paired t-test). **(F)** For V-ATPase inhibition experiment, control cells were treated with Bafilomycin A1 at the indicated concentration for the duration of the experiment. Images were taken at 0 and 16 h after wounding. Wound closures were quantified using TScratch software. Mean percentages of open wound area (± SD) are shown (*p<0.05, **p<0.01, n=3, Student's paired t-test)**.**

(Fig. 4.7)

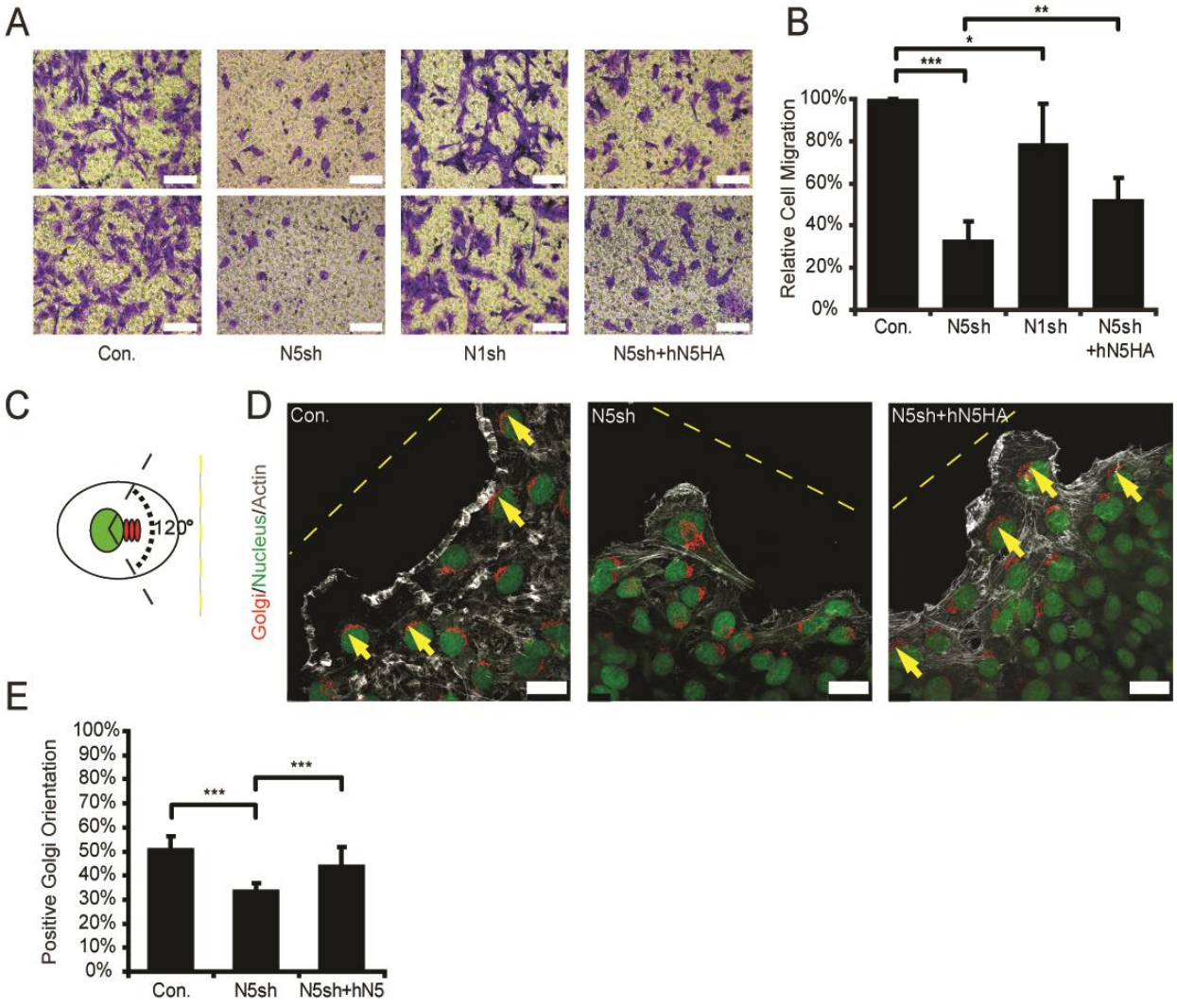
A
Con.
N5sh
N1sh
N5sh+hN5HA
B
Relative Cell Migration
100%
80%
60%
40%
20%
0%
***
*
**
Con.
N5sh
N1sh
N5sh
+hN5HA
C
120°
D
Golgi/Nucleus/Actin
Con.
N5sh
N5sh+hN5HA
E
Positive Golgi Orientation
100%
90%
80%
70%
60%
50%
40%
30%
20%
10%
0%
***
***
Con.
N5sh
N5sh+hN5

(Cont.) Figure 4.7 - NHE5 KD cells exhibit reduced cell motility and loss of cell polarity.

(A) 3D migrations of control, N5sh, N1sh and N5sh+hN5HA cells were analyzed by Transwell® migration assay. Equal numbers of cells were seeded to the upper chamber (serum-free), incubated for 6 h, fixed and stained with crystal violet. The migratory capability towards bottom chamber (20% FBS) were determined by counting the number of migrated cells at the bottom of the membrane. Representative images of crystal violet stained cells post incubation are shown. Bars = 500 μm. (B) The data represent mean percentage of migrated cell (± SEM) relative to control (*p<0.05, ***p<0.001, n=5-8, Student's paired t-test). (C) Polarity establishments of control, N5sh, and N5sh+hN5HA cells were examined by wound healing assay and immunofluorescence. Cells were labelled with a GM130 antibody (Red), DRAQ5 for nucleus (Green), and fluorescent phalloidin for F-actin (Grey). Correct polarity of the cell was defined as the Golgi residing within 120° angle anchored to the center of the nucleus and opens toward open wound. (D) Representative confocal images from one of the three sets of experiment are shown. Yellow dotted lines indicate the direction of open wound. Yellow arrows represent cells that displayed positive Golgi orientation. Bars = 10 μm. (E) Quantification of cells with positive orientation at the leading edge. The data represent mean percentage of positively oriented cells (± SD). Ten to fifteen images per cell type were taken and more than 300 cells were scored in each experiment (***p<0.001, n=3 Student's paired t-test).

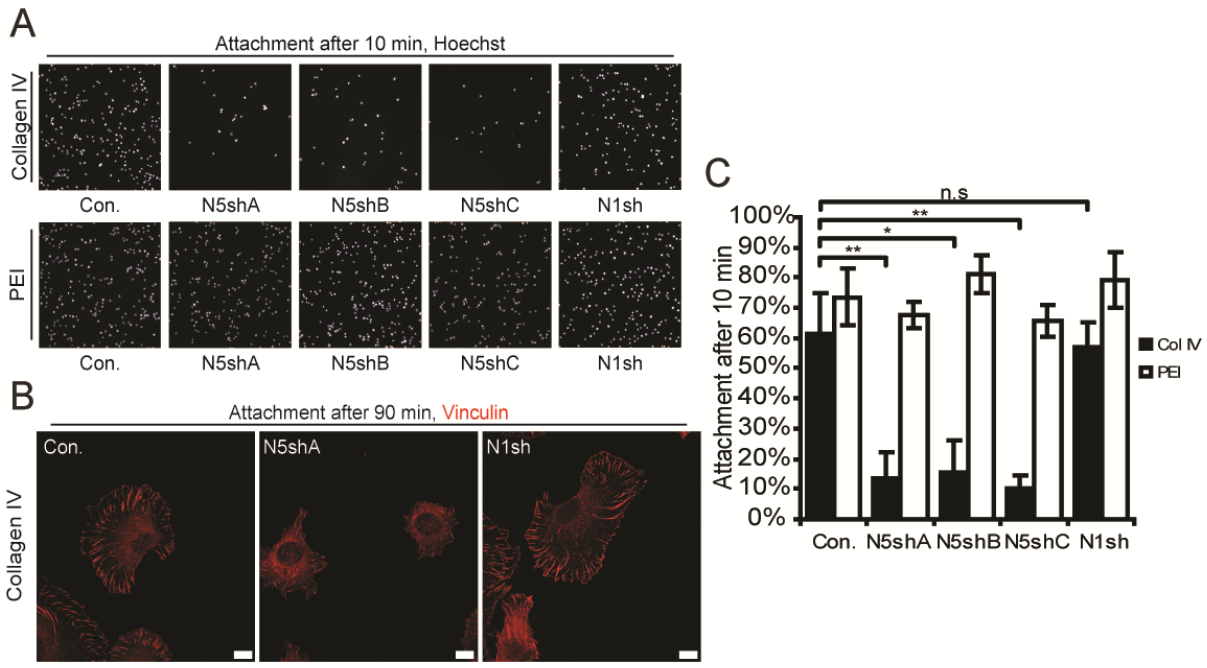

Figure 4.8 – NHE5 knockdown impairs cell spreading.

(A) Attachment of N5sh, N1sh, and control cells onto collagen coated surface was tested. Equal numbers of cells were seeded to collagen IV (Col IV, 0.06 µg/mL) or polyethyleneimine (PEI, 25 mM) coated 96-well plate. Cell attachment was terminated at 10 min and 90 min (end point) by removing the media. The wells were gently washed with PBS to remove non-adherent cells and fixed with 3% PFA-PBS supplemented with 500ng/mL. Quantification was done using Cellomics Arrayscan VTI high content screening system (Thermo Fischer Scientific) with protocol provided by the manufacturer. Representative images (nucleus only) of cell attachment at 10 min in Col IV- or PEI-coated plate are shown. **(B)** High resolution images of cells after 90 min of attachment on Col IV coated surface, with vinculin labelled in red. Note that NHE5 KD cells typically exhibit more disoriented spreading and smaller focal adhesion compared to control and NHE1 KD cells. Bars = 10 µm **(C)** Percentage of cells attachment after 10 min was calculated by normalizing the number of cells at 10 min to that of 90 min. (*p<0.05, **p<0.01, n.s=not significant).

5. Discussion

5.1 Endosomal pH and NHE5

Characterization of ion transporters in recent years has shed light on the understanding of endocytic networks and its regulatory role in cellular processes. Maintenance of intracellular pH has been implicated in processes such as endosome trafficking (Johnson, Dunn et al. 1993; Mohammad-Panah, Harrison et al. 2003; Orlowski and Grinstein 2007), signalling (Harrington, St Hillaire et al. 2011; Wiedmann, von Schwarzenberg et al. 2012; Diering, Numata et al. 2013), cell adhesion and migration (Onishi, Lin et al. 2007; Koivusalo, Welch et al. 2010; Magalhaes, Larson et al. 2011; Choi, Webb et al. 2013). It had been reported that elevated expression of luminal pH mediators, including V-ATPase, CLICs, and organellar NHEs, specifically NHE7 and NHE9, have implication in oncogenicity (Dozynkiewicz, Jamieson et al. 2012; Onishi, Lin et al. 2012; Wiedmann, von Schwarzenberg et al. 2012; Kondapalli, Llongueras et al. 2015). In this study, I investigated the pathological consequence of NHE5 up-regulation in C6 glioma cell line. I first showed NHE5 expression in C6 cells while NHE5 protein was barely detectable in hippocampal astrocyte obtained from post natal day 1 Sprague Dawley rat (Fig. 3.1A). The absence of NHE5 protein in cultured rat astrocytes is in agreement with the previous immunocytochemical studies suggesting the absence of NHE5-mRNA (Attaphitaya, Park et al. 1999; Baird, Orlowski et al. 1999) in glia-rich brain regions. It is tempting to hypothesize that NHE5 is upregulated in glioma, a possibility that requires future experiments.

Immunofluorescence analysis revealed that NHE5 is localized to a portion of

perinuclear endosomes positive for TfR or Rab11, but not with EEA1-positive endosomes. This is in agreement with the result observed in PC12, primary culture neuron, and heterologous over-expression system (Onishi, Lin et al. 2007; Diering, Church et al. 2009; Diering, Mills et al. 2011; Diering, Numata et al. 2013; Jinadasa, Szabo et al. 2014). In all cases, NHE5 exhibits partial co-localization with recycling endosomal markers, of which the highest degree of overlapping was observed with ADP-ribosylation factor 6 (ARF6)-positive endosomes in which Secretory carrier-associated membrane protein-2 (SCAMP2) is also present. Binding between NHE5 c-terminus and SCAMP2 is required for Arf6-mediated surface targeting of NHE5 (Diering, Church et al. 2009). In addition, interactions between NHE5 and receptor for activated C-kinase 1 (RACK1) facilitate NHE5-activity on the PM and potentially regulates integrin signalling and focal adhesion dynamics (Onishi, Lin et al. 2007). However, I was unable to detect membrane association upon serum stimulation (Fig. 3.1E), suggesting that NHE5 in C6 cells may have different recycling kinetics from that of neurons.

Given its intracellular localization and the ion specificity of NHE5 for Na^+, I postulate that NHE5 acidifies recycling compartments in C6 glioma. I showed that knockdown of NHE5 by expressing sequence specific shRNAs that reduced NHE5 expression by 50% alkalinizes pH of Tfn-positive recycling endosomes. As a control, increase in endosomal pH was also observed when V-ATPase was inhibited in control cells. Consistent with previous finding, disruption of endosomal pH accumulates Tfn to perinuclear endosomes, with minimal diffused vesicles in the periphery ((Johnson, Dunn et al. 1993), Fig. 3.3A, Fig. S2). It is important to note that while generating the human NHE5 complementation

clone, high NHE5 expression appears to be toxic to the cells. It is possible that excess NHE5 dysregulates endosomal pH homeostasis leading to cell death. This implies that maintaining endosomal pH at a narrow physiological range is crucial for the cells.

5.2 Physiological significance of organellar NHEs and endosomal pH

Members of the NHE family have been reported to play critical roles in vesicular pH regulation and loss of functions or dysregulation have been associated with various diseases. For example, the CNO-NHEs (NHE6-9) are ubiquitously expressed and function as endosomal/vesicular alkalinizer by catalyzing K^+/H^+ exchange. Loss of function mutations for NHE6 and NHE9 had been correlated to a variety of neurological disorders, including autism, attention deficient hyperactivity disorder, X-linked intellectual disability, and epilepsy (Kondapalli, Prasad et al. 2014). Expression of wild type NHE9, but not autism related mutants (L236S, S438P, and V176I) significantly alkalinizes endosomal pH. Increased activity of NHE9 stabilizes surface expression of TfR, GLAST, and increases Tfn and Glutamate uptake. Therefore, NHE9 appears to play important roles in modulating synaptic abundance of receptors required for neurotransmitter clearance (Kondapalli, Hack et al. 2013). Point mutations in NHE6 cause Christianson syndrome, an Angelman-like X-linked intellectual disability (Gilfillan, Selmer et al. 2008; Stromme, Dobrenis et al. 2011) whereas NHE6 knockout mice exhibit cerebellar atrophy (Stromme, Dobrenis et al. 2011). Endosomal alkalinization by NHE6 over-expression had been shown to affect clathrin-mediated endocytosis (CME), vesicular trafficking, and distribution of membrane lipids in various cells (Muro, Mateescu et al. 2006; Ohgaki, van et al. 2011; Xinhan, Matsushita et al. 2011). In addition, NHE7 over-expression in MDA-MB-231 cells facilitates cell adhesion, invasion, and anchorage-independent

growth (Onishi, Lin et al. 2012). More recently, Kondapalli and colleagues reported that NHE9 affects endo-lysosoaml pH and high expression of NHE9 is associated with poor prognosis in glioblastoma and resistance to chemotherapy.

The biological significance of NHE5 had been reported in several studies. In synapses, NMDA receptor activation recruits NHE5 to the dendritic spine, where acute acidification of synaptic cleft results in negative feedback inhibition of NMDA receptors and modulates synaptic plasticity (Diering, Church et al. 2009). In NHE5-expressing transporter-null CHO cells (AP-1), recruitment of NHE5 to the PM through RACK1 and integrin interaction enhances cell adhesion and spreading in a transporter activity-dependent manner (Onishi, Lin et al. 2007). NHE5 was also identified as an endosomal acidifier in neuroendocrine PC12 cells, in which membrane translocation is absent. In PC12 cells, NHE5 functions in maintenance of endosomal pH and facilitates PM targeting and signalling of TrkA (Diering, Numata et al. 2013). NHE5 depletion was shown to inhibit surface targeting of TrkA, NGF-mediated activation of MAPK and PI3K signalling pathways, and neurite extensions in PC12 or primary cortical neurons. These suggest that endosomal pH plays a critical role in neuritogenesis. Evidence of this includes work done by Harrington and co-workers that demonstrated luminal pH homeostasis is critical for spatially restricted ligand-specific TrkA signalling. In this study, the authors showed that acidic endosomal pH is required to differentiate between NT3- or NGF-TrkA signalling. The latter forms an interaction that is stable in the acidic endosomes and facilitates maturation of TrkA endosome. Mature NGF/TrkA “signosomes” are retrograde trafficking competent and support survival of the sympathetic neurons. In this module, endosomal pH plays a vital role in differential

activation for NGF-mediated long distance retrograde survival signalling or NT3 mediated intermediate axonal growth signalling, which contributes to neural plasticity.

5.3 NHE5 regulates surface availability of RTKs

Examination of two commonly studied RTKs in C6 cells, EGFR and c-Met with corresponding ligands revealed defects in ligand-mediated activation of MAPK and PI3K pathways in NHE5-depleted cells (Fig. 4.1). While EGF experiments also exhibit some difference, the degree of variation was not as drastic as that of HGF. Thus, I decided to focus on c-Met signalling for the most part of this study. It is important to note that many of the trafficking phenotypes observed for c-Met are likely conserved for EGFR as several tested phenotypes were paralleled.

Since NHE5 is functionally active in recycling endosomes and was previously shown to regulate membrane targeting of TrkA in PC12 (Diering, Numata et al. 2013), I postulate that NHE5 regulates trafficking of c-Met in C6 cells through an endosomal pH-dependent mechanism. I showed that alkalinization of recycling endosomal pH by genetic knockdown of NHE5 and Bafilomycin A1 treatment reduces surface abundance and polarized targeting of c-Met and EGFR, but not that of PM-resident proteins such as NKA or NHE1 (Fig. 4.2). Further biochemical analysis revealed that the rate of c-Met endocytosis is independent of NHE5 (Fig. 4.3A-B). However, recycling of c-Met to the PM is significantly reduced by NHE5-depletion, suggesting that homeostasis of endosomal pH is crucial for efficient PM targeting of c-Met (Fig. 4.3C-D). This is consistent with previous studies which reported endosomal pH perturbation by genetic knockdown or chemical inhibition of pH-regulator blocked retrograde PM targeting of

membrane receptors (Johnson, Dunn et al. 1993; Presley, Mayor et al. 1997; Dozynkiewicz, Jamieson et al. 2012; Diering, Numata et al. 2013). For instance, Wiedmann and co-workers had shown that chemical inhibition of V-ATPase or genetic knockdown of V_0 subunit in breast cancer cell line impaired translocation of EGFR to the lamellopodia of migrating cells, thereby prevented localized RTK signalling and effectively reduced cell migration and tumour metastasis both *in vitro* and *in vivo* (Wiedmann, von Schwarzenberg et al. 2012).

The vast majority of the activated RTKs are targeted to degradation within hours, allowing attenuation of signalling in a regulated manner. Integrins and TfR are mostly recycled and typically exhibit much lower turnover than most activated RTKs (Caswell, Vadrevu et al. 2009; Goh and Sorkin 2013). In scrambled shRNA control cells where expression of NHE5 is unaltered, a significant portion (60%) of internalized c-Met is recycled back to the PM (Fig. 4.3C-D). In contrast, NHE5-depleted cells showed significantly reduced membrane targeting of c-Met. Interestingly, no difference in the recycling of integrin β1 or TfR was observed (Fig. 4.3C-D, F-G). Previous studies have demonstrated that Integrin β1 can be recycled to the PM by various routes, including Rab11-, Rab21-, Rab25-, and, Rab4-dependent pathways (Caswell, Vadrevu et al. 2009; Bridgewater, Norman et al. 2012). Multiple accessory proteins regulate the recycling of integrins in distinct pathways (Ivaska, Vuoriluoto et al. 2005; Tayeb, Skalski et al. 2005; Pellinen and Ivaska 2006; Caswell, Spence et al. 2007; Jovic, Naslavsky et al. 2007; Pellinen, Tuomi et al. 2008; Caswell, Vadrevu et al. 2009; Bridgewater, Norman et al. 2012). For instance, recycling of integrin through Rab11 pathway is dependent on Akt-mediated inactivation of Glycogen Synthase Kinase 3 beta (GSK3β),

phosphorylation of ArfGAP with coiled-coil, ankyrin repeat and PH domains 1 (ACAP1), and Protein Kinase C-eta (PKCε) mediated phosphorylation of vimentin to release Integrin-containing vesicles from perinuclear compartment (Roberts, Woods et al. 2004; Ivaska, Vuoriluoto et al. 2005; Li, Ballif et al. 2005; Bridgewater, Norman et al. 2012). Intriguingly, Akt and PKCε activities are dispensable for the recycling of TfR, which also takes place in Rab11 endosomes (Bridgewater, Norman et al. 2012). This implicates that additional cargo-specific parameter(s) is involved in differentially modulated recycling of membrane receptors. Since recycling of integrin β1 and TfR follow multiple pathways (Maxfield and McGraw 2004; Grant and Donaldson 2009), it is possible that the pH-insensitive recycling routes may compensate the pH-sensitive recycling when endosomal pH is disturbed.

Recycling of c-Met faithfully follows the fast Rab4-dependent recycling and slow Arf6-dependent recycling pathways (Grant and Donaldson 2009; Hellberg, Schmees et al. 2009; Parachoniak, Luo et al. 2011; Goh and Sorkin 2013). Lakadamyali and co-workers showed that Tfn and RTK ligands were incorporated into distinct endosomes upon internalization and led to different outcomes (Lakadamyali, Rust et al. 2006), EGF and LDL were preferentially sorted into dynamic, nocodazole-sensitive early endosomes (DEEs) that rapidly acquired Rab7 (Rab5 and Rab7 positive). DEEs then matured and the cargoes of this compartment were mostly degraded. In contrast, Tfn was non-selectively incorporated into DEEs, and static, Rab5 and EEA1 positive early endosomes (SEEs). Due to faster maturing kinetics of DEEs, global distribution of Tfn appeared to be predominantly accumulated in SEEs. SEEs acquired Rab11 and recycled cargoes back to the PM. Interestingly, Tfn that entered DEEs also undergo

recycling, as the authors observed association of Tfn in peripheral tubular extensions in DEEs, implicating that recycling pathways exist in both SEEs and DEEs. It is tempting to investigate whether HGF/c-Met is also sorted to DEE and whether the recycling of this compartment is pH-regulated. Future studies focussed on ”Rabs-fingerprinting” of NHE5-positive endosomes could provide insights in identifying specific compartments that modulate RTKs recycling through pH-dependent mechanism(s).

In spite of the marked reduction of surface abundance of EGFR in NHE5 KD cells (Fig. 4.2C-D), the degree of signal activation by EGF in NHE5 KD and control cells was marginal (Fig. 4.1A). Although the precise mechanism is currently unknown, I postulate that EGF may not be sufficient to stimulate persistent EGFR signalling in C6 cells as the activation of Erk in control by EGF is both delayed and decreased in amplitude comparing to HGF stimulation. There are 7 known ligands for EGFR, including EGF, TGFα, amphiregulin, heparin binding EGF (HB-EGF), betacellulin, epiregulin, and epigen (Harris, Chung et al. 2003). Both TGFα and EGF expressions positively correlate with glioma grade (Tang, Steck et al. 1997). EGF and TGFα differ in the binding affinity to EGFR (Ebner and Derynck 1991). Stable EGF association to EGFR in endosomes enhances ubiquitination of the receptor and promote degradation, while labile interaction in TGFα-EGFR reroutes the receptor to recycling endosomes (Ebner and Derynck 1991; Longva, Blystad et al. 2002; Roepstorff, Grandal et al. 2009). Similar ligand-mediated down-regulation of c-Met had also been shown to occur through the same pathway. It had been reported that ligand-mediated ubiquitination of c-Met through c-Cbl is required for phosphorylation of Hrs at the endosomes and subsequent targeting of the ubiquitinated receptor to lysosomal degradation (Taher, Tjin et al. 2002; Abella, Peschard

et al. 2005). In this study, Abella and co-workers showed that a point mutation to the tyrosine 1004 abolishes HGF-dependent interaction between c-Cbl-TKB (tyrosine kinase binding domain) and c-Met, resulted in reduced receptor aberration and sustained signalling (Abella, Peschard et al. 2005). In addition, the proteasomes also play an important regulatory role in cellular expression of c-Met (Jeffers, Taylor et al. 1997; Hammond, Urbe et al. 2001; Abella, Peschard et al. 2005; Lefebvre, Ancot et al. 2012). The proteasomal degradation of c-Met is ligand-independent and this pathway is primarily involved in modulating c-Met turnover. Furthermore, Tulasne and colleagues demonstrated that proteasomal degradation of c-Met can occur under stressed condition in which cysteine-dependent aspartate-directed proteases (caspases) are activated (Tulasne, Deheuninck et al. 2004). It had been reported that Leucine-rich Repeat and Immunoglobulin-like domains protein (LRIG1) negatively regulates c-Met and EGFR in ligand- and Cbl-independent manners (Laederich, Funes-Duran et al. 2004; Shattuck, Miller et al. 2007). A more recent study revealed that the LRIG-mediated c-Met degradation is modulated by ubiquitin specific protease 8 (USP8) (Oh, Lee et al. 2014). Disrupting the interaction between USP8 and LRIG1 prevents deubiquitination of LRIG1 and the subsequent formation of LRIG1/c-Met complex, which is targeted to lysosome for degradation. Implications of USP8 in trafficking and stability of other RTKs had also been reported (Berlin, Schwartz et al. 2010; Byun, Lee et al. 2013; Reincke, Sbiera et al. 2015). For instance, loss of USP8 was shown to promote hyper-ubiquitination of EGFR and facilitate receptor degradation in Hrs-dependent manner (Berlin, Schwartz et al. 2010). However, the role of USP8 in RTKs degradation remains controversial as there are also studies that indicated USP8 (and deubiquitination of the receptors) promotes RTKs degradation (Row, Prior et al. 2006; Alwan and van Leeuwen 2007). It is possible

that the regulatory roles of USP8 on RTKs degradation is context dependent, where additional factors (such as LRIG1) can contribute to the opposite effect. Whereas USP8 can potentially promote degradation of selected RTKs, another endosomal deubiquitinase, AMSH (associated molecule with the Src homology 3 domain of signal transducing adaptor molecules) had been shown to promote recycling of the receptors through removal of the ubiquitin added by c-Cbl (McCullough, Clague et al. 2004). Interestingly, I found that HGF-induced c-Met degradation is facilitated by NHE5 depletion, implicating the pH-dependence in degradation of c-Met. In addition, c-Met degradation was partly inhibited by proteasomal inhibitor, but was unaltered by lysosomal block (Fig. 4.4B-C), suggesting that proteasomal degradation plays a dominant role in NHE5-regulated c-Met down-regulation. One possible interpretation is that NHE5 is involved in sorting of c-Met away from lysosomal degradation by facilitating receptor-ligand dissociation through luminal acidification. This reduces ubiquitination of the receptors and prevents lysosomal targeting. Under this scenario, it is possible that Bafilomycin A1 treatment increases cellular stress and activates alternative protease pathway (Nakashima, Hiraku et al. 2003), thus failing to protect c-Met from degradation. In contrast, proteasomal inhibition prevents the c-Met down-regulation by directly blocking proteasomal activity, lysosomal targeting (Abella, Peschard et al. 2005), and promoting recycling of c-Met (Hammond, Carter et al. 2003). It is important to note that the effect of MG-132 on c-Met stability in NHE5-depleted cells was partial, implicating an alternative NHE5-dependent degradation pathway(s) is yet to be determined.

To validate that endosomal pH modulates membrane protein recycling, I showed that endosomal alkalinization by primaquine blocks recycling of c-Met and TfR (Fig.

4.3E). This is consistent with previous findings that reported disruption of endosomal pH by V-ATPase inhibition, ionophores, or lysosomotrophic amines treatment impaired recycling of membrane receptors (Basu, Goldstein et al. 1981; Schwartz, Bolognesi et al. 1984; Johnson, Dunn et al. 1993; Presley, Mayor et al. 1997). Endosomal alkalinization was shown to induce structural change of the cytoplasmic β-turn motif (NPVY for LDLR or YTRF for TfR) and modulates interaction of cytoplasmic adaptors with recycling receptors (Basu, Goldstein et al. 1981; Presley, Mayor et al. 1997). A closely related NPXY motif is present in RTKs, including EGFR, TrkA, and c-Met, though the interaction of this motif with Shc primarily modulates RAS-MAPK signalling and is dispensable for the recycling of the RTKs (Pelicci, Giordano et al. 1995; Bolanos-Garcia 2005; Chen, Ieraci et al. 2005; Organ and Tsao 2011). It is likely that additional factor(s) besides targeting motif is responsible for the difference in vesicular trafficking between TfR and RTKs. Given the current data, it is possible that the presence of NHE5 in C6 cells provides an alternative pH-mediated pathway for the RTKs to escape the degradative fate and favours recycling of the receptors.

A previous study had shown that C6 cells secrete higher level of HGF, VEGF, and PGE2 than normal astrocytes do, thereby facilitating invasion of neural stem cells and brain microvascular endothelial cells across blood brain barrier (Diaz-Coranguez, Segovia et al. 2013). Increased secretion of HGF and surface availability of c-Met can function in parallel to promote sustained autocrine signalling, a hallmark for tumourigenesis.

5.4 NHE5 modulates Rho GTPases, Rac1 and Cdc42, activities

RTKs signalling activates subsets of signalling molecules, including MAPK, PI3K, Akt, and the cytoskeletal regulatory protein, Rho family GTPases (Lemmon and Schlessinger, 2010). Rho GTPases, Rac1 and Cdc42, are well-recognized effectors of HGF/c-Met that regulate cytoskeletal dynamics and the cell polarity establishment. Endocytic trafficking of RTKs, including c-Met and EGFR, had been implicated in spatial activation of Rac-1 (Joffre, Barrow et al. 2011; Wiedmann, von Schwarzenberg et al. 2012). Activated Rac1 and Cdc42 along with other actin-associated proteins induce formation of membrane ruffles, lamellipodia and fillopodia, which are F-actin-enriched structures located at the leading edge of migratory cells (Nobes and Hall 1995; Buchsbaum 2007). In actively migrating cells, Rac1 and Cdc42 are upregulated and their activities are regulated by GEFs, GTPase activating proteins (GAPs), and guanosine nucleotide dissociation inhibitors (GDIs). Deregulated activities of Rac1 and Cdc42 had been implicated in various tumours (Radu, Semenova et al. 2014). In C6 cells, Rac1 was activated by HGF/c-Met (Fig. 4.5E). This activity was significantly reduced by NHE5 depletion (Fig. 4.5F-G), consistent with the notion that disrupted endocytic trafficking of c-Met attenuates Rac1 signalling (Joffre, Barrow et al. 2011; Gherardi, Birchmeier et al. 2012). Peripheral membrane ruffle formation was also evident in control but not in NHE5 KD cells (Fig 4.6A-C). Coincidently, Cdc42 activity was similarly reduced in NHE5 KD cells (Fig. 4.5H-I). In addition to its role in modulating actin dynamics, Cdc42 is also known to regulate Par3/Par6/aPKC polarity complex formation and activation (Lin, Edwards et al. 2000; Etienne-Manneville 2004). Attenuated Cdc42 activity suggested the defect in polarity establishing capability, which was observed under unidirectional

migration (Fig 4.7D-E). In addition, recruitment of Rac1 to the PM was impaired in NHE5-deficient cells, as evident by reduced membrane association and localization to the leading edge (Fig. 4.5A-C). These results suggest that NHE5 regulates PM targeting and activity of Rac1, which are critical in establishing spatially restricted signals for cell migration (Palamidessi, Frittoli et al. 2008). Indeed, I observed that NHE5 KD or Bafilomycin A1 treatment impaired in directed cell migration and chemotaxis similar to defects observed by Rac1 perturbations (Fig 4.6D-F, Fig 4.7A-B, (Palamidessi, Frittoli et al. 2008; Hu, Shi et al. 2009; Wiedmann, von Schwarzenberg et al. 2012). The phenotype was partially rescued by exogenous expression of hNHE5 or overexpressing Rac1 into NHE5-deficient cells (Fig 4.6D-E), further validating that NHE5 acts on HGF-c-Met-Rac1 signalling axis to modulate cell motility.

Activation of Rac1 through HGF-c-Met signalling has been suggested to occur in the endosomes (Palamidessi, Frittoli et al. 2008; Menard, Parker et al. 2014). Palamidessi and colleagues showed that activation upon HGF stimulation, Rac1 and Tiam1, a Rac1 GEF, were localized to the periphery endosomes within 10 min in Rab5- and PI3K-Akt-dependent manner. Rab5 knockdown, over-expressions of a GTP-binding-deficient mutant, Rab5 S34N, or treatment with Wortmannin, a PI3K inhibitor, attenuated activation of Rac1 and peripheral membrane rufflings by HGF stimulation. Furthermore, over-expression of dominant negative dynamin, knockdown of clathrin heavy chain, or inhibition of endocytosis by lowering the temperature to 16ºC produced the same phenotypes, implicating that the integrity of CME is required for endosomal activation of Rac1 (Palamidessi, Frittoli et al. 2008). In a more recent study, Menard and colleagues demonstrated that differential c-Met-Rac1 signalling occurs at

distinct compartments. Specifically, HGF induced early (~10 min) activation of Rac1 in Rab4-/Rab5-positive peripheral endosomes and late/sustained activation (~30 min) in Rab7-positive perinuclear endosomes. The authors further showed that the sustained Rac1 activation was dependent on PKCα-modulated trafficking of c-Met from peripheral to perinuclear endosomes, PI3K activity, and Vav2, a Rac1 GEF. This late endosomal Rac1 activation was also shown to play an important role in actin reorganization at the cell front and the migration of the breast cancer cell lines (Menard, Parker et al. 2014). Given the similar effect of NHE5 KD on the actin cytoskeleton and continuous attenuation of Rac1 activity, it is possible that NHE5 is involved in directing c-Met from peripheral to perinuclear endosomes, and modulates sustained endosomal Rac1 signalling.

Recycling of Rac1 and c-Met had been implicated in cell migration and are mediated by Arf6, IQ-domain GTPase-activating protein 1 (IQGAP1), and GGA3 (Palamidessi, Frittoli et al. 2008; Hu, Shi et al. 2009; Parachoniak, Luo et al. 2011). Parachoniak and colleages demonstrated that the association between GGA3 and c-Met was required for recycling of the internalized receptors from Rab4. Depletion of GGA3 or Arf6 reduced recycling and promoted degradation of c-Met (Parachoniak, Luo et al. 2011). Consistent to this finding, I showed that impaired recycling of c-Met in NHE5 KD cells also promoted ligand-dependent degradation, implicating the functional similarity of NHE5 and GGA3/Arf6 as positive recycling modulators. In addition, activation of c-Met had been shown to facilitate membrane protrusion through Rho GTPase-mediated actin cytoskeleton remodelling in Arf6- and IQGAP-dependent manner (Palamidessi, Frittoli et al. 2008; Hu, Shi et al. 2009). Upon HGF-stimulation, Arf6 mediates recruitment of

IQGAP1 to the migrating edge in an Arf6 activity-dependent manner. IQGAP1 positively regulates cell migration by binding to Rac1-GTP and stabilizes activated conformation of the Rho GTPase (Kuroda, Fukata et al. 1996). Moreover, ARNO, an Arf6-GEF, had been shown to modulate Rac1 activation by promoting the recruitment of Dock180/ELMO1, a Rac-GEF, complex to the leading edge (Santy, Ravichandran et al. 2005). Altogether, these findings demonstrate that Arf6 is an important regulator for cell migration that modulates recycling and signalling of the upstream RTK (c-Met), and also plays a direct role in activating downstream Rho GTPases (Rac1 and Cdc42) in both endosomes and the plasma membrane. NHE5 was previously reported to co-localize with Arf6 and SCAMP2 in recycling endosomes, where interaction between SCAMP2 and NHE5 mediates PM translocation of NHE5 from recycling endosomes to the PM in an Arf6-dependent manner (Diering, Church et al. 2009). It is possible that the direct interaction between Arf6 and NHE5 in the endosomes may play a part in promoting endosomal signalling and recycling of Rac1 and c-Met. Intriguingly, I did not observe discernable expression of NHE5 in the PM of C6 cells (Fig 3.1), suggesting that active targeting of NHE5 to the PM is governed by a cell-type dependent and/or context-dependent mechanism(s). It is also possible that cell-surface biotinylation did not detect NHE5 recreuited to the PM because of spatially and/or temporally restricted nature of NHE5 recycling. The pH-dependent mechanism of NHE5-mediated sorting from the recycling compartments to the PM remains to be answered. Unveiling this mechanism may provide additional information about endocytic transport of specialized cargo and compartments that may lead to future development of therapeutics against oncogenic receptors.

5.5 Conclusion

In summary, I found that the endosomal acidifier NHE5 is a positive regulator of c-Met recycling in C6 glioma cells. Reduced expression of NHE5 resulted in loss of c-Met on cell surface through impaired PM targeting and enhanced degradation, and attenuated downstream signalling targets such as Akt, Erk, Rac1, and Cdc42 (Fig 5.1). These coincided with defects in cell motility, including impaired wound-healing, chemotaxis, reduced actin dynamics and loss of cell polarity, indicating an overall reduced fitness of NHE5-depleted cells. This study highlights a critical role of NHE5/endosome pH in mediating distinct recycling pathway and promoting persistent RTK signalling that contributes to glioma pathogenesis. Future experiment will focus on understanding the precise mechanism of NHE5/pH-regulated cargo-specific recycling processes, in hope to rationalize targeting NHE5 or other endosomal pH regulators as a viable strategy against cancer metastasis.

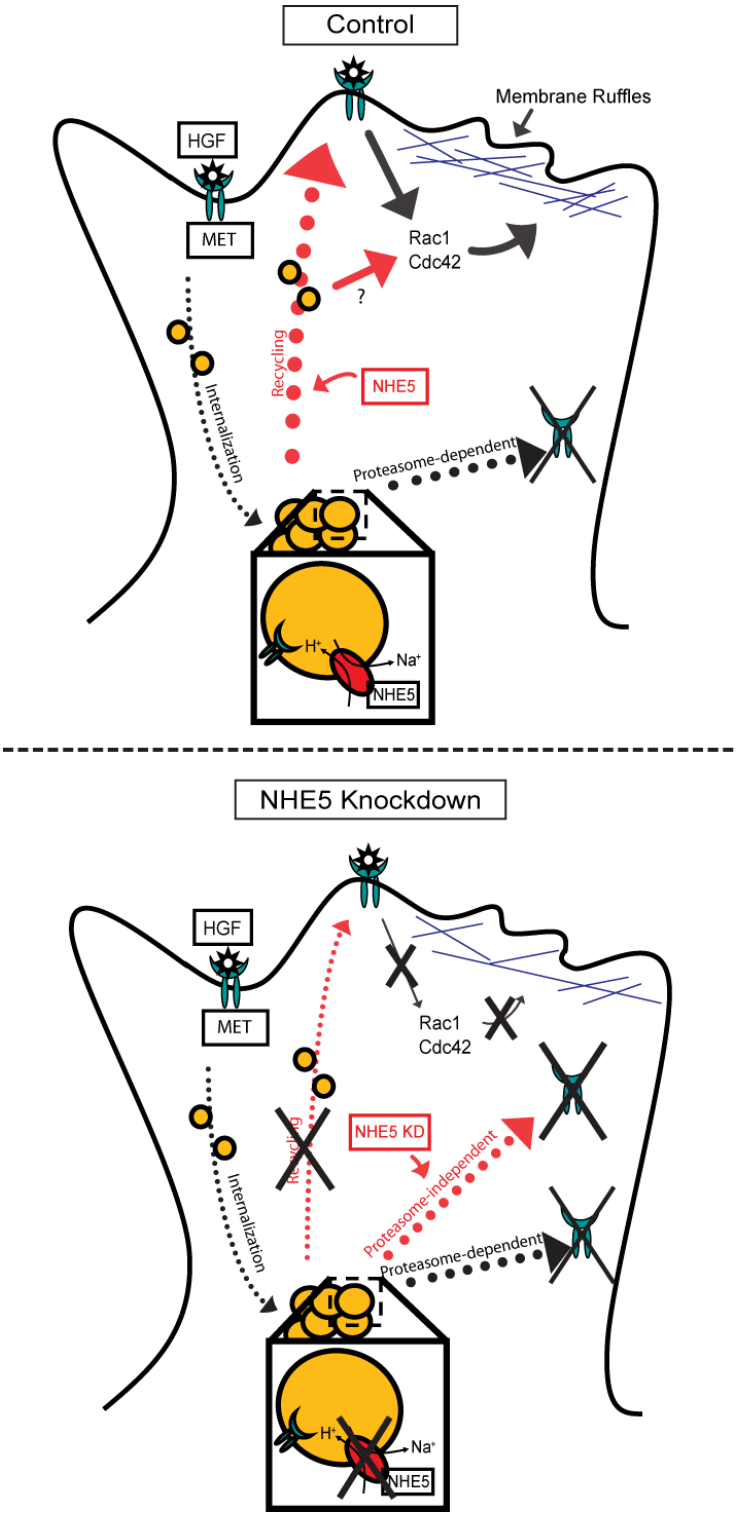

Figure 5.1 – Summary of NHE5 regulation in c-Met trafficking and signalling.
This cartoon summarizes trafficking (dotted arrow) and signalling of c-Met in control and NHE5-depleted cells. Solid arrows depict downstream effect. Processes influenced by NHE5 are colored in red.

Bibliography

Abella, J. V., P. Peschard, et al. (2005). "Met/Hepatocyte growth factor receptor ubiquitination suppresses transformation and is required for Hrs phosphorylation." Mol Cell Biol **25**(21): 9632-9645.

Alwan, H. A. and J. E. van Leeuwen (2007). "UBPY-mediated epidermal growth factor receptor (EGFR) de-ubiquitination promotes EGFR degradation." J Biol Chem **282**(3): 1658-1669.

Attaphitaya, S., K. Nehrke, et al. (2001). "Acute inhibition of brain-specific Na^+/H^+ exchanger isoform 5 by protein kinases A and C and cell shrinkage." Am J Physiol Cell Physiol **281**(4): C1146-1157.

Attaphitaya, S., K. Park, et al. (1999). "Molecular cloning and functional expression of a rat Na+/H+ exchanger (NHE5) highly expressed in brain." J Biol Chem **274**(7): 4383-4388.

Bachmann, O., B. Riederer, et al. (2004). "The Na^+/H^+ exchanger isoform 2 is the predominant NHE isoform in murine colonic crypts and its lack causes NHE3 upregulation." Am J Physiol Gastrointest Liver Physiol **287**(1): G125-133.

Bailey, M. A., G. Giebisch, et al. (2004). "NHE2-mediated bicarbonate reabsorption in the distal tubule of NHE3 null mice." J Physiol **561**(Pt 3): 765-775.

Baird, N. R., J. Orlowski, et al. (1999). "Molecular cloning, genomic organization, and functional expression of Na^+/H^+ exchanger isoform 5 (NHE5) from human brain." J Biol Chem **274**(7): 4377-4382.

Basu, S. K., J. L. Goldstein, et al. (1981). "Monensin interrupts the recycling of low density lipoprotein receptors in human fibroblasts." Cell **24**(2): 493-502.

Baum, M., K. Twombley, et al. (2012). "Proximal tubule Na^+/H^+ exchanger activity in adult NHE8-/-, NHE3-/-, and NHE3-/-/NHE8-/- mice." Am J Physiol Renal Physiol **303**(11): F1495-1502.

Baumgartner, M., H. Patel, et al. (2004). "Na^+/H^+ exchanger NHE1 as plasma membrane scaffold in the assembly of signalling complexes." Am J Physiol Cell Physiol **287**(4): C844-850.

Bazzini, C., G. Botta, et al. (2001). "The presence of NHE1 and NHE3 Na^+-H^+ exchangers and an apical cAMP-independent Cl^- channel indicate that both absorptive and secretory functions are present in calf gall bladder epithelium." Exp Physiol **86**(5): 571-583.

Becker, A. M., J. Zhang, et al. (2007). "Ontogeny of NHE8 in the rat proximal tubule." Am J Physiol Renal Physiol **293**(1): F255-261.

Berlin, I., H. Schwartz, et al. (2010). "Regulation of epidermal growth factor receptor ubiquitination and trafficking by the USP8.STAM complex." J Biol Chem **285**(45): 34909-34921.

Biemesderfer, D., P. A. Rutherford, et al. (1997). "Monoclonal antibodies for high-resolution localization of NHE3 in adult and neonatal rat kidney." Am J Physiol **273**(2 Pt 2): F289-299.

Bolanos-Garcia, V. M. (2005). "MET meet adaptors: functional and structural implications in downstream signalling mediated by the Met receptor." Mol Cell Biochem **276**(1-2): 149-157.

Bornens, M. (2008). "Organelle positioning and cell polarity." Nat Rev Mol Cell Biol **9**(11): 874-886.

Bosse, T., J. Ehinger, et al. (2007). "Cdc42 and phosphoinositide 3-kinase drive Rac-mediated actin polymerization downstream of c-Met in distinct and common pathways." Mol Cell Biol **27**(19): 6615-6628.

Bourguignon, L. Y., P. A. Singleton, et al. (2004). "CD44 interaction with Na^+-H^+ exchanger (NHE1) creates acidic microenvironments leading to hyaluronidase-2 and cathepsin B activation and breast tumor cell invasion." J Biol Chem **279**(26): 26991-27007.

Brant, S. R., C. H. Yun, et al. (1995). "Cloning, tissue distribution, and functional analysis of the human Na^+/N^+ exchanger isoform, NHE3." Am J Physiol **269**(1 Pt 1): C198-206.

Brett, C. L., M. Donowitz, et al. (2005). "Evolutionary origins of eukaryotic sodium/proton exchangers." Am J Physiol Cell Physiol **288**(2): C223-239.

Brett, C. L., D. N. Tukaye, et al. (2005). "The yeast endosomal Na^+K^+/H^+ exchanger Nhx1 regulates cellular pH to control vesicle trafficking." Mol Biol Cell **16**(3): 1396-1405.

Bridgewater, R. E., J. C. Norman, et al. (2012). "Integrin trafficking at a glance." J Cell Sci **125**(Pt 16): 3695-3701.

Brisson, L., V. Driffort, et al. (2013). "NaV1.5 Na^+ channels allosterically regulate the NHE-1 exchanger and promote the activity of breast cancer cell invadopodia." J Cell Sci **126**(Pt 21): 4835-4842.

Brown, D., T. G. Paunescu, et al. (2009). "Regulation of the V-ATPase in kidney epithelial cells: dual role in acid-base homeostasis and vesicle trafficking." J Exp Biol **212**(Pt 11): 1762-1772.

Buchsbaum, R. J. (2007). "Rho activation at a glance." J Cell Sci **120**(Pt 7): 1149-1152.

Byun, S., S. Y. Lee, et al. (2013). "USP8 is a novel target for overcoming gefitinib

resistance in lung cancer." Clin Cancer Res **19**(14): 3894-3904.
Cai, W., S. L. Rook, et al. (2000). "Mechanisms of hepatocyte growth factor-induced retinal endothelial cell migration and growth." Invest Ophthalmol Vis Sci **41**(7): 1885-1893.
Cardone, R. A., V. Casavola, et al. (2005). "The role of disturbed pH dynamics and the Na^+/H^+ exchanger in metastasis." Nat Rev Cancer **5**(10): 786-795.
Casey, J. R., S. Grinstein, et al. (2010). "Sensors and regulators of intracellular pH." Nat Rev Mol Cell Biol **11**(1): 50-61.
Caswell, P. T., H. J. Spence, et al. (2007). "Rab25 associates with alpha5beta1 integrin to promote invasive migration in 3D microenvironments." Dev Cell **13**(4): 496-510.
Caswell, P. T., S. Vadrevu, et al. (2009). "Integrins: masters and slaves of endocytic transport." Nat Rev Mol Cell Biol **10**(12): 843-853.
Cha, B. and M. Donowitz (2008). "The epithelial brush border Na^+/H^+ exchanger NHE3 associates with the actin cytoskeleton by binding to ezrin directly and via PDZ domain-containing Na^+/H^+ exchanger regulatory factor (NHERF) proteins." Clin Exp Pharmacol Physiol **35**(8): 863-871.
Chen, Z. Y., A. Ieraci, et al. (2005). "A novel endocytic recycling signal distinguishes biological responses of Trk neurotrophin receptors." Mol Biol Cell **16**(12): 5761-5772.
Choi, C. H., B. A. Webb, et al. (2013). "pH sensing by FAK-His58 regulates focal adhesion remodeling." J Cell Biol **202**(6): 849-859.
Christianson, A. L., R. E. Stevenson, et al. (1999). "X linked severe mental retardation, craniofacial dysmorphology, epilepsy, ophthalmoplegia, and cerebellar atrophy in a large South African kindred is localised to Xq24-q27." J Med Genet **36**(10): 759-766.
Christoforidis, S., H. M. McBride, et al. (1999). "The Rab5 effector EEA1 is a core component of endosome docking." Nature **397**(6720): 621-625.
Chu, J., S. Chu, et al. (2002). "Apical Na^+/H^+ exchange near the base of mouse colonic crypts." Am J Physiol Cell Physiol **283**(1): C358-372.
Cinar, A., M. Chen, et al. (2007). "NHE3 inhibition by cAMP and Ca^{2+} is abolished in PDZ-domain protein PDZK1-deficient murine enterocytes." J Physiol **581**(Pt 3): 1235-1246.
Cordat, E. and J. R. Casey (2009). "Bicarbonate transport in cell physiology and disease." Biochem J **417**(2): 423-439.
Dai, J., J. Li, et al. (2004). "ACAP1 promotes endocytic recycling by recognizing recycling sorting signals." Dev Cell **7**(5): 771-776.

de Silva, M. G., K. Elliott, et al. (2003). "Disruption of a novel member of a sodium/hydrogen exchanger family and DOCK3 is associated with an attention deficit hyperactivity disorder-like phenotype." J Med Genet **40**(10): 733-740.

Denker, S. P., D. C. Huang, et al. (2000). "Direct binding of the Na--H exchanger NHE1 to ERM proteins regulates the cortical cytoskeleton and cell shape independently of H^+ translocation." Mol Cell **6**(6): 1425-1436.

Diaz-Coranguez, M., J. Segovia, et al. (2013). "Transmigration of neural stem cells across the blood brain barrier induced by glioma cells." PLoS One **8**(4): e60655.

Diehl, H. and R. Markuszewski (1989). "Studies on fluorescein-VII The fluorescence of fluorescein as a function of pH." Talanta **36**(3): 416-418.

Diering, G. H., J. Church, et al. (2009). "Secretory Carrier Membrane Protein 2 Regulates Cell-surface Targeting of Brain-enriched Na^+/H^+ Exchanger NHE5." J Biol Chem **284**(20): 13892-13903.

Diering, G. H., F. Mills, et al. (2011). "Regulation of dendritic spine growth through activity-dependent recruitment of the brain-enriched Na^+/H^+ exchanger NHE5." Mol Biol Cell **22**(13): 2246-2257.

Diering, G. H., Y. Numata, et al. (2013). "Endosomal acidification by Na^+/H^+ exchanger NHE5 regulates TrkA cell-surface targeting and NGF-induced PI3K signalling." Mol Biol Cell **24**(21): 3435-3448.

Dixit, M. P., L. Xu, et al. (2004). "Effect of angiotensin-II on renal Na^+/H^+ exchanger-NHE3 and NHE2." Biochim Biophys Acta **1664**(1): 38-44.

Donowitz, M., C. Ming Tse, et al. (2013). "SLC9/NHE gene family, a plasma membrane and organellar family of Na^+/H^+ exchangers." Mol Aspects Med **34**(2-3): 236-251.

Dozynkiewicz, M. A., N. B. Jamieson, et al. (2012). "Rab25 and CLIC3 collaborate to promote integrin recycling from late endosomes/lysosomes and drive cancer progression." Dev Cell **22**(1): 131-145.

Ebner, R. and R. Derynck (1991). "Epidermal growth factor and transforming growth factor-alpha: differential intracellular routing and processing of ligand-receptor complexes." Cell Regul **2**(8): 599-612.

Etienne-Manneville, S. (2004). "Cdc42--the centre of polarity." J Cell Sci **117**(Pt 8): 1291-1300.

Forgac, M. (2007). "Vacuolar ATPases: rotary proton pumps in physiology and pathophysiology." Nat Rev Mol Cell Biol **8**(11): 917-929.

Fortin Ensign, S. P., I. T. Mathews, et al. (2013). "Implications of Rho GTPase Signalling in Glioma Cell Invasion and Tumor Progression." Front Oncol **3**: 241.

Fuster, D. G. and R. T. Alexander (2014). "Traditional and emerging roles for the SLC9

Na+/H+ exchangers." Pflugers Arch **466**(1): 61-76.

Gage, R. M., K. A. Kim, et al. (2001). "A transplantable sorting signal that is sufficient to mediate rapid recycling of G protein-coupled receptors." J Biol Chem **276**(48): 44712-44720.

Garbern, J. Y., M. Neumann, et al. (2010). "A mutation affecting the sodium/proton exchanger, SLC9A6, causes mental retardation with tau deposition." Brain **133**(Pt 5): 1391-1402.

Gattineni, J., D. Sas, et al. (2008). "Effect of thyroid hormone on the postnatal renal expression of NHE8." Am J Physiol Renal Physiol **294**(1): F198-204.

Gawenis, L. R., J. M. Greeb, et al. (2005). "Impaired gastric acid secretion in mice with a targeted disruption of the NHE4 Na^+/H^+ exchanger." J Biol Chem **280**(13): 12781-12789.

Gherardi, E., W. Birchmeier, et al. (2012). "Targeting MET in cancer: rationale and progress." Nat Rev Cancer **12**(2): 89-103.

Gilfillan, G. D., K. K. Selmer, et al. (2008). "SLC9A6 mutations cause X-linked mental retardation, microcephaly, epilepsy, and ataxia, a phenotype mimicking Angelman syndrome." Am J Hum Genet **82**(4): 1003-1010.

Goh, L. K. and A. Sorkin (2013). "Endocytosis of receptor tyrosine kinases." Cold Spring Harb Perspect Biol **5**(5): a017459.

Gould, G. W. and J. Lippincott-Schwartz (2009). "New roles for endosomes: from vesicular carriers to multi-purpose platforms." Nat Rev Mol Cell Biol **10**(4): 287-292.

Goyal, S., S. Mentone, et al. (2005). "Immunolocalization of NHE8 in rat kidney." Am J Physiol Renal Physiol **288**(3): F530-538.

Grant, B. D. and J. G. Donaldson (2009). "Pathways and mechanisms of endocytic recycling." Nat Rev Mol Cell Biol **10**(9): 597-608.

Gross, E., K. Hawkins, et al. (2001). "The stoichiometry of the electrogenic sodium bicarbonate cotransporter NBC1 is cell-type dependent." J Physiol **531**(Pt 3): 597-603.

Guan, Y., J. Dong, et al. (2006). "NHE2 is the main apical NHE in mouse colonic crypts but an alternative Na+-dependent acid extrusion mechanism is upregulated in NHE2-null mice." Am J Physiol Gastrointest Liver Physiol **291**(4): G689-699.

Hammond, D. E., S. Carter, et al. (2003). "Endosomal dynamics of Met determine signalling output." Mol Biol Cell **14**(4): 1346-1354.

Hammond, D. E., S. Urbe, et al. (2001). "Down-regulation of MET, the receptor for hepatocyte growth factor." Oncogene **20**(22): 2761-2770.

Hara-Chikuma, M., B. Yang, et al. (2005). "ClC-3 chloride channels facilitate endosomal acidification and chloride accumulation." J Biol Chem **280**(2): 1241-1247.

Harrington, A. W., C. St Hillaire, et al. (2011). "Recruitment of actin modifiers to TrkA endosomes governs retrograde NGF signalling and survival." Cell **146**(3): 421-434.

Harris, R. C., E. Chung, et al. (2003). "EGF receptor ligands." Exp Cell Res **284**(1): 2-13.

Hayashi, H., K. Szaszi, et al. (2004). "Inhibition and redistribution of NHE3, the apical Na+/H+ exchanger, by Clostridium difficile toxin B." J Gen Physiol **123**(5): 491-504.

Hellberg, C., C. Schmees, et al. (2009). "Activation of protein kinase C alpha is necessary for sorting the PDGF beta-receptor to Rab4a-dependent recycling." Mol Biol Cell **20**(12): 2856-2863.

Hiebsch, R. R., T. J. Raub, et al. (1991). "Primaquine blocks transport by inhibiting the formation of functional transport vesicles. Studies in a cell-free assay of protein transport through the Golgi apparatus." J Biol Chem **266**(30): 20323-20328.

Hill, J. K., C. L. Brett, et al. (2006). "Vestibular hair bundles control pH with (Na^+, K^+)/H^+ exchangers NHE6 and NHE9." J Neurosci **26**(39): 9944-9955.

Hisamitsu, T., K. Yamada, et al. (2007). "Functional importance of charged residues within the putative intracellular loops in pH regulation by Na^+/ H^+ exchanger NHE1." FEBS J **274**(16): 4326-4335.

Honasoge, A. and H. Sontheimer (2013). "Involvement of tumor acidification in brain cancer pathophysiology." Front Physiol **4**: 316.

Hsu, V. W., M. Bai, et al. (2012). "Getting active: protein sorting in endocytic recycling." Nat Rev Mol Cell Biol **13**(5): 323-328.

Hu, B., B. Shi, et al. (2009). "ADP-ribosylation factor 6 regulates glioma cell invasion through the IQ-domain GTPase-activating protein 1-Rac1-mediated pathway." Cancer Res **69**(3): 794-801.

Huotari, J. and A. Helenius (2011). "Endosome maturation." EMBO J **30**(17): 3481-3500.

Ivaska, J., K. Vuoriluoto, et al. (2005). "PKCepsilon-mediated phosphorylation of vimentin controls integrin recycling and motility." EMBO J **24**(22): 3834-3845.

Jeffers, M., G. A. Taylor, et al. (1997). "Degradation of the Met tyrosine kinase receptor by the ubiquitin-proteasome pathway." Mol Cell Biol **17**(2): 799-808.

Jinadasa, T., E. Z. Szabo, et al. (2014). "Activation of AMP-activated protein kinase regulates hippocampal neuronal pH by recruiting Na^+/H^+ exchanger NHE5 to the cell surface." J Biol Chem **289**(30): 20879-20897.

Joberty, G., C. Petersen, et al. (2000). "The cell-polarity protein Par6 links Par3 and

atypical protein kinase C to Cdc42." Nat Cell Biol **2**(8): 531-539.
Joffre, C., R. Barrow, et al. (2011). "A direct role for Met endocytosis in tumorigenesis." Nat Cell Biol **13**(7): 827-837.
Johnson, L. S., K. W. Dunn, et al. (1993). "Endosome acidification and receptor trafficking: bafilomycin A1 slows receptor externalization by a mechanism involving the receptor's internalization motif." Mol Biol Cell **4**(12): 1251-1266.
Joseph, C., J. Gattineni, et al. (2013). "Glucocorticoids Reduce Renal NHE8 Expression." Physiol Rep **1**(2).
Jovic, M., N. Naslavsky, et al. (2007). "EHD1 regulates beta1 integrin endosomal transport: effects on focal adhesions, cell spreading and migration." J Cell Sci **120**(Pt 5): 802-814.
Kagami, T., S. Chen, et al. (2008). "Identification and biochemical characterization of the SLC9A7 interactome." Mol Membr Biol **25**(5): 436-447.
Klonis, N. and W. H. Sawyer (1996). "Spectral properties of the prototropic forms of fluorescein in aqueous solution." J Fluoresc **6**(3): 147-157.
Koivusalo, M., C. Welch, et al. (2010). "Amiloride inhibits macropinocytosis by lowering submembranous pH and preventing Rac1 and Cdc42 signalling." J Cell Biol **188**(4): 547-563.
Kondapalli, K. C., A. Hack, et al. (2013). "Functional evaluation of autism-associated mutations in NHE9." Nat Commun **4**: 2510.
Kondapalli, K. C., J. P. Llongueras, et al. (2015). "A leak pathway for luminal protons in endosomes drives oncogenic signalling in glioblastoma." Nat Commun **6**: 6289.
Kondapalli, K. C., H. Prasad, et al. (2014). "An inside job: how endosomal Na^+/H^+ exchangers link to autism and neurological disease." Front Cell Neurosci **8**: 172.
Kuroda, S., M. Fukata, et al. (1996). "Identification of IQGAP as a putative target for the small GTPases, Cdc42 and Rac1." J Biol Chem **271**(38): 23363-23367.
Lacroix, J., M. Poet, et al. (2004). "A mechanism for the activation of the Na/H exchanger NHE-1 by cytoplasmic acidification and mitogens." EMBO Rep **5**(1): 91-96.
Laederich, M. B., M. Funes-Duran, et al. (2004). "The leucine-rich repeat protein LRIG1 is a negative regulator of ErbB family receptor tyrosine kinases." J Biol Chem **279**(45): 47050-47056.
Lagarde, A. E., A. J. Franchi, et al. (1988). "Effect of mutations affecting Na^+: H^+ antiport activity on tumorigenic potential of hamster lung fibroblasts." J Cell Biochem **36**(3): 249-260.
Lakadamyali, M., M. J. Rust, et al. (2006). "Ligands for clathrin-mediated endocytosis are differentially sorted into distinct populations of early endosomes." Cell **124**(5):

997-1009.

Lawrence, S. P., N. A. Bright, et al. (2010). "The sodium/proton exchanger NHE8 regulates late endosomal morphology and function." Mol Biol Cell **21**(20): 3540-3551.

Le, T. L., A. S. Yap, et al. (1999). "Recycling of E-cadherin: a potential mechanism for regulating cadherin dynamics." J Cell Biol **146**(1): 219-232.

Lefebvre, J., F. Ancot, et al. (2012). "Met degradation: more than one stone to shoot a receptor down." FASEB J **26**(4): 1387-1399.

Lemmon, M. A. and J. Schlessinger (2010). "Cell signalling by receptor tyrosine kinases." Cell **141**(7): 1117-1134.

Levkowitz, G., H. Waterman, et al. (1999). "Ubiquitin ligase activity and tyrosine phosphorylation underlie suppression of growth factor signalling by c-Cbl/Sli-1." Mol Cell **4**(6): 1029-1040.

Li, J., B. A. Ballif, et al. (2005). "Phosphorylation of ACAP1 by Akt regulates the stimulation-dependent recycling of integrin beta1 to control cell migration." Dev Cell **9**(5): 663-673.

Lin, D., A. S. Edwards, et al. (2000). "A mammalian PAR-3-PAR-6 complex implicated in Cdc42/Rac1 and aPKC signalling and cell polarity." Nat Cell Biol **2**(8): 540-547.

Lin, P. J., W. P. Williams, et al. (2007). "Caveolins bind to (Na^+, K^+)/H^+ exchanger NHE7 by a novel binding module." Cell Signal **19**(5): 978-988.

Lin, P. J., W. P. Williams, et al. (2005). "Secretory carrier membrane proteins interact and regulate trafficking of the organellar (Na^+,K^+)/H^+ exchanger NHE7." J Cell Sci **118**(Pt 9): 1885-1897.

Lin, R., R. Murtazina, et al. (2011). "D-glucose acts via sodium/glucose cotransporter 1 to increase NHE3 in mouse jejunal brush border by a Na^+/H^+ exchange regulatory factor 2-dependent process." Gastroenterology **140**(2): 560-571.

Liu, L., P. H. Schlesinger, et al. (2011). "High capacity Na^+/H^+ exchange activity in mineralizing osteoblasts." J Cell Physiol **226**(6): 1702-1712.

Longva, K. E., F. D. Blystad, et al. (2002). "Ubiquitination and proteasomal activity is required for transport of the EGF receptor to inner membranes of multivesicular bodies." J Cell Biol **156**(5): 843-854.

Lukashova, V., T. Jinadasa, et al. (2013). "The Na^+/H^+ exchanger NHE5 is sorted to discrete intracellular vesicles in the central and peripheral nervous systems." Adv Exp Med Biol **961**: 397-410.

Lukashova, V., E. Z. Szabo, et al. (2011). "CK2 phosphorylation of an acidic Ser/Thr di-isoleucine motif in the Na^+/H^+ exchanger NHE5 isoform promotes association

with beta-arrestin2 and endocytosis." J Biol Chem **286**(13): 11456-11468.
Magalhaes, M. A., D. R. Larson, et al. (2011). "Cortactin phosphorylation regulates cell invasion through a pH-dependent pathway." J Cell Biol **195**(5): 903-920.
Mak, H. H., P. Peschard, et al. (2007). "Oncogenic activation of the Met receptor tyrosine kinase fusion protein, Tpr-Met, involves exclusion from the endocytic degradative pathway." Oncogene **26**(51): 7213-7221.
Malakooti, J., R. Y. Dahdal, et al. (1999). "Molecular cloning, tissue distribution, and functional expression of the human Na^+/H^+ exchanger NHE2." Am J Physiol **277**(2 Pt 1): G383-390.
Maldonado-Baez, L., C. Williamson, et al. (2013). "Clathrin-independent endocytosis: a cargo-centric view." Exp Cell Res **319**(18): 2759-2769.
Markunas, C. A., K. S. Quinn, et al. (2010). "Genetic variants in SLC9A9 are associated with measures of attention-deficit/hyperactivity disorder symptoms in families." Psychiatr Genet **20**(2): 73-81.
Masereel, B., L. Pochet, et al. (2003). "An overview of inhibitors of Na^+/H^+ exchanger." Eur J Med Chem **38**(6): 547-554.
Maxfield, F. R. and T. E. McGraw (2004). "Endocytic recycling." Nat Rev Mol Cell Biol **5**(2): 121-132.
Mayor, S. and R. E. Pagano (2007). "Pathways of clathrin-independent endocytosis." Nat Rev Mol Cell Biol **8**(8): 603-612.
McCullough, J., M. J. Clague, et al. (2004). "AMSH is an endosome-associated ubiquitin isopeptidase." J Cell Biol **166**(4): 487-492.
Menard, L., P. J. Parker, et al. (2014). "Receptor tyrosine kinase c-Met controls the cytoskeleton from different endosomes via different pathways." Nat Commun **5**: 3907.
Mezzacappa, C., Y. Komiya, et al. (2012). "Activation and function of small GTPases Rho, Rac, and Cdc42 during gastrulation." Methods Mol Biol **839**: 119-131.
Mohammad-Panah, R., R. Harrison, et al. (2003). "The chloride channel ClC-4 contributes to endosomal acidification and trafficking." J Biol Chem **278**(31): 29267-29277.
Morrow, E. M., S. Y. Yoo, et al. (2008). "Identifying autism loci and genes by tracing recent shared ancestry." Science **321**(5886): 218-223.
Muro, S., M. Mateescu, et al. (2006). "Control of intracellular trafficking of ICAM-1-targeted nanocarriers by endothelial Na^+/H^+ exchanger proteins." Am J Physiol Lung Cell Mol Physiol **290**(5): L809-817.
Musch, M. W., D. L. Arvans, et al. (2009). "Functional coupling of the downregulated in

adenoma Cl-/base exchanger DRA and the apical Na^+/H^+ exchangers NHE2 and NHE3." Am J Physiol Gastrointest Liver Physiol **296**(2): G202-210.

Nakamura, N., S. Tanaka, et al. (2005). "Four Na^+/H^+ exchanger isoforms are distributed to Golgi and post-Golgi compartments and are involved in organelle pH regulation." J Biol Chem **280**(2): 1561-1572.

Nakashima, S., Y. Hiraku, et al. (2003). "Vacuolar H^+-ATPase inhibitor induces apoptosis via lysosomal dysfunction in the human gastric cancer cell line MKN-1." J Biochem **134**(3): 359-364.

Nobes, C. D. and A. Hall (1995). "Rho, rac, and cdc42 GTPases regulate the assembly of multimolecular focal complexes associated with actin stress fibers, lamellipodia, and filopodia." Cell **81**(1): 53-62.

Noel, G., D. K. Tham, et al. (2009). "Interdependence of laminin-mediated clustering of lipid rafts and the dystrophin complex in astrocytes." J Biol Chem **284**(29): 19694-19704.

Numata, M. and J. Orlowski (2001). "Molecular cloning and characterization of a novel $(Na^+,K^+)/H^+$ exchanger localized to the trans-Golgi network." J Biol Chem **276**(20): 17387-17394.

Oh, Y. M., S. B. Lee, et al. (2014). "USP8 modulates ubiquitination of LRIG1 for Met degradation." Sci Rep **4**: 4980.

Ohgaki, R., M. Matsushita, et al. (2010). "The Na^+/H^+ exchanger NHE6 in the endosomal recycling system is involved in the development of apical bile canalicular surface domains in HepG2 cells." Mol Biol Cell **21**(7): 1293-1304.

Ohgaki, R., I. S. C. van, et al. (2011). "Organellar Na^+/H^+ exchangers: novel players in organelle pH regulation and their emerging functions." Biochemistry **50**(4): 443-450.

Onishi, I., P. J. Lin, et al. (2007). "RACK1 associates with NHE5 in focal adhesions and positively regulates the transporter activity." Cell Signal **19**(1): 194-203.

Onishi, I., P. J. Lin, et al. (2012). "Organellar $(Na^+, K^+)/H^+$ exchanger NHE7 regulates cell adhesion, invasion and anchorage-independent growth of breast cancer MDA-MB-231 cells." Oncol Rep **27**(2): 311-317.

Organ, S. L. and M. S. Tsao (2011). "An overview of the c-MET signalling pathway." Ther Adv Med Oncol **3**(1 Suppl): S7-S19.

Orlowski, J. and S. Grinstein (2007). "Emerging roles of alkali cation/proton exchangers in organellar homeostasis." Curr Opin Cell Biol **19**(4): 483-492.

Ouyang, Q., S. B. Lizarraga, et al. (2013). "Christianson syndrome protein NHE6 modulates TrkB endosomal signalling required for neuronal circuit development."

Neuron **80**(1): 97-112.
Palamidessi, A., E. Frittoli, et al. (2008). "Endocytic trafficking of Rac is required for the spatial restriction of signalling in cell migration." Cell **134**(1): 135-147.
Parachoniak, C. A., Y. Luo, et al. (2011). "GGA3 functions as a switch to promote Met receptor recycling, essential for sustained ERK and cell migration." Dev Cell **20**(6): 751-763.
Pelicci, G., S. Giordano, et al. (1995). "The motogenic and mitogenic responses to HGF are amplified by the Shc adaptor protein." Oncogene **10**(8): 1631-1638.
Pellinen, T. and J. Ivaska (2006). "Integrin traffic." J Cell Sci **119**(Pt 18): 3723-3731.
Pellinen, T., S. Tuomi, et al. (2008). "Integrin trafficking regulated by Rab21 is necessary for cytokinesis." Dev Cell **15**(3): 371-385.
Pennock, S. and Z. Wang (2008). "A tale of two Cbls: interplay of c-Cbl and Cbl-b in epidermal growth factor receptor downregulation." Mol Cell Biol **28**(9): 3020-3037.
Pizzonia, J. H., D. Biemesderfer, et al. (1998). "Immunochemical characterization of Na+/H+ exchanger isoform NHE4." Am J Physiol **275**(4 Pt 2): F510-517.
Poea-Guyon, S., M. R. Ammar, et al. (2013). "The V-ATPase membrane domain is a sensor of granular pH that controls the exocytotic machinery." J Cell Biol **203**(2): 283-298.
Praetorius, J., D. Andreasen, et al. (2000). "NHE1, NHE2, and NHE3 contribute to regulation of intracellular pH in murine duodenal epithelial cells." Am J Physiol Gastrointest Liver Physiol **278**(2): G197-206.
Presley, J. F., S. Mayor, et al. (1997). "Bafilomycin A1 treatment retards transferrin receptor recycling more than bulk membrane recycling." J Biol Chem **272**(21): 13929-13936.
Puthenveedu, M. A., B. Lauffer, et al. (2010). "Sequence-dependent sorting of recycling proteins by actin-stabilized endosomal microdomains." Cell **143**(5): 761-773.
Qin, A., T. S. Cheng, et al. (2012). "V-ATPases in osteoclasts: structure, function and potential inhibitors of bone resorption." Int J Biochem Cell Biol **44**(9): 1422-1435.
Radu, M., G. Semenova, et al. (2014). "PAK signalling during the development and progression of cancer." Nat Rev Cancer **14**(1): 13-25.
Reincke, M., S. Sbiera, et al. (2015). "Mutations in the deubiquitinase gene USP8 cause Cushing's disease." Nat Genet **47**(1): 31-38.
Roberts, M. S., A. J. Woods, et al. (2004). "Protein kinase B/Akt acts via glycogen synthase kinase 3 to regulate recycling of alpha v beta 3 and alpha 5 beta 1 integrins." Mol Cell Biol **24**(4): 1505-1515.
Roepstorff, K., M. V. Grandal, et al. (2009). "Differential effects of EGFR ligands on

endocytic sorting of the receptor." Traffic **10**(8): 1115-1127.
Row, P. E., I. A. Prior, et al. (2006). "The ubiquitin isopeptidase UBPY regulates endosomal ubiquitin dynamics and is essential for receptor down-regulation." J Biol Chem **281**(18): 12618-12624.
Sabolic, I., C. M. Herak-Kramberger, et al. (2002). "NHE3 and NHERF are targeted to the basolateral membrane in proximal tubules of colchicine-treated rats." Kidney Int **61**(4): 1351-1364.
Sage, S. O., T. J. Rink, et al. (1991). "Resting and ADP-evoked changes in cytosolic free sodium concentration in human platelets loaded with the indicator SBFI." J Physiol **441**: 559-573.
Sahai, E. and C. J. Marshall (2002). "RHO-GTPases and cancer." Nat Rev Cancer **2**(2): 133-142.
Santy, L. C., K. S. Ravichandran, et al. (2005). "The DOCK180/Elmo complex couples ARNO-mediated Arf6 activation to the downstream activation of Rac1." Curr Biol **15**(19): 1749-1754.
Schultheis, P. J., L. L. Clarke, et al. (1998). "Targeted disruption of the murine Na^+/H^+ exchanger isoform 2 gene causes reduced viability of gastric parietal cells and loss of net acid secretion." J Clin Invest **101**(6): 1243-1253.
Schwartz, A. L., A. Bolognesi, et al. (1984). "Recycling of the asialoglycoprotein receptor and the effect of lysosomotropic amines in hepatoma cells." J Cell Biol **98**(2): 732-738.
Schwede, M., K. Garbett, et al. (2014). "Genes for endosomal NHE6 and NHE9 are misregulated in autism brains." Mol Psychiatry **19**(3): 277-279.
Scita, G. and P. P. Di Fiore (2010). "The endocytic matrix." Nature **463**(7280): 464-473.
Scott, C. C. and J. Gruenberg (2011). "Ion flux and the function of endosomes and lysosomes: pH is just the start: the flux of ions across endosomal membranes influences endosome function not only through regulation of the luminal pH." Bioessays **33**(2): 103-110.
Seger, R. and E. G. Krebs (1995). "The MAPK signalling cascade." FASEB J **9**(9): 726-735.
Shattuck, D. L., J. K. Miller, et al. (2007). "LRIG1 is a novel negative regulator of the Met receptor and opposes Met and Her2 synergy." Mol Cell Biol **27**(5): 1934-1946.
Sheldon, C., Y. M. Cheng, et al. (2004). "Concurrent measurements of the free cytosolic concentrations of H+ and Na+ ions with fluorescent indicators." Pflugers Arch **449**(3): 307-318.
Shin, J. M., K. Munson, et al. (2009). "The gastric HK-ATPase: structure, function, and

inhibition." Pflugers Arch **457**(3): 609-622.
Sigismund, S., E. Argenzio, et al. (2008). "Clathrin-mediated internalization is essential for sustained EGFR signalling but dispensable for degradation." Dev Cell **15**(2): 209-219.
Simonsen, A., R. Lippe, et al. (1998). "EEA1 links PI(3)K function to Rab5 regulation of endosome fusion." Nature **394**(6692): 494-498.
Smardon, A. M., H. I. Diab, et al. (2014). "The RAVE complex is an isoform-specific V-ATPase assembly factor in yeast." Mol Biol Cell **25**(3): 356-367.
Sorkin, A. and M. Von Zastrow (2002). "Signal transduction and endocytosis: close encounters of many kinds." Nat Rev Mol Cell Biol **3**(8): 600-614.
Stock, C. and A. Schwab (2006). "Role of the Na/H exchanger NHE1 in cell migration." Acta Physiol (Oxf) **187**(1-2): 149-157.
Stromme, P., K. Dobrenis, et al. (2011). "X-linked Angelman-like syndrome caused by Slc9a6 knockout in mice exhibits evidence of endosomal-lysosomal dysfunction." Brain **134**(Pt 11): 3369-3383.
Sun, A. M., Y. Liu, et al. (1998). "Expression of Na^+/H^+ exchanger isoforms in inner segment of inner medullary collecting duct." J Membr Biol **164**(3): 293-300.
Symons, M. (2011). "Rac1 activation comes full circle." EMBO J **30**(19): 3875-3877.
Szaszi, K., A. Paulsen, et al. (2002). "Clathrin-mediated endocytosis and recycling of the neuron-specific Na^+/H^+ exchanger NHE5 isoform. Regulation by phosphatidylinositol 3'-kinase and the actin cytoskeleton." J Biol Chem **277**(45): 42623-42632.
Taher, T. E., E. P. Tjin, et al. (2002). "c-Cbl is involved in Met signalling in B cells and mediates hepatocyte growth factor-induced receptor ubiquitination." J Immunol **169**(7): 3793-3800.
Takahashi, Y., K. Hosoki, et al. (2011). "A loss-of-function mutation in the SLC9A6 gene causes X-linked mental retardation resembling Angelman syndrome." Am J Med Genet B Neuropsychiatr Genet **156B**(7): 799-807.
Tang, P., P. A. Steck, et al. (1997). "The autocrine loop of TGF-alpha/EGFR and brain tumors." J Neurooncol **35**(3): 303-314.
Tayeb, M. A., M. Skalski, et al. (2005). "Inhibition of SNARE-mediated membrane traffic impairs cell migration." Exp Cell Res **305**(1): 63-73.
Temkin, P., B. Lauffer, et al. (2011). "SNX27 mediates retromer tubule entry and endosome-to-plasma membrane trafficking of signalling receptors." Nat Cell Biol **13**(6): 715-721.
Tulasne, D., J. Deheuninck, et al. (2004). "Proapoptotic function of the MET tyrosine

kinase receptor through caspase cleavage." Mol Cell Biol **24**(23): 10328-10339.

van Weert, A. W., H. J. Geuze, et al. (2000). "Primaquine interferes with membrane recycling from endosomes to the plasma membrane through a direct interaction with endosomes which does not involve neutralisation of endosomal pH nor osmotic swelling of endosomes." Eur J Cell Biol **79**(6): 394-399.

Vivanco, I. and C. L. Sawyers (2002). "The phosphatidylinositol 3-Kinase AKT pathway in human cancer." Nat Rev Cancer **2**(7): 489-501.

Wakabayashi, S., T. Hisamitsu, et al. (2003). "Mutations of Arg440 and Gly455/Gly456 oppositely change pH sensing of Na^+/H^+ exchanger 1." J Biol Chem **278**(14): 11828-11835.

Weinman, E. J., D. Steplock, et al. (2000). "NHERF associations with sodium-hydrogen exchanger isoform 3 (NHE3) and ezrin are essential for cAMP-mediated phosphorylation and inhibition of NHE3." Biochemistry **39**(20): 6123-6129.

Wellhauser, L., C. D'Antonio, et al. (2010). "ClC transporters: discoveries and challenges in defining the mechanisms underlying function and regulation of ClC-5." Pflugers Arch **460**(2): 543-557.

Wiedmann, R. M., K. von Schwarzenberg, et al. (2012). "The V-ATPase-inhibitor archazolid abrogates tumor metastasis via inhibition of endocytic activation of the Rho-GTPase Rac1." Cancer Res **72**(22): 5976-5987.

Xinhan, L., M. Matsushita, et al. (2011). "Na^+/H^+ exchanger isoform 6 (NHE6/SLC9A6) is involved in clathrin-dependent endocytosis of transferrin." Am J Physiol Cell Physiol **301**(6): C1431-1444.

Xu, H., H. Chen, et al. (2008). "Gastrointestinal distribution and kinetic characterization of the sodium-hydrogen exchanger isoform 8 (NHE8)." Cell Physiol Biochem **21**(1-3): 109-116.

Xu, H., B. Zhang, et al. (2010). "Transcriptional inhibition of intestinal NHE8 expression by glucocorticoids involves Pax5." Am J Physiol Gastrointest Liver Physiol **299**(4): G921-927.

Yokouchi, M., T. Kondo, et al. (1999). "Ligand-induced ubiquitination of the epidermal growth factor receptor involves the interaction of the c-Cbl RING finger and UbcH7." J Biol Chem **274**(44): 31707-31712.

Yun, C. H., S. Oh, et al. (1997). "cAMP-mediated inhibition of the epithelial brush border Na^+/H^+ exchanger, NHE3, requires an associated regulatory protein." Proc Natl Acad Sci U S A **94**(7): 3010-3015.

Zerial, M. and H. McBride (2001). "Rab proteins as membrane organizers." Nat Rev Mol Cell Biol **2**(2): 107-117.

Zhang, J., I. A. Bobulescu, et al. (2007). "Characterization of Na^+/H^+ exchanger NHE8 in cultured renal epithelial cells." Am J Physiol Renal Physiol **293**(3): F761-766.